PARTITIONING SUBSURFACE WATER FLUXES USING COUPLED HYDRUS-MODFLOW MODEL., CASE STUDY OF LA MATA CATCHMENT, SPAIN

GEZAHEGN DEME
March 15, 2011

SUPERVISORS:

Dr., Ir. M.W., Lubczynski (1st)

MSc., Ir. G.N. Parodi (2nd)

ADVISOR:

MSc., Enrico Balugani (PhD Candidate)

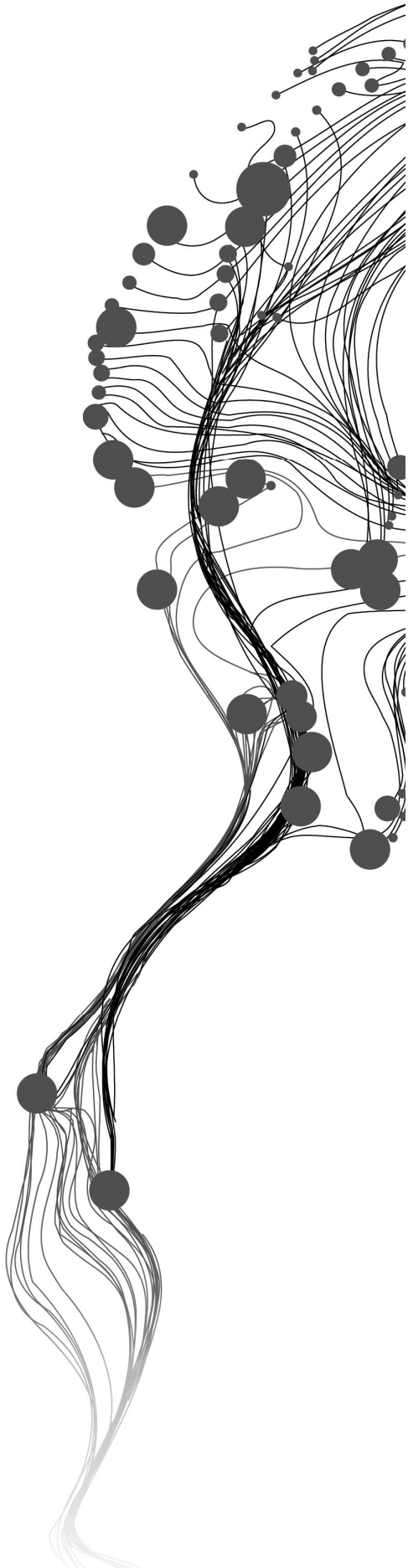

PARTITIONING SUBSURFACE WATER FLUXES USING COUPLED HYDRUS-MODFLOW MODEL., CASE STUDY OF LA MATA CATCHMENT, SPAIN

GEZAHEGN DEME

Enschede, The Netherlands, March 15, 2011

Thesis submitted to the Faculty of Geo-Information Science and Earth Observation of the University of Twente in partial fulfilment of the requirements for the degree of Master of Science in Geo-information Science and Earth Observation.
Specialization: Water Resources and Environmental Management

SUPERVISORS:

Dr., Ir. M.W., Lubczynski
MSc., Ir. G.N., Parodi
ADVISOR:
MSc., Enrico Balugani (Ph D candidate)

THESIS ASSESSMENT BOARD:
Prof., Dr. Z., Su (Chair)
Prof., Dr. Okke Batelaan (External Examiner, Brussel University - Dept. of Hydrology and Hydraulic Engineering)

ABSTRACT

Spatial and temporal variation of dry season subsurface water fluxes in granitic La Mata catchment in Spain, ~5km^2 has been assessed using a coupled HYDRUS-MODFLOW model. The data sources used were from field measurements, remote sensing, laboratory analysis of soil samples, meteorological measurements and groundwater level monitoring, recession curve analysis, slug and pumping tests and geophysical measurements.

This study is mainly aimed to obtain dry season quantities of different subsurface fluxes such as water that leaves aquifer vertically upward i.e bottom flux (BF), evaporation from groundwater (Eg), change in the storage of unsaturated zone (Eu if negative), transpiration from groundwater (Tg), transpiration from unsaturated zone (Tu) and out flow in the catchment through drains. The study was carried out comparing dry season fluxes of September 2009 and September 2010. The vadose zone flow complexity was analyzed through unsaturated zone model HYDRUS 1D, transpiration using sap flow measurements partitioned aplying isotope tracing and transient groundwater modelling with MODFLOW for spatio-temporal groundwater balance.

The calibration of the coupled HYDRUS MODFLOW model resulted in maps showing spatial and temporal variability of the subsurface fluxes in the catchment. All the subsurface fluxes showed a tendency of decline from the beginning to the end of September 2009 and 2010.

In September 2009 the average BF for the entire catchment decreased from 0.984 mmd^{-1} to 0.889 mmd^{-1}, Eg decreased from 0.064 mmd^{-1} to 1.914 mmd^{-1}, no evaporation from unsaturated zone (Eu) throughout the month, Tg decreased from 0.13 mmd-1 to 0.06 mmd-1, Tu from 0.092 mmd^{-1} to 0.078 mmd^{-1}, and out flow to Sardon River coinciding with the fault zone from 31.5 m3d^{-1} to 0.00m3d^{-1}in 2009.

In September 2010 the average BF decreased from 1.46 mmd^{-1} to 1.118 mmd^{-1}, Eg from 1.703 mmd^{-1} to 0.069 mmd^{-1}, no evaporation from unsaturated zone (Eu) throughout the month, Tg decreased from 0.109 mmd^{-1} to 0.084 mmd^{-1} and Tu from 0.15mmd^{-1} to 0.12 mmd^{-1} and groundwater out flow to Sardon River coinciding with the fault zone from 0.085 m3d^{-1} to 0.064 m3d^{-1}.

The total amount of water that leaves the catchment because of all the subsurface fluxes is 0.302 mmd^{-1} in September 2009 and 0.311 mmd^{-1} in September 2010, which is significant as compared to the annual mean value of precipitation (about 500 mmy^{-1}) or estimated recharge (about 10-100 mmy^{-1}).

ACKNOWLEDGEMENTS

Great thanks to the everlasting almighty God who created me and always with me during all my activities and such successes. It is my great pleasure to express my sincere gratitude to the Netherlands Government through the Netherlands Fellowship Program (NFP) for providing me the scholarship from which I gained a lot most of all the knowledge. I am grateful to my employer, the Oromia Water Resources Bureau for granting me leave to undertake the studies and for all the help they have delivered so far.

Beyond words, I have plenty of thanks for my supervisors Dr. Ir. M.W. Lubczynski and MSc, Ir.G.N. Parodi and advisor MSc,Enrico Balugani (PhD Candidate) for enabling me carry out the task through guidance, suggestions, scientific comments during the field work, throughout the course and the research work.

I would like to thank especially Msc Alain F. Pascal and also MSc. Leonardo Reyes Acosta for their suggestions, guidance and all their roles in my research beginning from the field work.

I have to thank also my field work team mates Yesrib Bahiru Shifa, Cisneros Vaca (Cesar Ramiro), Mutasa (Collen) for the time we spent together in Salamanca Spain and also in the cluster.

I am grateful for all ITC staffs especially for Water Resources Department staffs particularly to our program director A.V.Lieshout for his support and care during the course and his beneficial comments on research proposal and midterm presentations.

Thanks to Prof..Dr. Z. (Bob) Su, Dr. A.S.M. (Ambro), Dr. ir. (Christiaan) van der Tol and Dr.Ir. C.M.M. (Chris) Mannaertse for their encouraging words, ideas, suggestions and comments during research progress and proposal presentations.

I reserve much gratitude to Dr. J. B. Boudewijn de Smeth for his assistance during the tedious laboratory works, his valuable comments on the laboratory results and his trial to ease my work (writing the thesis using single hand) due to my minor disability.

My special thanks to all my friends, especially the Ethiopian students community in ITC, my colleagues and classmates (all WREM_2009 students) and ITC student community for all the good and rough times we shared and for their moral and physical support.

Thanks also to my colleague Asrat Dewo who maintained the connection between me and my Bureau and the country by updating me with all the information during the whole period of my study.

Last but not least, my heartfelt appreciation goes to my lovely wife Shola, my daughters Wangary and Nayady and the whole family for their incessant support, especially Alemayehu Beyene who have been forwarding me up-to-date information at home during the whole period of my stay in the Netherlands.

Gezahegn

TABLE OF CONTENTS

LIST OF FIGURES

LIST OF TABLES

ABREVIATIONS AND DEFINITIONS

BF: Bottom flux, is the rate (L/T) at which water leaves the top of groundwater table either due to evaporation or capillary rise.

DEM:Digital elevation model

ET: Evapotranspiration

ET0: Reference evapotranspiration

Eu: Evaporation from unsaturated zone: Water that leaves and contributed by unsaturated zone to the atmosphere

E: Evaporation: Water the leaves the soil to the atmosphere

Eg: Evaporation from groundwater: Water that leaves saturated zone to the atmosphere

FAO:World Food Organization

G: Soil heat flux

GPS: The Global Positioning System (a space-based global navigation satellite system that provides reliable location and time information in all weather)

HYDRUS: Windows-based modelling environment for analysis of water flow and solute transport in variably saturated porous media

K: Hydraulic conductivity

LAI: Leaf Area Index

LW: Long wave radiation

MRC : Master recession curve

MODFLOW: Modular 3D finite-difference ground-water flow model

NTG : Natural thermal gradient

PT: Potential transpiration

REC: Recharge

RF: Rainfall

Rn/Rnl: Net radiation/Net long wave radiation

ROSETTA: A computer program for estimating soil hydraulic parameters with hierarchical pedotransfer function

SM: Soil moisture

SPAW:Soil Plant - Atmosphere – Water Field & Pond Hydrology

SW: Shortwave radiation

T: Transpiration

TDP: Thermal dissipation probes

TF: Top flux, evaporation from soil (the rate (L/T) at which water leaves soil to the atmosphere)

Tt: Transpiration of tree

U: Wind speed

GWL: Groundwater Level/Water Level

WUT: Water up take

Q.P: *Quercus Pyrenaica*

Q.I: *Quercus Ilex*

1. Introduction

1.1. Background

The demand of fresh water all over the world is increasing every year. The main causes for this increment are population growth, increase of water use, increase of water demand by industry and agriculture (Twarakavi et al.2008). On the other hand, depletion because of over exploitation and or due to reduction in recharge and the threatening of this fresh water by contamination especially due expansion of industry to the developing world in addition to local human contamination is intensifying (Earth, 2010).

More than 98% of the available fresh water is groundwater which by far exceeds the volume of surface water (Fetter, 2001). Nearly one third of all humanity relies almost exclusively on groundwater (Earth, 2010). However, the rise in demand is causing this resource to be depleted and abstracted in ways which compromise freshwater ecosystem health (Smakhtin, 2008). Of course, groundwater is advantageous in its being relatively less susceptible to both climate change and contamination compared to surface water bodies(Kumar & Shah, 2010). Therefore, groundwater systems are vital to both society and the environment, supporting food production and many other ecosystem services. Sustainable management of this vital resource for future generations requires a sound understanding of how groundwater might respond to the inevitable changes in future climate (Makoto & lan, 2010), land cover or abstraction.

Research on the coupling of unsaturated zone and saturated zone is experiencing a recent expansion driven by ecological water requirements, climate change, and the need for better quantified water budgets(Twarakavi et al.2008). A number of robust computer models are now available for addressing questions about the hydrologic connection between the vadose zone, surface water and groundwater. In addition, as also mentioned by Twarakavi, new measurement techniques, such as distributed fiber optic temperature monitoring, are being developed and tested to obtain data to constrain these models. Similarly this study is concerned with quantification and partitioning of subsurface fluxes of La Mata catchment in Spain for the period of 1 to 30 September 2009 and 2010 using a coupled model (HYDRUS-MODFLOW), HYDRUS 1D and isotope tracing method for transpiration.

Therefore this research aimed at contributing to the knowledge on subsurface water regime of La Mata catchment through numerical modelling by coupling unsaturated zone model with saturated zone model so as to quantify the subsurface water fluxes during the dry season. September is selected because of its being the last dry month as shown on Figure 1 where the impact of the preceding months is expected to exist. The years 2009 and 2010 have relatively different weather condition as it was referred from About.com Spain travel (2010) and also observed from the daily waether records of the catchment from monitoring network station installed by ITC. The main fluxes during this time are flow through drainage, evaporation and transpiration that are from both unsaturated and saturated zones of the catchment. This result can be used as a reference for groundwater management of the catchment under consideration.

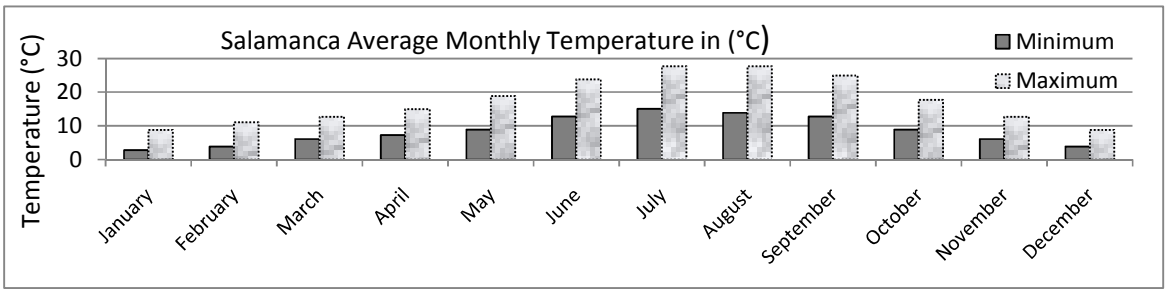

Figure 1. Salamanca Average Monthly Temperature, Source: (About.com Spain Travel, 2010)

1.2. Research Problem

The hydrological cycle in arid and semi-arid climates is highly controlled by the subsurface fluxes such as evaporation and transpiration. Their effect is not limited only to water in the unsaturated zone but also to groundwater. The correct quantification of these fluxes is therefore essential for improving the water balance, the resource management and evaluation (Johnson et al., 2010). This research aimed to accurately quantify the spatially and temporally variable dry season discharging fluxes by coupling unsaturated and saturated zone models and using HYDRUS 1D and isotope tracing for partitioning of the fluxes in a nearly 4.5km^2 wide catchment of La Mata.

1.3. Research Questions

1.3.1. General Research Question

What is the role and quantities of the subsurface fluxes in water budget of the La Mata catchment?

1.3.2. Specific Research Question

- How can coupling of the unsaturated and saturated zone models be established for the catchment?
- What is the spatial and temporal distribution of the subsurface fluxes in the study area?
- What are the groundwater recession characteristics of the La Mata catchment?
- To which main hydraulic parameters the model is most sensitive?

1.4. Research Objectives

1.4.1. General objective

To reliably model the La Mata Catchment subsurface discharge fluxes using the coupled model.

1.4.2. Specific objectives

1. To setup and calibrate the coupled models to simulate subsurface discharging fluxes in dry seasons of 2009 and 2010 for the catchment.
2. To partition subsurface fluxes (in to unsaturated & saturated) and find spatial & temporal variations of the partitioned subsurface fluxes during the study period in the catchment.
3. To analyse groundwater recession characteristics of the catchment.
4. To test the sensitivity of the model to main input hydraulic parameters.
5. To compare model simulated water levels with that of piezometric measurements.
6. To compare model outputs (the fluxes) with outputs obtained by other methods

1.5. Assumptions

- Total evaporation (E)≈ the sum of evaporation from unsaturated zone (Eu) & saturated zone (Eg)
- Recharge is zero during the dry season.
- Water that leaves groundwater as a vapour is neglected
- Tree transpiration is related with ground projection of canopy area (CA limits the tree transpiration).

1.6. Hypothesis

- The contribution from groundwater to total evaporation increases with time during dry season in semi-arid area (Yang et al.,2000) at expense of Eu.

1.7. Relevance

Quantitative estimate of subsurface discharge fluxes in arid and semi-arid climatic regions are of primary importance for constraining catchment scale numerical model of groundwater flow system. In addition the

study area has shallow groundwater depth and coarse textured dominated soil cover where the evaporation and transpiration from groundwater is expected to play an important role in the water cycle of the catchment (Menking, et al., 2000). By quantifying the fluxes water resource of the catchment will be evaluated by this study and its output can be used for water resource management of the catchment.

Therefore modelling of these discharge fluxes is essential for subsurface resource evaluation of the area. The existence of dense hydrologic data and massive basement below the top alluvium and fractured rock makes the catchment an ideal site to apply such models that are data demanding but efficient to describe the fluxes (Twarakavi, Simunek, & Seo, 2008). As a result the output of such studies can be used for groundwater management plans that require accurate quantities of water budget components.

Since accurate estimate of transpiration from both unsaturated and saturated zones by trees in the catchment was done by the last year MSc student, Agbakpe (2010) using sap flow measurement, the result including the data from the campaign of September 2009 was used for this study (as an input or for comparison). The major subsurface fluxes, especially evaporation from saturated and unsaturated zones and the spatial distribution of the fluxes is accurately estimated only by this study using sap flow measurement, unsaturated zone (HYDRUS 1D) Model and saturated zone 3D (MODFLOW) model.

According to the study by Twarakavi et al (2008), the one-dimensional unsaturated flow package HYDRUS, recently developed for the groundwater model MODFLOW, was evaluated and compared with other contemporary modelling approaches used to characterize vadose zone effects in groundwater models and concluded that the HDRUS package for MODFLOW demonstrated a significant improvement in modelling accuracy for large scale problems. Hence coupling unsaturated and saturated zone using this package is found suitable for modelling the subsurface discharge fluxes of the study area.

"Pikul et al. (1974) and Niswonger et al. (2006) noted that the coupling approach probably provides the most efficient solution for groundwater flow models, especially for large-scale applications" (Twarakavi, et al., 2008). The catchment under consideration is also favourable as it is only about 5km2; a well-equipped monitoring station, eddy covariance tower, rain gauge station, flume measurements, different data loggers and many previous works related to groundwater modelling exist for such data demanding model.

1.8. Study Area and Literature Review

1.8.1. Description of the Study Area

Sardon is an intermittent stream with a catchment area of 80km^2 that discharges to a perennial river, Rio-Tormes found in Salamanca Province, central-western Spain as shown on Figure 2. La Mata stream is a tributary of Sardon stream with a catchment of an elongated shape South East to North West and areal coverage of about 4.5km^2 and it is close to an out let of Sardon stream. The centre of the study area (La Mata Catchment) lies on UTM coordinate of 738900W longitude and 4553700N latitude (ED 1950 datum, Zone 29).

In the study area there exist a meteorological station, monitoring network station and Eddy tower that are found in north western part of the study area and can be accessed by a feeder road of 4km from the Ledesma highway.

Several ITC MSc research for more than a decade and PhD research since few years ago have been done concerning Sardon catchment. The studies dealt with modelling, groundwater assessment, groundwater resource evaluation, geological, hydrological, evapotranspiration, tree transpiration, hydro geophysical characteristics and etc. Among those researches pertaining to groundwater flow modelling of Sardon area Shakya (2001), Lubczynski & Gurwin (2005) and (Ermias, 2010) established the fully transient modelling of Sardon area by integrating GIS & Remote sensing for the input parameters calculation, while the emphasis of Ruwan Rajapakse (2009), Uria cornejo (2000) was on modelling of recharge and solute transport.

Studies like that of Lubczynski & Gurwin (2005) which deals with integration of various data sources for transient groundwater modelling with spatio-temporally variable fluxes is among the published ones.

The catchment of Sardon is characterized by an asymmetric development, with area west of the river having more gentle topography and longer drainage. The better development of soil and more cultivated land at this side indicates the existence of more weathering. Immediately east of the main Sardon river, where La Mata is found, several areas fall in the 'undulating' and 'rolling' classes (Shakya, 2001). The low lying areas of La Mata mostly along the river channel have slopes in the range of 16-33% whilst the high altitudes around the catchment boundary are almost flat.

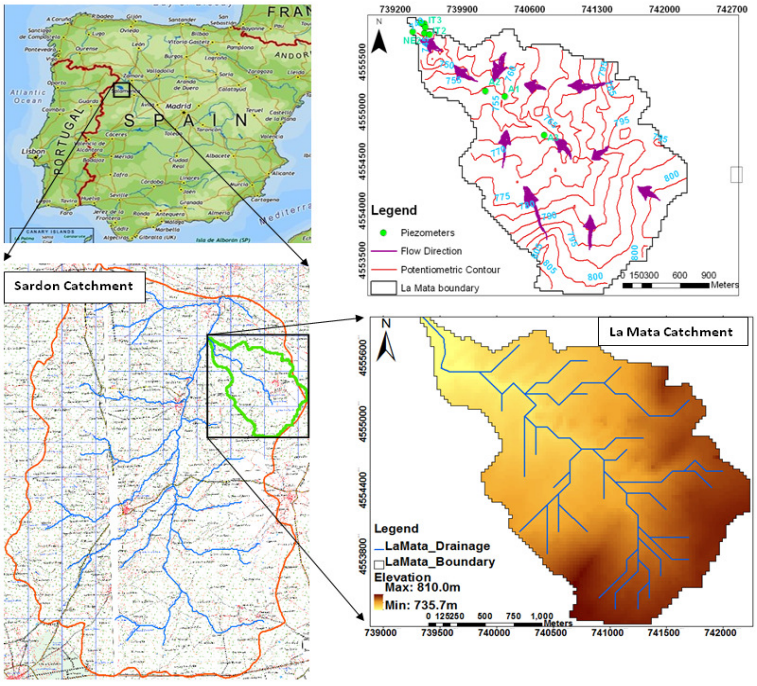

Figure 2. Location map of the study area and groundwater flow over Potentiometric Surface Contour

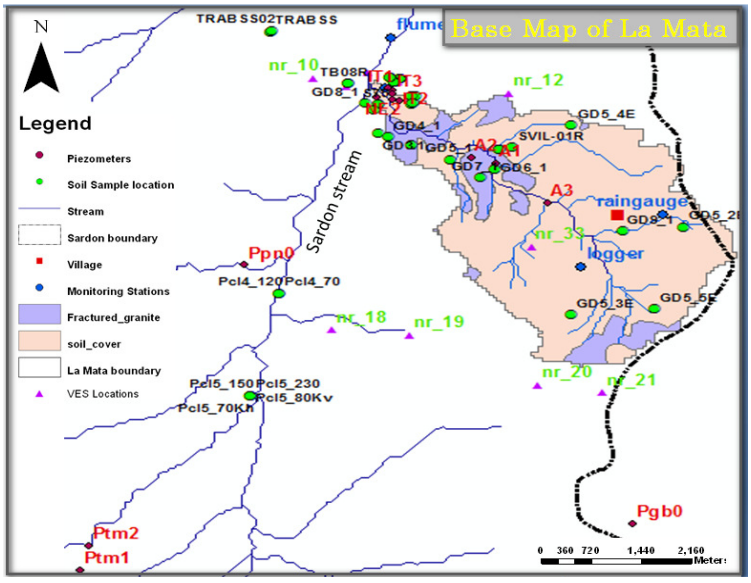

Figure 3. Base Map of La Mata Catchment

According to the previous studies and also from field observation three layers were identified in the study area (Figure 4). These are (1). the upper thin (5-10m) unconsolidated layer, (2). fractured granite layer with intercalation of granodiorites, schist & gneisses and (3) massive quartzites (Attanayake, 1999) and (Tesfai,

2000). As it can be observed from Geologic map of Sardon by Attanayake (1999), Granodiorites, strongly foliated granite and Lecuogranite formed the La Mata area (Figure 3).

The land cover of La Mata is characterized by natural vegetations like woody shrubs, deciduous *Quercus pyrenaica* and evergreen *Quercus ilex*, Escobar shrub and short grass (Figure 17-top right). Among these natural vegetations the dominant ones in the study area are the *Quercus pyrenaica* which covers 12% and *Quercus ilex* tree species that cover 19% of the study area, according Agbakpe (2010). The remaining part of the study area are covered by bushes, grass and mixed bush with trees.

The area is used mainly for pasture because the soils contain large proportion of weathered granite, which make them generally unsuitable for agriculture (Lubczynski & Gurwin, 2005)

The study area has an elevation of 736-810m above mean sea level (Figure 2-bottom right) with semi-arid climate which is typical for the central part of the Iberian Peninsula. The region has two rainfall periods. These are April to June and November to February. The mean annual rainfall is about 500mm/yr while the temperature and potential evapotranspiration ranges from ~5^{o}c to ~22^{o}c and ~0.5mm/d to ~5mm/d respectively (Lubczynski & Gurwin, 2005)

The drainage network of La Mata is dense as compared to its width and is largely influenced by La Mata. Runoff processes are low in this area which is typical for semi-arid hard rock catchments. These entire factors together with the thin and low retention capacity upper unconsolidated layer caused the area to have high and rapid subsurface runoff. La Mata is situated in this part of the catchment with land surface slope that ranges from 0 to 33%. Among the studies mentioned above, only one is limited to the study area, estimating tree groundwater transpiration of La Mata catchment by Agbakpe (2010)

Hydrogeology of the catchment is largely influenced by the granitic composition, weathering and fracturing processes in the area (Lubczynski & Gurwin, 2005). Hydrostratigraphic succession of the study area is characterized by alluvial deposit & weathered granite at the top, the second layer is fractured granite followed by massive granite with gneiss inclusions at the bottom. The depth to water table in the area ranges 0-3m in the valleys and up to 4m at upper part of the catchment area. The groundwater flow regime is towards the North following the major Sardon fault (Shakya, 2001) at regional level while towards the fault (North West) at La Mata level as it can be deduced from the drainage pattern of this sub catchment.

1.8.2. Sap flow, Transpiration and its Partitioning

Oak (genus name *Quercus*) is a dominant natural vegetation in the form either tree or a shrub in the study area. They are further subdivided in to evergreen *Quercus ilex (Q. ilex)* and the deciduous *Quercus pyrenaica (Q. P.)* locally named "encina" and "roble" respectively (Rwasoka, 2010)

Q. ilex is typical Mediterranean vegetation and grows to a height of about 20-27m, although only about 6m (average) in the study area. This tree has an ability to harvest water from atmospheric, shallow and deep subsurface moisture with water up take mechanism called hydraulic lift (David, et al., 2007).

Q. pyrenaica is also typical vegetation to Iberian Peninsula and grows to a height of up to 25m, although only about 6 m (average) in the study area Agbakpe (2010). This tree has osmotic adjustment capacity to face drought stresses a deep tap root that develops several horizontal roots, mainly in the shallow subsurface conditions like in the study area. The estimated bark radius of *Q.I.* is 1cm & 1.5cm for *Q.P.* Agbakpe (2010)

These trees maintain transpiration rates above 0.7 mm day−1 during the summer drought. By that time, more than 70% of the transpired water was being taken from groundwater sources (David, et al., 2007). The transpiration rate have been estimating by many scientists using sap flow measurement, which is a measurement made using temperature difference created due to the flow of water through xylem of a tree.

Sap flow is a biological term that describes water passing through conductive xylem of tree stems or branches. It is commonly expressed in unit volume per unit of stem circumference that is rescaled to a whole tree if needed. Once related to specific area (i.e., stem segment, conductive part of stem or entire cross-sectional area of tree stem or branch) it is called sap flux (water flux quantity per unit area) instead. In this document, the term sap flow always describes the volume of ascending sap.

Transpiration rate of a tree is assumed to be related to its biometric dimensions. According to the study of Agbakpe (2010) *Quercus pyrenaica* has an average breast height stem diameter of 28m and sapwood depth of

5.3 cm. The majority of sap flow is concentrated within the first 0-3.5cm of the stem and decreases towards heartwood, not linearly but exponentially according to Kosner et al. (1998).

Based on sap flow data processing steps after Lu et al. (2004) the equations used for conversion of temperature difference in to transpiration rate are the following.

$K = \frac{\Delta Tm - \Delta T}{\Delta T}$ ----------Equation 1 $v = 0.000119 * K^{1.231}$----------Equation 2

Qs=Jv*Ax, where Jv=v*3600----------Equation 3 TPA=Qs/CA----------Equation 4

Where K is sap flow index, v is sap velocity, Jv is hourly sap flux density, Qs is sap flow (equivalent to tree transpiration, Tt in cm^3/h), ΔTm is maximum temperature diff. (that occurs usually at night where sap flow is low or nil), ΔT is measured temperature difference, Ax is xylem or sapwood area (in cm^2), TPA transpiration per unit area, CA canopy area.

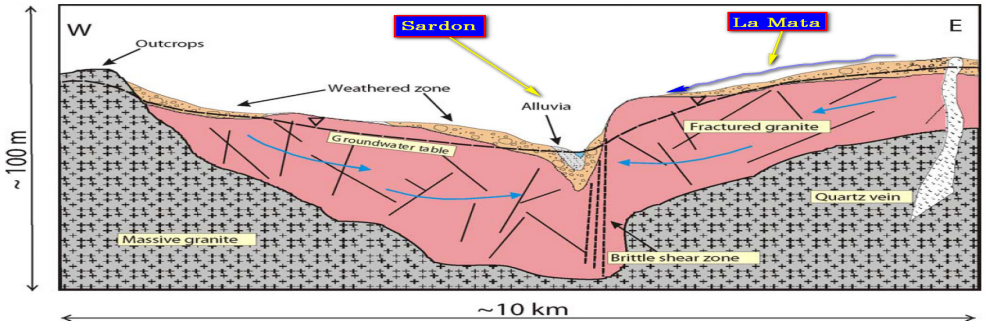

Figure 4. Schematic Cross Section Across Sardon Catchment (Source:(Tesfai, 2000))

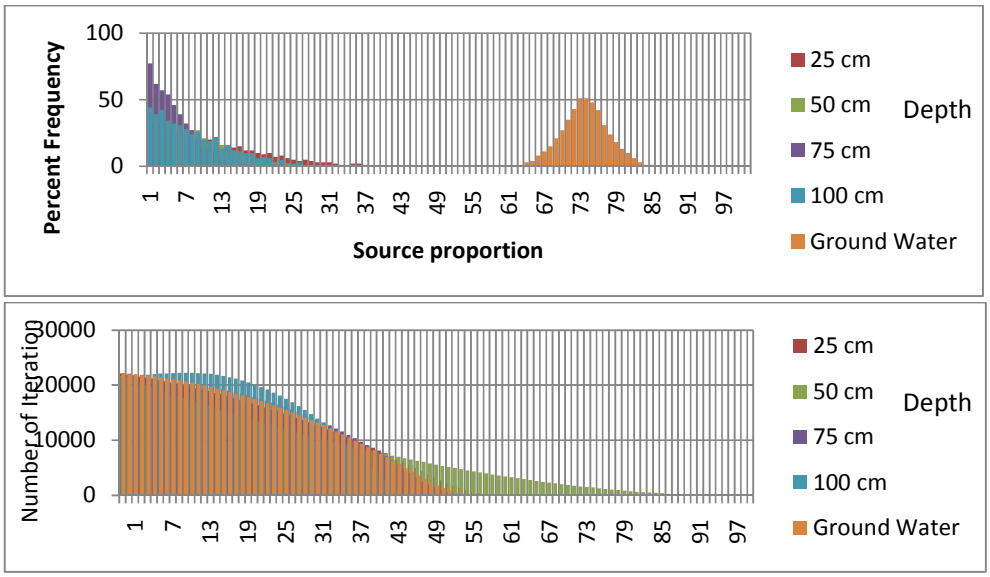

Figure 5. Proportion of transpiration per depth (A) *Q.Ilex* and (B) *Q. Pyrenaica* from Reyes-Acosta (2010)

According to a study of Reyes-Acosta & Lubczynski (2011) on the partitioning of transpiration depths of the two species in the study area as presented in Figure 5, it was observed that *Q.p.* transpires about 40% from groundwater while *Q. i.* is about 72% during 12:00 to 18:00 hrs of the day and 40% during the remaining time. The first graph shows a probabilistic measurement of the frequency of different mixes in certain number of iterations (25000) the most probable (>70% of the iterations, pooling the bars with the higher frequency) source was groundwater with a percentage range between 70&-75%. All the other sources show the higher probability at much lower percentages. On the second graph the % from groundwater, has the highest probability in a range between 1- 20%, together with all the other sources also contributing.

2. Materials and Method

2.1. General

Both ground based and remote sensing data were collected for preprocessing or to use as direct inputs to the models. The data required for the characterization of the unsaturated zone are obtained mainly from field-work, monitoring network, eddy covariance tower and laboratory analysis. Some of the data used for preprocessing like data related to hydrostratigraphic layer determination are obtained from previous works or reports. The main data sources & their location are shown on table 1 and the base map of La Mata catchment figure 3 respectively. The weather data are Temperature, Wind speed, Net Radiation, Short wave radiation, Long wave radiation, Soil moisture, Water levels, well reports, & Matrix potential.

Table 1. Available Data and their Sources

	Data/Material	Source & Cost	Remark
1	DEM	Web, ITC Archive	5m resolution
2	Topographic map	ITC Archive	
3	Soil hydraulic parameters	Field & Laboratory	
4	GPS	ITC Archive	
5	Geologic map & or Soil map	ITC Archive	
6	**Quickbird image	ITC Archive	2.4m resolution at nadir
7	Vegetation map	ITC Archive	
8	Geophysical data/map	ITC Archive	
9	Thickness of weathered & fractured layer	ITC Archive + field	Geophysical & geological report
10	Piezometr locations	Using GPS	
11	Transpiration rate of Tree species	Field + ITC Archive	
12	**Weather data	Monitoring station	
13	Feddes's and Some Soil Parameters	Literature, Software	

2.2. Data Sources

There has been rapid improvement in development of sophisticated numerical codes like the coupling used for this study are able to address wide range of water related problems very efficiently, provided that the appropriate data is available (Lubczynski & Gurwin, 2005). Since care must be taken for the input data, much effort is made to get reliable data. Some of the data obtained for this research cannot be used directly as an input and some others may have gaps either spatial or temporal or some have scale problems. So in this case pre-processing works such as: Recession Curve technique, correlation, interpolation extrapolation, up scaling or downscaling and etc. are used to fulfil missed data of water levels, variables that do not fit the scale of the study and to obtain some aquifer hydraulic parameters; conversion of infiltration result or data measured using permeameter to saturated hydraulic conductivity; conversion of wind speed values measured at 10m in to 2m; calculation of ETo from monitoring and eddy covariance station data, conversion of temperature difference to sap flow or transpiration and etc. are done.

2.2.1. Remote Sensing

For this research the Quickbird and Landsat remote sensing observation data sets are used to map the vegetation cover, soil cover and to improve the already studied (but at smaller scale) distribution of fractures in the study area. These data are used for aquifer geometry, ETo estimation and partitioning of transpiration.

2.2.2. Field Measurement

Some of the data for this study were and also must be directly collected from in situ measurement of the variables such as soil profiles dimension, spatial variation of soil textures & types, infiltration capacity or hydraulic conductivity of soils as shown on figure 6. Sampling is another task during filed-work. It is necessary to take representative soils samples for further analysis at laboratory, because some properties of soils like accurate texture analysis cannot be determined on the field. Soil type and their lateral and vertical variation are observed on the field by auguring and also from samples of machine based drilling that was conducted during the field work.

Field observation also helped to have clear idea on boundary conditions, to take measurements of stream that are used as an input for the model, observing the real situation of the study area for ease classification of the land cover and conceptualize the model. Recording GPS locations of some ground references, piezometers, out crops and etc were also essential for the classification, zoning for the unsaturated model and also for calibration of the model.

Sap flow of three representative trees from each species was also measured to calculate the amount of water that is taken from groundwater by trees.

Figure 6. Auguring for soil sampling and study of water table depth (left) and infiltration test to estimate in situ vertical saturated hydraulic conductivity of the soil (right)

Sampling

Soil samples are collected as shown on Figure 6, from several places to derive their hydraulic parameters and to accurately identify their textural classes in laboratory. At the same time depth to groundwater was also studied through hand auguring to a depth of up to 3m where possible. The auguring is always followed by sampling using both sampler and sample bags. Samples from the sampler are used to derive soil hydraulic parameters such as saturated hydraulic conductivity, residual soil moisture content and saturated soil moisture content in laboratory. Similarly samples collected in sample bags are also used to retrieve soil hydraulic parameters using soft wares like SPAW and Rossetta in addition to soil texture analysis. These values are used as an input for unsaturated zone model, HYDRUS.

Samples from soil outcrops (Figure 23) from four places in the catchment were also taken; especially in the valleys soil profile having a thickness of up to 3 m were observed. The samples were taken from different depths of such profiles and used to determine (in laboratory) type of material and corresponding hydraulic properties which was used as an input for the model.

To locate relevant places for representative soil sampling previous studies concerning soil classes was first reviewed. Reconnaissance survey of the soils in the catchment was done to observe the real properties of the soils on the field. According to the observation the soil thickness and soil profile of the catchment found varying with change of the slope. It is thick at plain areas especially valleys and thin at sloppy areas. Based on this variation laterally and vertically representative samples were taken from twelve spots (Figure 3) by auguring and from four places found as an out crop (exposed soil profiles).

Measuring In Situ Soil Hydraulic Parameters

Some hydraulic property of the sample soils like infiltration capacity and or saturated hydraulic conductivity were analyzed in the field using double ring method as shown in Figure 6 (right). The rate of infiltration is determined as the amount of water per surface area and time unit that penetrates the soil. This rate was calculated on the basis of the measuring results and the Law of Darcy.

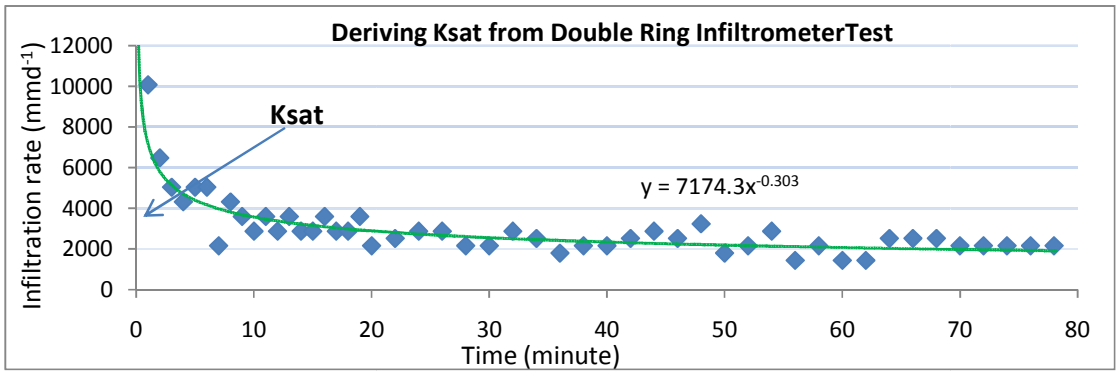

Figure 7. A plot of infiltration rate using double ring method about 500m up stream of junction of La Mata and Sardon

Figure 8. While conducting texture analysis (left) and hydraulic conductivity test (right) in laboratory

Figure 9. Installation of sap flow measurement (left) and arrangement of TDP in a tree (right), source (Mapanda 2003)

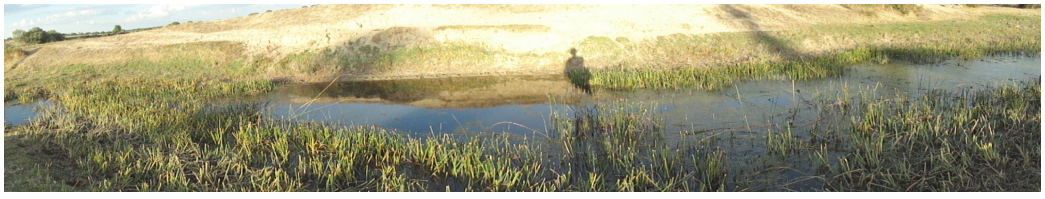

Figure 10. Sardon Stream (in September), boundary of the catchment at its out let (assigned drain boundary condition)

From the standard set of the double ring infiltrometer sets of stainless steel rings the one with 53cm and 28 cm outer and inner diameter was used for infiltration test. Several measurements were taken simultaneously at a place so as to obtain the mean result. As vertically infiltrated water runs away to the sides, the outer ring of the infiltrometer serves as a separation. The measurements exclusively take place in the inner ring through which the water runs virtually vertical.

The infiltration rates were plotted versus time as shown in figure 7 to identify saturated hydraulic conductivity of the top soil, which is used as an input for HYDRUS. Saturated hydraulic conductivity is the infiltration rate that can be read from the y-axis where the graph is flattened. It can also be calculated by inserting the time at which last measurement is taken (where saturation becomes almost constant) in to the equation of the graph drawn.

Sap Flow and Biometric Measurements of Trees

Three cluster and representative trees from *Q.Ilex* and *Q.Pyrenaica* were selected and sap flow of these trees were measured to calculate transpiration in September 2010 as shown on Figure 9. The biometric measurement is attached to this document (Appendix D). A record of previous study Leonardo Reyes (2010) was used to calculate Tg and Tu in September 2009. Daily average values of sap flow of each species are finally used to calculate the corresponding daily transpiration rates of the trees which at the end partitioned in to unsaturated and saturated zone transpiration based on the study of Leonardo Reyes (2010) (Figure 5). The partitioned transpiration rates are finally used to create maps and also as an input to the models. Sap flow Tg estimate is preferred, because it is more reliable than using model estimation as it is the direct measurement of water that flows through xylem of a tree. The conversion of sap flow to transpiration is done by dividing the total volume of water that flows up through tree xylem to the canopy area of the tree. The procedure is explained in detail on the literature review section of this document and biometric measurement is annexed.

In order to upscale transpiration from tree to canopy, the biometric up scaling functions obtained from study of Agbakpe (2010) was used. The data was corrected for NTG (natural temperature gradient) using an hourly record of NTG at monitoring network station. For the details of sap flow study of La Mata area, MSc theses of Agbakpe (2010) and Rwasoka (2010) can be referred since detailed description of the process is beyond the scope of this thesis.

Boundary Condition Observation

It was observed that the granitic rocks around the water divides are less fractured and found at shallower depth as compared to the central part of the catchment which can be considered a no flow boundary for the catchment. Both Sardon and La Mata (around its junction with Sardon) act as a drain as it was observed on the field. Both streams have water in their valleys at this location which is collected there by being drained from the top aquifer of the catchment as shown in Figure 10.

2.2.3. Monitoring Network and Eddy Tower Station

There are automatically recording monitoring network station called Trabadillo and Eddy tower station, at downstream end or western side of the catchment. The existence of the stations in such a small catchment makes the data representation more reliable. The station is equipped with different sensors having different channels that record data in the user defined/adjusted interval, in this case between 10 minutes to one hour. Some of the data that are recorded by this station include rainfall, air temperature, wind speed, solar radiation, soil temperature, humidity, groundwater level, matrix potential and soil moisture. Most of these data were used to calculate input parameters of the models like water levels or hydraulic heads, reference evapotranspiration rates, correction of sap flow measurement for natural thermal gradient (NTG), creation of Master recession curves and etc.

2.2.4. Laboratory Analysis

The soil texture analysis of the collected samples was done in laboratory using pipette method to determine the proportion by weight of sand, silt and clay of each sample. Constant head and falling head methods were

used for hydraulic conductivities, WP4 method for determination of residual moisture content. Totally the parameters such as saturated and unsaturated hydraulic conductivities of soils, specific yield, residual moisture content, saturated soil moisture content, storage coefficient of the soils and constants or coefficients were determined using these laboratory analyses. Most of these parameters are direct inputs of the unsaturated model, so the accurate measurement of the parameters are necessary for better results and much effort was needed in order to get accurate parameters.

2.2.5. Literatures and Software

Data such as geological map, soil map, land cover map, geophysical surveying results, published and unpublished previous studies on the study area by the previous MSc and PhD students were used for accomplishment of this work. For instance a study of (2000), (Abubeker, 2010), (Agbakpe, 2010), (Salinas, 2010) and unpublished study of the PhD candidate Leonardo Reyes Acosta(2010) are used to study lineament distribution, geophysical condition, equations concerning tree transpiration rate of the two dominant species in the area and its partitioning in to Tg and Tu respectively.
Suggested values of Feddes's parameters for the water stress response function of the *Q.I* and *Q.P.* and pore connectivity parameters of soils were referred from the data base of HYDRUS 1D. Parameters like the inverse of air entry value (α), pore connectivity parameter (L) and pore size distribution index (N) are determined using softwares such as HYDRUS 1D, SPAW and ROSSETTA (laboratory result as an input).

2.3. Model, Software and Package Selection

To achieve the objectives of this research the first step was a choice of appropriate software. Based on:

- Software availability, taking its quality (applicability) and cost in to account
- Non complexity of the software or its being user friendly
- Memory and time it needs to run or to simulate and
- Availability of the Inputs of the model or software and its capability to partition the subsurface fluxes

Table 2. Comparison of the Recharge–Evapotranspiration (REC-ET), Unsaturated Zone Flow (UZF1), and Variably Saturated Flow (VSF) packages for MODFLOW. Source: (Twarakavi, et al., 2008)

Characteristic	REC-ET	UZF1	VSF	HYDRUS
Descript on of vadose zone processes	Water balance at the land surfce	one-dimensional kinematic wave equation	3D Richards equation	One dimensional Richards equation
Characterization of vadose zone flow processes	poor	better	best	better than UZF1, not as good as VSF
Vadose zone flow modelling capabilities	REC and ET only	ET, root water uptake, and infiltration	ET, root water uptake, ponding & infiltration	many capabilities as available in HYDRUS-1D
Applicability across larger spatial domains	yes	yes	difficult due to computational effort	yes
Computational effort	low	moderate	very high	moderate
Range of groundwater modelling scenarios	large†	large†	large†	large†
Applicability to arid and semiarid areas	not very applicable; needs extensive calibration	very applicable for deep water tables, less applicable for shallow water tables where capillary rise is significant process	highly applicable	highly applicable

† Since it is based on MODFLOW

For evaluation of hydrologic process like modeling under consideration, water flow through the vadose zone should be appropriately taken into account. However, due to the complex and computationally demanding modeling of vadose zone flow processes is often handicapped as mentioned by Scanlon et al., by the lack of data necessary to characterize the hydraulic properties of the subsurface environment. Consequently, it is rarely been properly represented in hydrologic models. (Scanlon et al.,2003).
A more promising approach to properly represent vadose zone flow processes in groundwater models involves coupling groundwater and vadose zone models. The HYDRUS Package for MODFLOW-2000 (Harbaugh et al.,2000) was developed to consider the effects of infiltration, soil moisture storage, evaporation, plant water uptake, precipitation, and water accumulation at the ground (Fig 11 & 12)
Among the available packages for MODFLOW, HYDRUS is preferred for this study for different reasons summarized in the Table 2 and especially its capability to compute capillary rise and recharge at water table level (Twarakavi, et al., 2008). The author analyzed the performance of the HYDRUS package for various case studies that involve different spatial and temporal scales. As it can be observed from this summary the model is helpful to achieve the aim of this research (estimating partitioned subsurface fluxes).
As a result coupled HYDRUS-MODFLOW is preferred for the modeling of the subsurface fluxes of the catchment and Arc GIS, ILWIS and Excel are used for geographic information system processes, HYDRUS 1D for partitioning evaporation & stable isotope method for partitioning transpiration.

2.4. Model Solution

2.4.1. Introduction

After the selection of appropriate model, software and package, data that are required as inputs are identified and those which require preprocesses are processed. The modeling was started with data collection, followed by data preprocessing, setting up the model, extracting out puts of the model, post processing, analysis of the result and finally concluded based on the result as shown in detail on the flow chart of figure 11 and schematic representation of the modeling (Figure 12).

2.4.2. Conceptual Model Design

To simplify the field problem and organize the associated data so that the system can be analysed the conceptual model was built based on the field observation and data gathered concerning the catchment. Based on the obtained information the conceptual model was made closer to the field situation as much as possible. So natural hydro geological boundaries were identified, hydrostratigraphic units were defined , water budget was prepared and flow system was defined (Anderson & Woessner, 1972).
The catchment has three main layers. The first layer is the upper unconsolidated sediment that covers most part of the catchment or alluvial deposit along the streams. This layer is a weathered product of the lower granitic rock characterised by primary porosity and it acts as unconfined layer. The second is the highly weathered top part of granitic rock which is semi confined type as observed from previous works and obtained from borehole log of drilling during the field campaign. This layer unlike the first layer is characterised by secondary porosities caused by faults and fractures most of them trending East-West in the La Mata catchment. The third layer is the massive granitic rock that acts as the bottom boundary.
Most part of the study area is covered by sandy loam soil. As a result the area has moderate run off and the soil has low retention capacity, which leads to moderate recharge capacity. However due to the low precipitation, high evapotranspiration and thin aquifer layer the catchment has low yield, as also observed from the bore holes in the study area. Both La Mata and Sardon drain the catchment during dry season; the flow of groundwater is towards these streams in all directions of the catchments as it is indicated on figure 2. Evaporation and transpiration by the two tree species are the two main dominant water budget components of the catchment especially during dry season. No abstraction and flow between the neighbouring aquifers

2.4.3. Numerical Model Design

2.4.3.1. Coupling Unsaturated with Saturated Zone

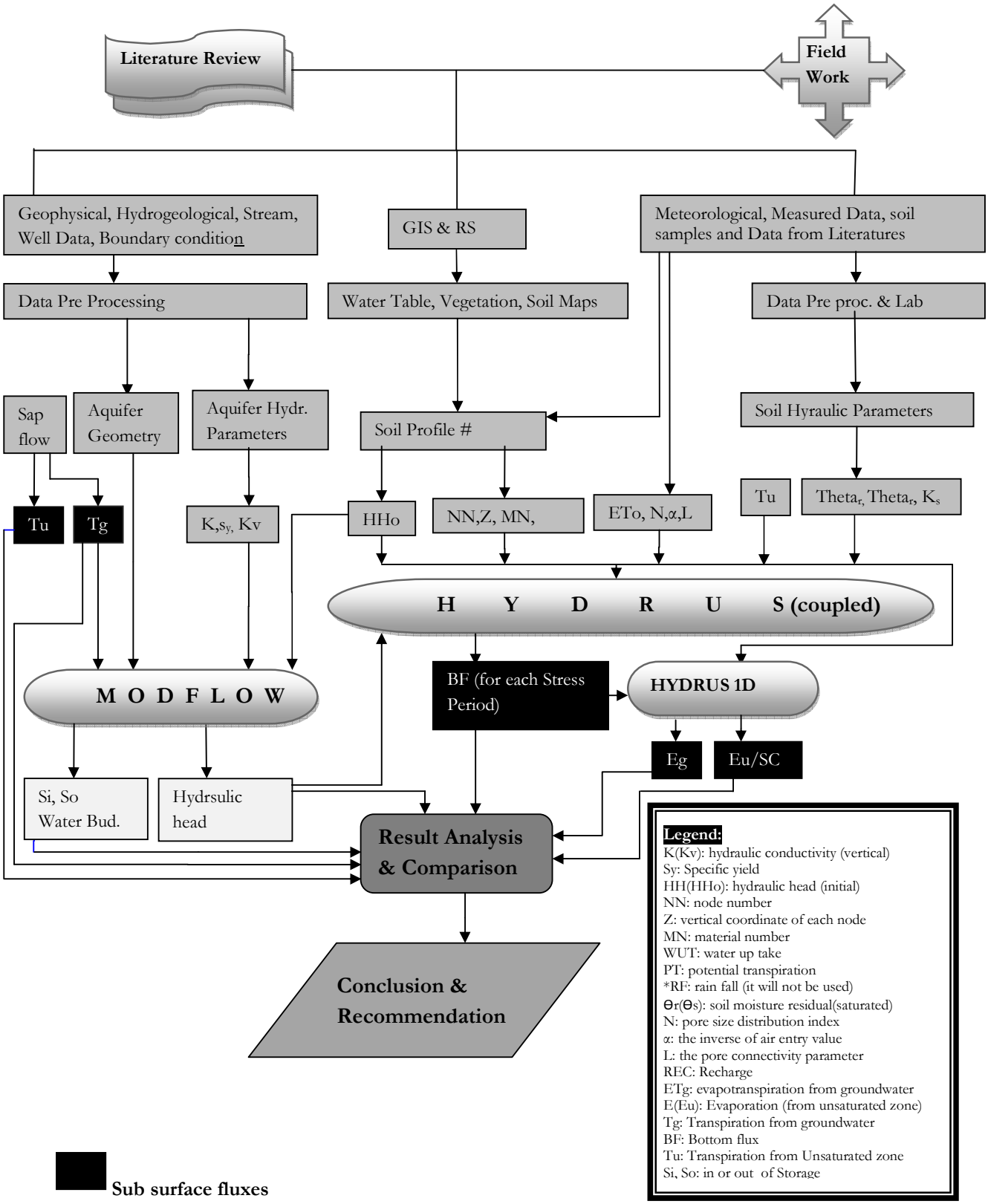

Figure 11. Flow Chart Showing Sequence and the Main Processes of the Study

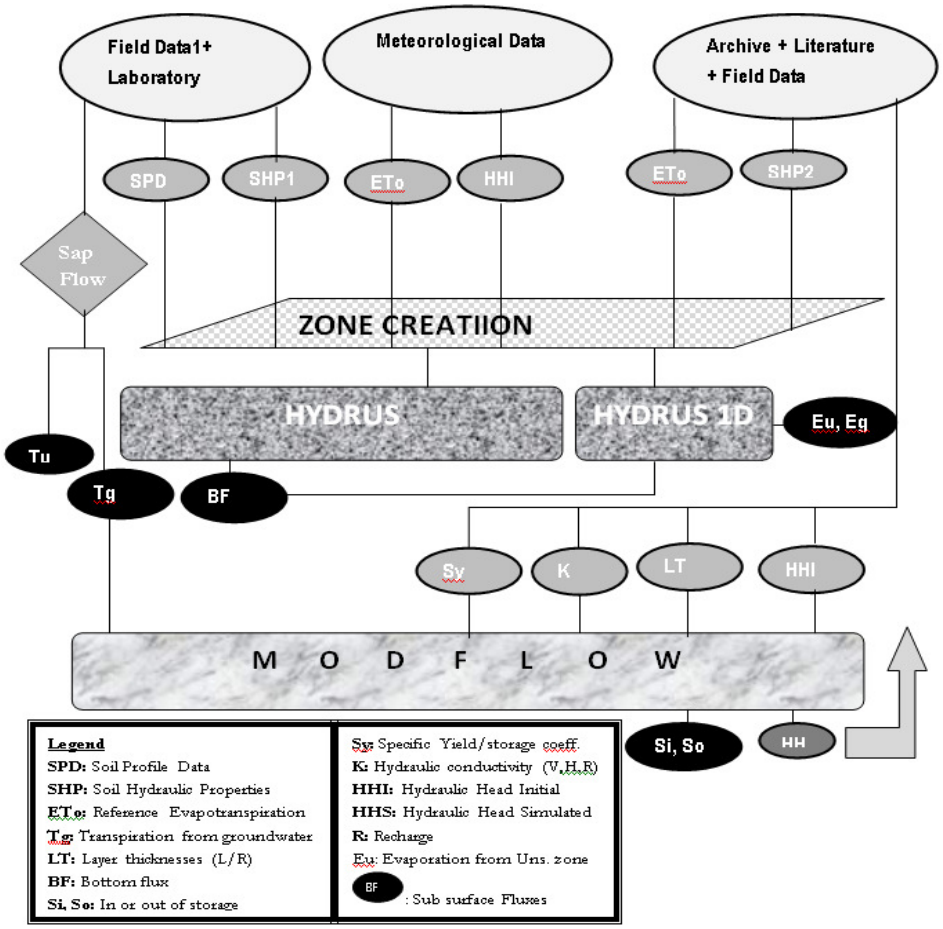

Figure 12. Schematic representation of the coupling and the output subsurface fluxes

2.4.3.2. Unsaturated Zone Numerical Model Design

Introduction:

The HYDRUS package for MODFLOW consists of two sub-models that interact in space and time: HYDRUS sub-model (vadose zone) and MODFLOW sub-model (groundwater).

The HYDRUS package considers the main processes and factors affecting fluxes in the vadose zone, such as precipitation, infiltration, evaporation, redistribution, capillary rise, water accumulation at the ground surface, surface runoff, soil moisture storage and plant water uptake. The HYDRUS package then calculates the recharge or evaporation from groundwater which will be used by MODFLOW to simulate hydraulic head as shown in the figure below.

Initial Conditions

The area is divided in to twelve zones (Figure 14), each zone having their own unsaturated soil profile. The unsaturated zone finite element mesh was constructed by dividing the soil profile into one dimensional linear elements connected at nodal points. The element dimensions should be relatively small at locations where large hydraulic gradients (around the top) are expected but the ratio of the neighboring elements doesn't exceed 1.5. Soil hydraulic properties also need to be considered when defining element dimensions. It was also mentioned to note that the bottom of the soil profile needs to be below the water table throughout the simulation. Two meter is estimated based on the trends of the recession curves of the piezometers in the catchment as the maximum value that the water level might decline during the simulation period and pressure head at each profile is therefore set at least at two meter below the bottom of unsaturated zone.

The HYDRUS Package solves the Richards equation and determines the flux at the bottom of the soil profile using time sub-steps for each MODFLOW time step. MODFLOW receives the flux as recharge and

calculates a new water depth for the time step, which is assigned as the new pressure head at the bottom of the soil profile in the HYDRUS Package for the next MODFLOW time step.

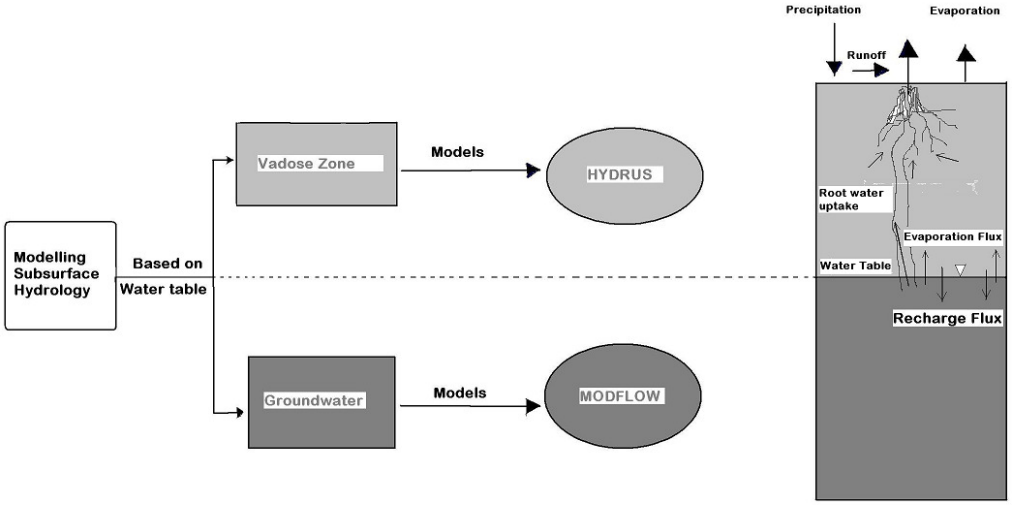

Figure 13. Schematic representation of Coupled HYDRUS-MODFLOW

Governing Flow Equation

The one-dimensional unsaturated flow package is used to describe the effects of the main water fluxes at the ground surface described by a modified form of the Richards equation, which is expressed as:

$$\frac{\partial \theta}{\partial t} = \frac{\partial}{\partial z}\left(K \frac{\partial h}{\partial z} + K \right) - S \qquad \text{Equation 5}$$

Where θ is volumetric soil water content [dimensionless], t is time [T], Z is the spatial coordinate [L] (+ upward), K is unsaturated hydraulic conductivity at the current pressure head [LT^{-1}], h is water pressure head [L] and S is the s ink term [T^{-1}].

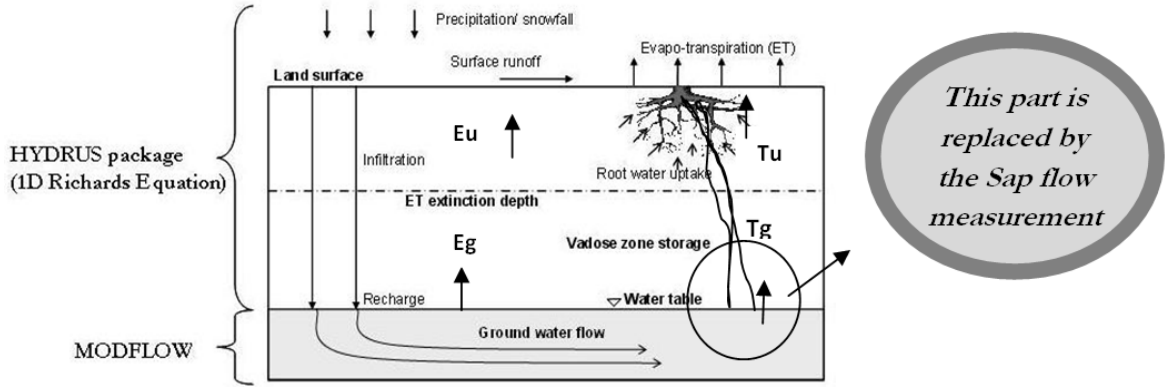

Figure 14. Schematic descriptions of redistribution of the fluxes and how the HYDRUS package computes them for MODFLOW: Source: (Twarakavi, et al., 2008)

This solution requires the initial distribution of the pressure head within the flow domain. At the beginning of a simulation, tables of water contents, hydraulic conductivities, and specific water capacities are prepared for each soil type from the specified input of hydraulic parameters. Then depending on various hydrological and topological conditions, the HYDRUS package predicts both positive (downward) recharge and negative (upward, capillary rise) discharge fluxes. Water table fluxes at any cell are directly influenced by surface infiltration, evaporation, and transpiration, as well as pumping rates in and around a particular cell.

Zone, Soil Profile Creation and Time Discretization

The catchment as also mentioned above is divided into twelve zones as shown in figure 17, based on the variation in water level or hydraulic head, thickness of the soil cover which mainly follows slope in the study area, lateral and vertical variation of soil texture and similarity in surface elevation. To create the twelve zones first soil thickness map was created based on point data of geological map (soil map, based not only on lateral but also vertical variation), geophysical survey and auguring results. Map of classified slopes was created from the DEM data. Water levels were created from point data of piezometers, extrapolated water levels from recession curve for dry piezometers, augured pits and water levels in the drains (streams). By taking the classified soil thickness map in to account the classified slope map was intersected with classified water level maps and finally zones with similar properties were identified so as to assign similar soil profile parameters for each zone. The main factors for creation of a zone are:

- Existence of vegetation
- Similarity in water table depth: Water level map is created from point data of piezometers, naturally leaking water from aquifer and auguring wells (previous and new)
- Similarity in soil profile: mapping using augering wells soil profile and using the slope of the catchment as a function of soil profile. That means the area is classified based on the slope justified by augering.
- Similarity in surface elevation

Soil Profiles were created using 28 sampling results of previous studies, texture analysis of 19 samples, infiltration test of double ring method at 5 places and permeameter test of 25 samples as it can be observed from the base map of the catchment (figure 3). These laboratory and field analysis has two purposes; to prove or disprove the field observation (slope is a function of soil thickness) and soil succession and to discretize the soil profiles and quantify soil hydraulic parameters for each soil horizon.

Soil profile that represents respective zone is prepared for each zone. The soil profile is divided in to linear elements connected at nodal points that are numbered from bottom to surface. The element dimensions according to the manual of the model should be relatively small at locations where large hydraulic gradients are expected. Such a region is usually located close to the soil surface where highly variable meteorological factors can cause rapid changes in the soil water content and corresponding pressure heads. Therefore, relatively small elements are recommended near the soil surface, with gradually larger sizes deeper in the soil profile. Accordingly the discretization of the soil profile is made 0.01m at the top and 1m at the bottom.

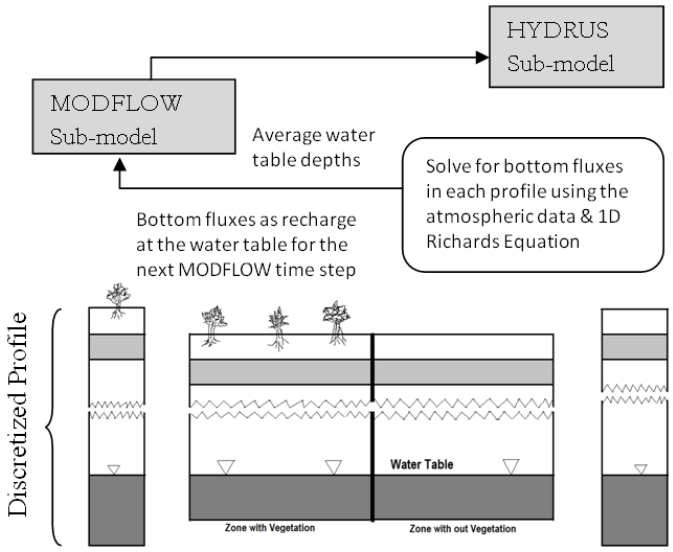

Figure 15. Schematic representation of soil profiles, Adopted from Twarakavi,(2008)

Flow chart: zone Creation

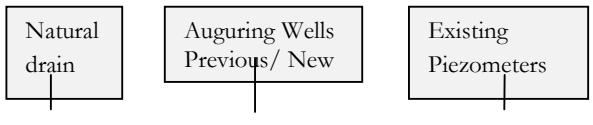

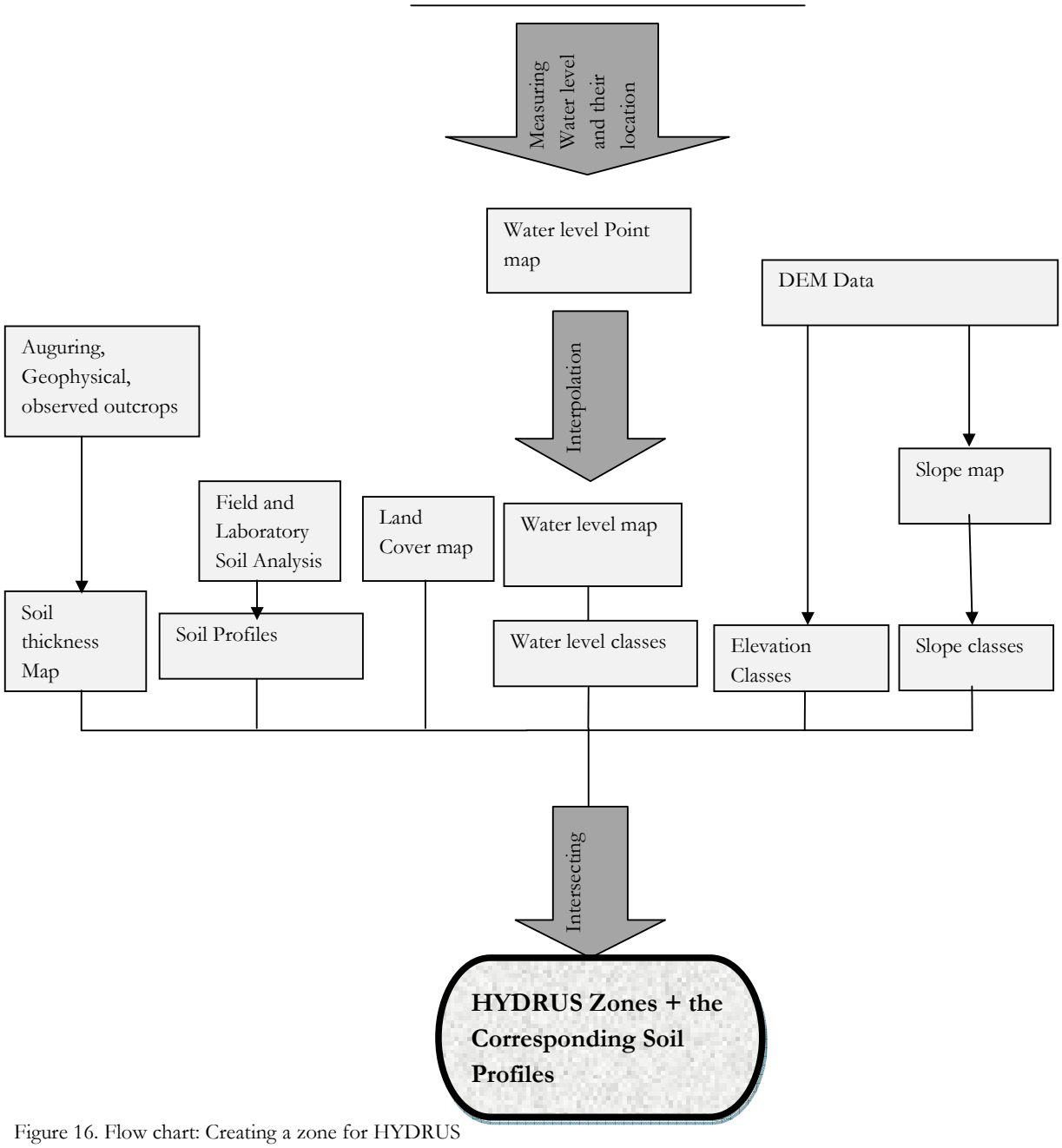

Figure 16. Flow chart: Creating a zone for HYDRUS

Soil hydraulic properties also need to be considered when defining element dimensions. Coarse textured soils generally require a finer discretization than fine-textured soils (loams, clays). The following figure shows how the created soil profiles are assigned to the corresponding zones.

Selection of the time steps are critical steps in model design as they have strong influence on the numerical result (Anderson & Woessner, 1972). Time will be discretized based on the temporal variation in inputs (those inputs which vary temporally) of HYDRUS, such as precipitation, potential transpiration and potential evaporation. Since hourly data of the indirect causes of the change of these factors like wind speed, humidity, radiation, temperature and etc. are available it is possible to discretize the study periods starting from daily. Since the input variables like PET and Tg that cause water table change vary daily a day is used as time step.

The process of analyzing one dimensional water flow begins with the discretization of the soil profile into finite elements, and definition of the vertical distribution of hydraulic and other parameters characterizing the soil profile (Figure 13). The soil profile needs to represent materials from the surface to the bottom of the profile where the profile must always be saturated at the bottom at any time during the simulation. The bottom of the profile is therefore selected for each zone based on the maximum draw down that was observed in the piezometers of the catchment since at least last five years and that is about one meter. But a drawdown of two meter is selected for safety.

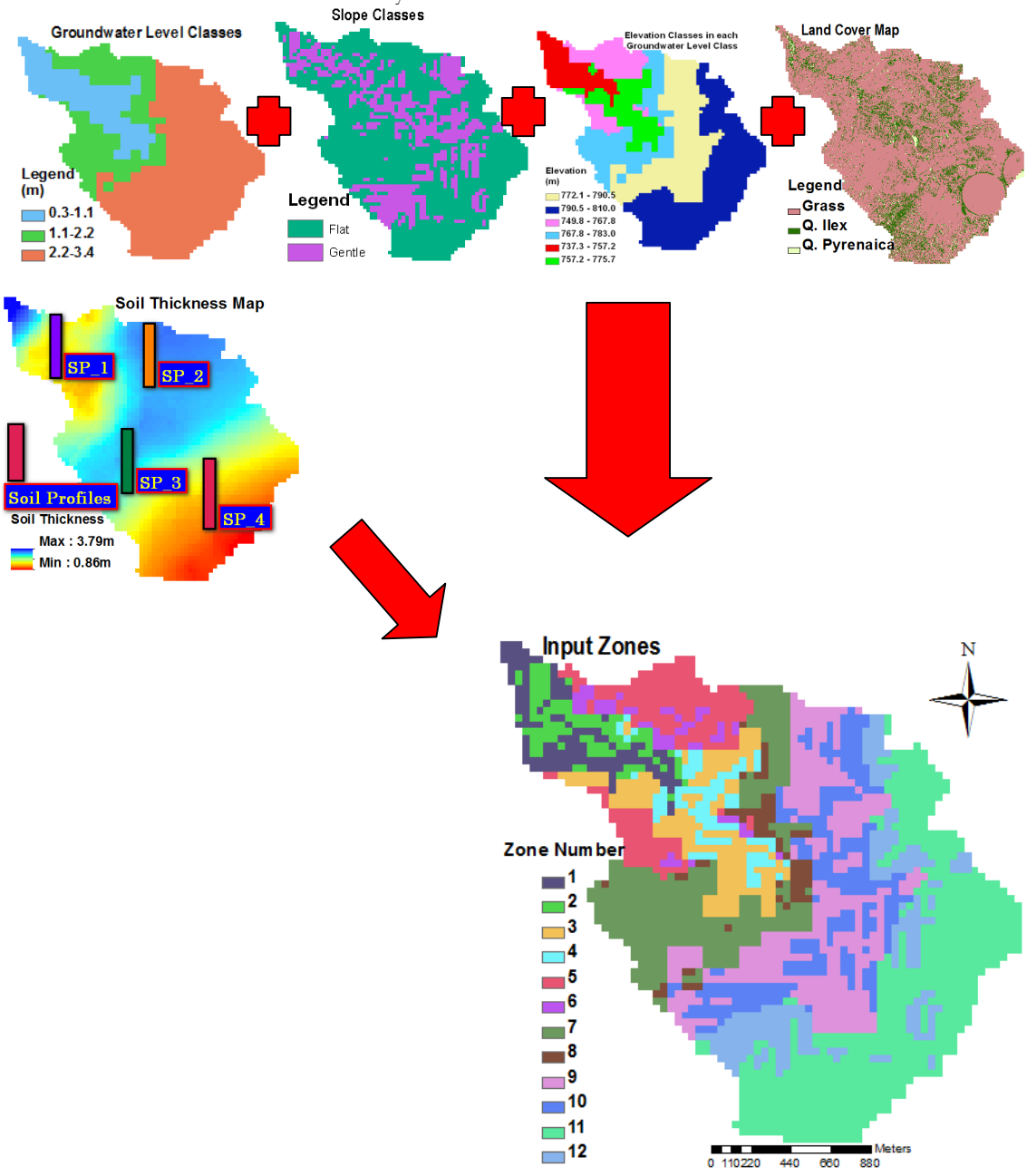

Figure 17. The twelve zones of the catchment with similar soil hydraulic properties, elevation and water levels

Boundary Condition

MODFLOW zone arrays identify cells to which each unsaturated soil profile applies. The HYDRUS Package determines the flux from the variably saturated rigid porous medium and connects to MODFLOW as a head dependent flux boundary. Information about the average depth to water in each MODFLOW zone is delivered to the HYDRUS Package, which returns a flux calculated using its own time discretization for each MODFLOW time step. The flux is applied to every cell in the zone. The HYDRUS Package uses prescribed pressure head and flux boundaries, and boundaries controlled by atmospheric conditions such as precipitation, evaporation, and transpiration **(Twarakavi, et al., 2008)**

The bottom boundary for the unsaturated zone model of the La Mata catchment is selected based on the maximum expected water level decline during the simulation periods (September, 2009,2010) for each year. Since unsaturated zone model is one dimensional and the simulation is done for each zone separately lateral boundary condition will not be considered for this model

Input Data

❖ **Precipitation:** There are two rainfall seasons in the study area November to February and April to June. But there is no variation temporally according to previous studies within the Sardon catchment. Since the study area is just a sub area of Sardon catchment no spatial variation is expected. These variations (temporal variation of rainfall) together with that of temperature influence the recharge and evapotranspiration of this area. Since it is one of the inputs of the unsaturated zone model, good record of this variable is important and it is available. However it is not needed for this study due to the period of the study (dry season).

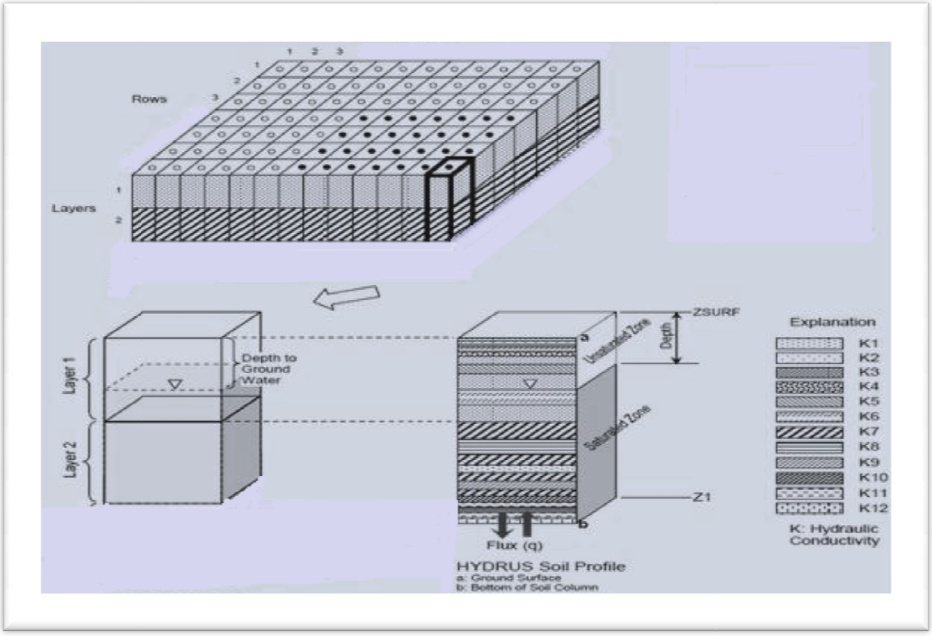

Figure 18. Discretizing aquifer system in MODFLOW and the HYDRUS soil profile: One profile for each MODFLOW zone. (Twarakavi, et al., 2008)

❖ **Transpiration:** most part of the study area is covered by grasses and the remaing by the two tree species and out crops of highly fractured granite at few places. The area was dry for the whole time of the simulation periods. Since only the trees transpire during this time, they are considered in the model using the sap flow measurement. It is possible to consider transpiration in the coupled model directly. However it is not considered directly in this model because of the availability of sap flow data (a more direct way of measuring transpiration) for both simulation periods. There for sap flow measurements were used instead of estimating transpiration rates using HYDRUS.

❖ **Evaporation:** It is the major and more important hydrologic cycle component of the catchment especially during dry season, which also varies temporally and spatially. Its variability originates from its dependence on variable factors such as humidity, water temperature, air temperature, air humidity, type of vegetation cover and depth to groundwater.

In order to estimate the actual Evaporation or transpiration the model requires reference evaporation, a representation of the environmental demand that represents the ET rate of a short green crop, completely shading the ground, of uniform height and with adequate water status in the soil profile (Thornthwaite, 1948) as an input. The reference surface is a hypothetical grass reference crop with an assumed crop height of 0.12 m, a fixed surface resistance of 70 s m^{-1} and an albedo of 0.23. The reference surface closely resembles an extensive surface of green, well-watered grass of uniform height, actively growing and completely shading the ground. The fixed surface resistance of 70 s m^{-1} implies a moderately dry soil surface resulting from about a weekly irrigation frequency. It can be estimated from the meteorological measurements as it depends only on climatic factors like temperature, humidity solar radiation, soil heat fluxes and etc.

The FAO Penman-Monteith method is selected as the method by which the evapotranspiration of this reference surface (ET_o) can be unambiguously determined, and as the method which provides consistent ET_o values in all regions and climates (Allen et al.,1998). As mentioned in this paper the relatively accurate and consistent performance of the Penman-Monteith approach in both arid and humid climates has been indicated in both the ASCE and European studies.

This reference evapotranspiration value calculated using the hourly records of atmospheric variables at a meteorological station and also at eddy covariance tower is used to estimate the amount of water that evaporates from the area not covered by trees. The water uptake from groundwater in the profile of HYDRUS zones is not used for that part of the study area covered by trees; the direct measurement of water through xylem of a tree, sap flow measurement is used as a direct input to the recharge package of MODFLOW.

Since the wind speed measurement at eddy covariance station is at 10m the transfer equation:

$$U2 = Uz\frac{4.87}{\ln(67.8z-5.42)}$$ ----------Equation 6,

is used to transfer the wind speed measured at 10 in to the 2m wind speed, as referred from literature of FAO for ETo calculation, where U2 is wind speed at 2m Uz is wind speed at zm and z is level at which measurement of wind speed is taken. From the original Penman-Monteith equation and the equations of the aerodynamic and surface resistance, the FAO Penman-Monteith method to estimate ET_o can be derived:

$$\mathrm{ET_0} = \frac{0.408\Delta(\mathrm{Rn}-\mathrm{G})+\gamma\frac{900}{\mathrm{T}+273}\mathrm{U_2}(\mathrm{e_s}-\mathrm{e_a})}{\Delta+\gamma(1+0.34\mathrm{U_2})}$$ ----------Equation 7.

Where: ET_o reference evapotranspiration [mm day^{-1}], R_n net radiation at the crop surface [MJ m^{-2} day^{-1}], G soil heat flux density [MJ m^{-2} day^{-1}], T mean daily air temperature at 2 m height [°C], u_2 wind speed at 2 m height [m s^{-1}], e_s saturation vapour pressure [kPa], e_a actual vapour pressure [kPa], e_s - e_a saturation vapour pressure deficit [kPa], Δ slope vapour pressure curve [kPa $°C^{-1}$], ɣ psychrometric constant [kPa $°C^{-1}$].

The daily estimate of ETo calculated for September 2009 and 2010 as shown on figure 19 in both ways (using measured long wave radiation (Rnl) and the one calculated from estimate of Rnl based on day number and location) have similar trends except the lower value of the one using measurements of net long wave radiation during both years.

❖ **Initial Hydraulic Heads:** five piezometers in and the surrounding of La Mata catchment are equipped with automatic groundwater level recording loggers. They hourly record absolute and atmospheric pressures above the logger sensor at each piezometer or well. The automated records of the loggers are converted to a true water level or hydraulic heads of each piezometer or well. Once the initial hydraulic head is assigned (average hydraulic head value of all grids in the zone) as an input for each zone of the unsaturated model, it receives hydraulic head for the next time step from the saturated model. For those piezometers

that are dry during the first time step the hydraulic head at that location was calculated using the extrapolation of the recession curves or its equation (Equation equation) of the corresponding piezometer as shown on figure 26.

Time during which the piezometer is dry is considered zero and the water level is considered initial water level. Then the value of water level on the curve at September 1 of 2009 and 2010 was used to assign for the location of the piezometer. Then these values of hydraulic heads at each piezometer are interpolated to obtain hydraulic head values at every cell of the model. These cell values are used to calibrate the model for both (September 2009 and 2010) simulation periods respectively. Single value of hydraulic head was assigned to each HYDRUS zone.

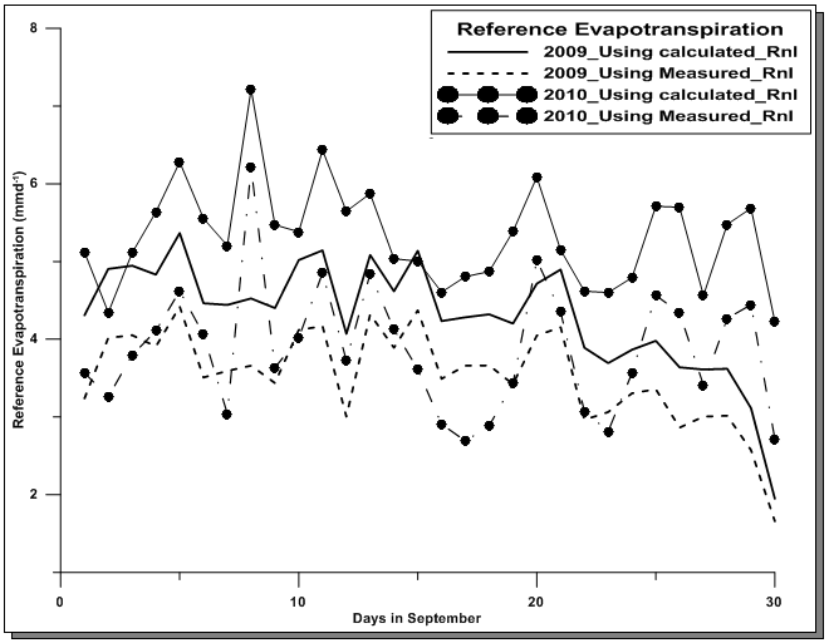

Figure 19. ETo calculated Using measured and estimated net long wave radiation (Rnl), September 2009 and 2010

❖ **Saturated Hydraulic Conductivity (Ksat):** the infiltration capacity of the top soil is measured on field using double ring method. To achieve good measuring results it is important to take into account several factors that may influence the measurement: the surface vegetation, the extent to which the soil has been compacted, the soil moisture content and the soil layers (strata). The best measuring results are obtained at 'field capacity' of the soil (Eijkelkamp, 2010).The soil type is the main factor for infiltration in addition cracks and slope of the terrain where the test is carried out should also be taken in to account while selecting representative sites for the infiltration.

The rate of infiltration is determined as the amount of water per surface area and time unit that penetrates the soil. This rate can be calculated on the basis of the measuring results and the Law of Darcy. The rate of infiltration on dry soil is higher at the beginning of injection, decreases gradually with time and finally becomes constant as it was observed from the plots of cumulative time versus infiltration rate. From the plot then this constant value is taken as the saturated hydraulic conductivity of the soil.

To obtain saturated hydraulic conductivity in laboratory using permeameter undisturbed soil samples are taken and put in to metallic rings of 53cm circumference and a volume of 100cm3 with a closed ring holder as described on user manual of the equipment. The permeameter method is mainly used to provide estimates of the hydraulic conductivity of the soil near saturation. There are two types of permeameter methods of measuring Ksat, the constant head that is used for non-cohesive high permeability sediments like sand and failing head method which is more suitable for cohesive, intermediate to low permeability

sediments such as clays and silts as described in manual obtained from the mentioned web site. For this study both methods were applied based on the sample soil property or type.

For the constant head method the permeameter has a chamber with spill way to provide a supply of water at a constant head so that the water moves through the samples a steady state. The hydraulic conductivity is then determined using Darcy's law.

$$K = \frac{V*L}{A*t*h}$$ ----------Equation 8

Where K is hydraulic conductivity, V (m/d) is the volume of water discharging in time t, L is the length of sample, A is cross-sectional area of sample (m^2) and h (m) is hydraulic head difference over the sample.

❖ **Saturated Water Content:** To measure the porosity (a property of a soil related to saturated water content) of the sample, it is first saturated and weighted. Then the water was drained by gravity and weight at different time steps until drain ceases. This weight was plotted versus time to obtain field capacity and also specific yield. The drained samples were oven dried at 105^0C for 24 hours and weighted. Then the porosity (volume of pore space) is simply the weight of saturated sample minus the oven dried weight multiplied by density of water. Saturated water content by weight is calculated from the volume of pore space divide to the volume of sample.

❖ **Residual Water Content, Soil Moisture and Soil Matrix Potential:** The soil moisture at Trabadillo station is measured by TDR-based Steven Hydra probe sensor as that can be derived from the corresponding reading of dielectric permittivity using different equations as described by Bellingham (2007). They are placed at depths of 25, 50, 75 and 100cm and they have been reading matrix potential with in an interval of an hour. This data in addition to laboratory analysis of sampled soils is used to determine hydraulic parameters like wilting point but this data is used mainly as one of the alternatives to determine the residual soil moisture content of the soil around the station as it is one of the inputs of HYDRUS**.**

The other alternative to estimate residual soil moisture is using WP4 instrument, which is used to measure matrix potential of soils with low soil moisture contents. The WP4-T has a measurement range from 0 to -300 MPa and 3 to 6.5 pF (saturation to air dry) with an accuracy of 0.1MPa or better. The WP4-T senses the dew point of water vapour with a cooled mirror located above a sample in a closed chamber. Sample temperature is monitored with a built-in infrared thermometer, and the WP4-T.s internal pettier cooler sing. Using this instrument those samples for which other hydraulic parameters was measured is dried and again wetted to different levels by taking small amount. Then the wetted soil is measured for matrix potential and weighted to later calculate the soil moisture content. Then the pF curve is drawn from the soil moisture content versus pF values read by WP4 to estimate the residual water content of the sample in this case. Similarly the residual soil moisture of all the samples was calculated and the result is summarized in table 3.

❖ **Pore size distribution Index and Pore connectivity Parameter:** A complete analysis of the pore size distribution of a soil is useful for predicting water infiltration rates, water availability, plants, water-storage capacity, and aeration status. However, for many practical soil management decisions, detailed pore size distribution may not be needed. "'A single number characterizing the important aspects of the distribution would suffice and even be preferable for people not specifically trained in soil physics (Bolt et al., 1959)"(Cary & Hayden, 1973). For this reason these parameters were derived using models developed for this purpose, models like HYDRUS 1D and ROSETTA. The models use soil texture class (percentage of sand, silt clay and or bulk density) and give the soil hydraulic parameters as an output. For this study only Pore size distribution Index (N) and Pore connectivity Parameter (L) are required.

❖ **Texture Analysis:** Texture analysis is done to determine the percentage of sand, silt and clay in a sample soil. Those findings are plugged into a texture analysis triangle (shown in figure 17) to determine soil classification. The soil classes should be known to divide the catchment in to zones with similar soil property. In addition the hydraulic parameters of each soil sample are estimated using models like SPAW, ROSETTA and HYDRUS 1D that needs the texture class or proportion of sand, silt and clay as an input. Hydraulic parameters derived from texture analysis are saturated and unsaturated hydraulic conductivities, saturated soil moisture content, residual soil moisture content, and inverse of air entry value, pore connectivity parameter and pore distribution index.

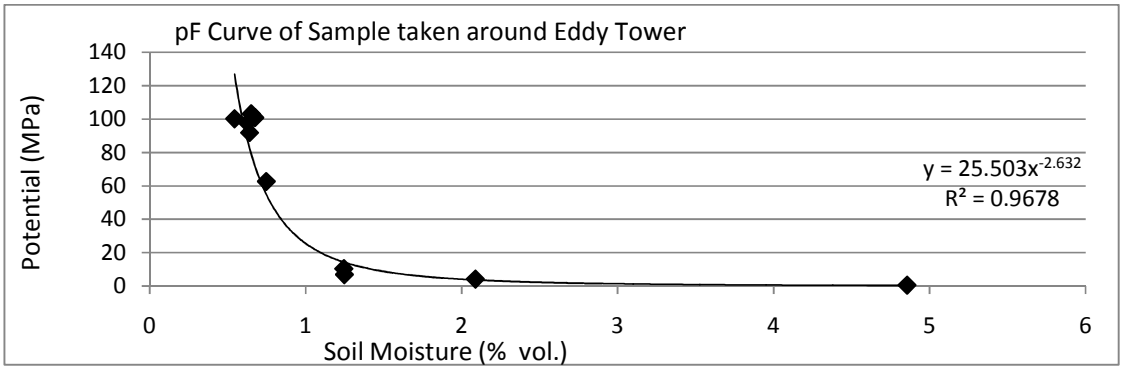

Figure 20. pF curve of a soil sample taken from right bank of La Mata stream (around the eddy tower) drawn using WP4 measurement (Residual soil moisture ≈ 0.05)

The texture analysis was done by taking soil samples from representative locations in to plastic bags some of the locations overlaping with the samples taken using the sampler in to metallic sample rings to compare the results.

Texture analysis is one of the methods used to obtain some hyraulic property of the corresponding soils. For instance some samples cannot stick in to the mettalic ring, it is some times also difficult to auger deep at some locations but there exist an out crop of thick soil layers.

Finally soil hydraulic measurements taken using different methods are compared and the more reliable one is used incase the values are not correlable as an input to the unsaturated model for those locations where results are obtained by more than two methods. But result of only one of the methods was used for those locations where more than two ways of measurements are not possible based on the summary of the results shown in table 3. For instance augering up to a depths of 4m might be difficult, in this case alternative methods of taking samples from valley cut or exposures in to plastic samplle bags was apllied. Doble ring infiltrometer can only be applied to the top part of the soil layers. But it has an advantage as it the measurement is conducted on an in situ sample of the soil. To obtain dense distribution of hydraulic conductivity values in the study area these three methods are applied.

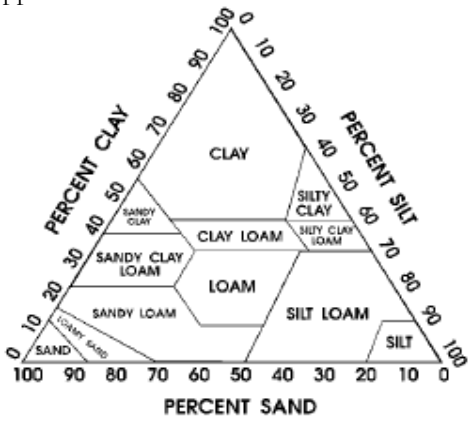

Figure 21. Texture Analysis Triangle for soil classe Determination

Based on the sample texture analysis almost all the soil material in this catchment lies under sandy loam classes as it can be observed from the graphs of all the samles ploted together (Figure 20).

Based on the texture analysis some hydraulic parameters were derived using SPAW model. This result is summurized in table 3.

As it can be observed from the table above the value of Ksat measured in laboratory using permeameter in most cases is higher than that of field measurement taken by double ring method and also the one derived from texture analysis using models like SPAW. There are uncertainties in both methods caused by different

factors affecting the measurement like sampling from a place that doesn't best represents the area. The former is more susceptible to such factors as it is taken from very small part of the area as compared to even the area covered by double ring method. In addition the initial compaction of the material may be reduced while sampling due to the hammering or hitting.

Table 3. The identified soil materials in the area

Description	Material Number	Corresponding Hydraulic Parameters					
		Ksat	Θ_{sat}	Θ_r	α	L	N
Very fine sandy loam	1	0.031	0.404	0.1433	2.28	2.215	0.5
Fine sandy loam	2	0.058	0.391	0.1433	1.89	1.916	0.5
Medium sandy loam	3	0.069	0.391	0.124	1.516	1.5	0.5
Medium coarse sandy loam	4	0.087	0.417	0.075	1.51	1.14	0.5
Coarse sandy loam	5	0.09	0.417	0.075	1.51	0.85	0.5

Twelve soil profiles that belong to the twelve zones as shown in table 3 are finally created based on the succession and thickness of the soil material, water level and surface elevation.

At most parts of the study area as it was indicated also in the table 3, it was observed that the soil texture becomes coarser as depth increases.

Based on the result of all these samples the area is classified in to three main soil profile types:

i. Thin fine to medium sandy loam followed by coarse sandy loam: Gentle sloped parts of the catchment.
ii. Fine sandy loam followed by medium sandy loam then coarse sandy loam: plain but upstream of the catchment.
iii. Thin fine sandy loam, thin coarse sandy loam, thicker medium sandy loam and fine sandy loam: Plain but downstream of the catchment (that part of the area closer the to the main stream Sardon).

Therefore the area is summarized to five main soil materials (five main sandy loam varieties) as shown in table 3 and their corresponding hydraulic parameter values are assigned to the corresponding zone following the above description.

❖ **Feddes's Parameters:** The parameters for the water stress response function differ for different plants. "Wesseling (1991) and Taylor and Ashcroft (1972) provided a database of suggested values for different plants"(Seo, Šimunek, & Poeter, 2007). The parameters of the plant in the data base of HYDRUS 1D that resembles the two species found in the study are were assigned to the model as an input for zones containing trees so as to incorporate transpiration from unsaturated zone.

2.4.3.3. Saturated Zone Numerical Model Design

Introduction

Precipitation, transpiration and reference evaporation rates for each profile of the soil zones as discussed above are the driving forces for such coupled model. These data together with hydraulic parameters of each soil layer are used by HYDRUS to calculate the input flux, recharge or capillary rise for next time step of MODFLOW. Therefore, there is no need to use MODFLOW Evapotranspiration (ET) and recharge (REC) Packages simultaneously in the same vertical column with the HYDRUS Package. But for more accurate representation of input transpiration rates sap flow measurements conducted during the study period is used as a negative recharge using recharge package in MODFLOW for this study.

The flux either positive or negative is calculated at the bottom of the soil profile, which must always be saturated as also mentioned above (pressure at this boundary is equal to the height of saturated column above that elevation). The flux is applied to the MODFLOW layer which can be specified first layer or the highest active cell. For instance if layer one is selected and layer one goes dry, then the simulated recharge is not input to the simulation (Seo et al.,2007). The governing 3D model equation the unconfined aquifers is:

$$\frac{\partial}{\partial x}\left(K_x \frac{\partial h}{\partial x}\right) + \frac{\partial}{\partial y}\left(K_y \frac{\partial h}{\partial y}\right) + \frac{\partial}{\partial z}\left(K_z \frac{\partial h}{\partial z}\right) = S_s \frac{\partial h}{\partial t} - W \quad \text{----------Equation 9}$$

Where Kx, Ky and Kz are components of Hydraulic conductivity tensors, Sy specific storage and W is general sink/source term, that intrinsically positive and defines the volume of inflow to the system per unit volume of aquifer per unit time.

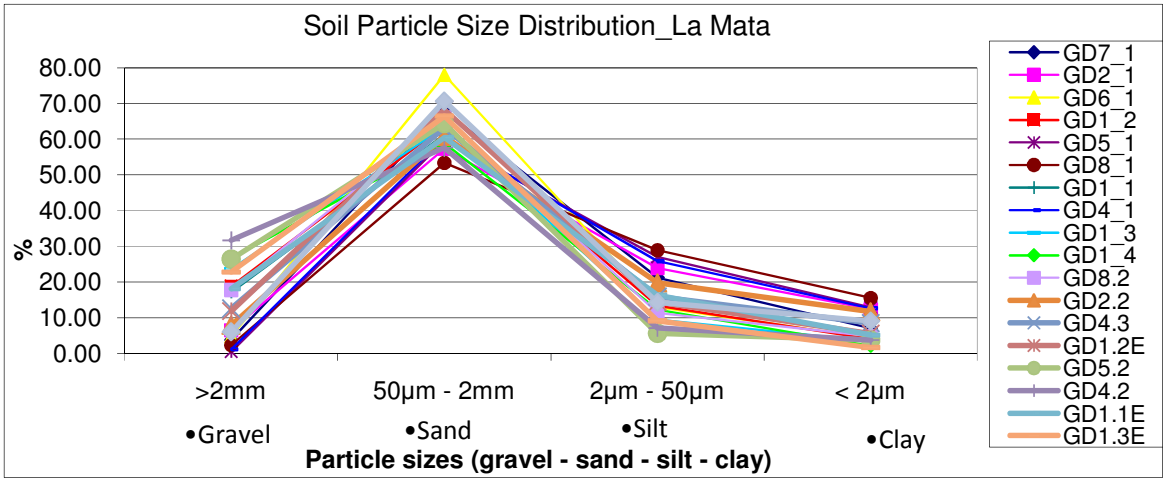

Figure 22. Particle size distribution of all the samples taken from representative locations in the catchment

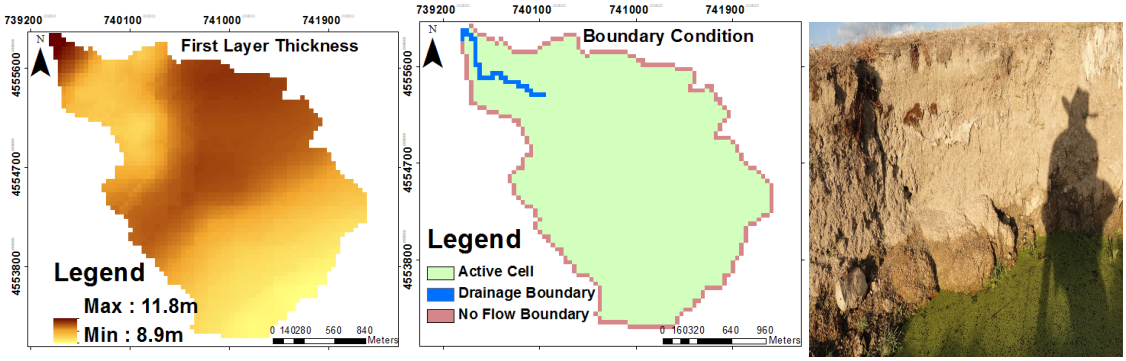

Figure 23. First layer thickness (left), Boundary condition of the first layer (middle) and Stream Draining (right)

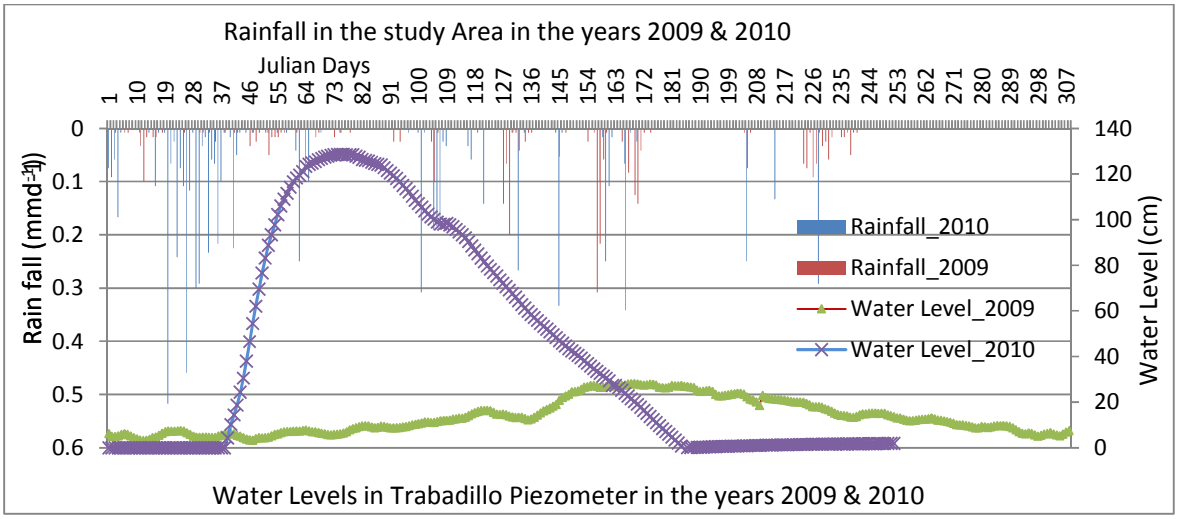

Figure 24. Water level and Rainfall in the year 2009 and 2010

Input Data

❖ **Grid Design:** Taking the size, lateral hydro stratigraphic variation, fracture distribution, topography of the catchment, its fitness to the DEM grid distribution and the upper limit of the PMWIN used in to account a regular square grid of 40X40 meters was selected for the model. The area is bounded with in a rectangle of 72X69 cells or 4,968cells (area of 7.94 square kilometer) out of which 2832 cells (about 4.531 square kilometer) are part of the catchment.

❖ **Aquifer Geometry:** The number of the layers and their thickness are estimated based on geological map of the area, available borehole geologic logs and geophysical surveying conducted in the area especially the VES data gathered by the previous MSc students, the thesis from Tesfay and Abubeker were the main sources. Accordingly the hydro stratigraphic units of the catchment are divided in to three layers including the bottom massive granite. Then the thickness of the first layer found by integrating all available data mentioned at each cell is subtracted from DEM values of each cell to obtain the bottom elevation of the first layer (Figure 21-right) using ArcGIS. Similarly bottom elevation of the second layer is obtained and finally exported to MODFLOW.

Both layers above the massive granitic rock are hydro geologically unconfined aquifers. So the first layer which is composed of soil or alluvial deposit and highly weathered granite was assigned the MODFLOW layer type 1 (strictly unconfined). Figure 4 shows three main hydro stratigraphic units and location of La Mata in relation to Sardon catchment. The second layer which is composed of fractured granite can be considered semi confined type of aquifer as it was observed from the drilling conducted in September 2010. This layer is assigned the MODFLOW layer type 3 (where transmissivity of each cell vary with saturated thickness).

❖ **Boundary Conditions:** Bottom boundary of the model is massive granite (no flow) as shown on Figure 21. In such basement rocks the streams follow selectively weak zones like faults, whereas resistant rocks become water divides as also studied by previous MSc researches like that of Ratnayake (2000) for both surface and groundwater catchment. Surface catchment boundaries of La Mata stream which are also boundaries for groundwater catchment of this stream are therefore considered as the lateral boundaries in the model (no flow boundary), except few cells around the outlet of this catchment, which are assigned drain boundary as shown on Figure 23 (middle). These cells are assigned a drain boundary because this part of the catchment is bounded by main Sardon stream which has water at its boundary with La Mata catchment during the whole month of September and the water level is recharged by the surrounding aquifers including the aquifer of La Mata catchment as shown in Figure 23 (right).

The stream is treated as a drain in the model by assigning the MODFLOW Drain boundary condition. Based on the field observation La Mata is assigned to a drain boundary for only about 1.5km (thirty seven cells) up stream of the out let as only this part of the stream is draining the aquifer during the study period. The depth of the drain is taken one meter below surface elevation at an average for both streams.

❖ **Initial Hydraulic Head:** The groundwater responds to subsequent changes of subsurface fluxes like recharge, evaporation, transpiration and interflow by rising or falling of the water table. Well hydrograph can be used to estimate the groundwater levels at piezometers that do not fully penetrate the aquifer. When they get dried during dry seasons by extrapolating the graph or using equation of the recession segment written as Equation 10 and the initial value of groundwater depth (H_o) one can estimate depth to groundwater (Figure 25 & Figure 31) (Posavec, Parlov, & Nakić, 2010). Depth to groundwater was estimated for dry piezometers for this study so as to increase the density of point measurements of hydraulic head in the catchment.

$H = H_o e^{-\propto t}$----------Equation 10

Where H is the required groundwater table, H_o water level before dried out, $e^{-\propto}$ recession constant, t time

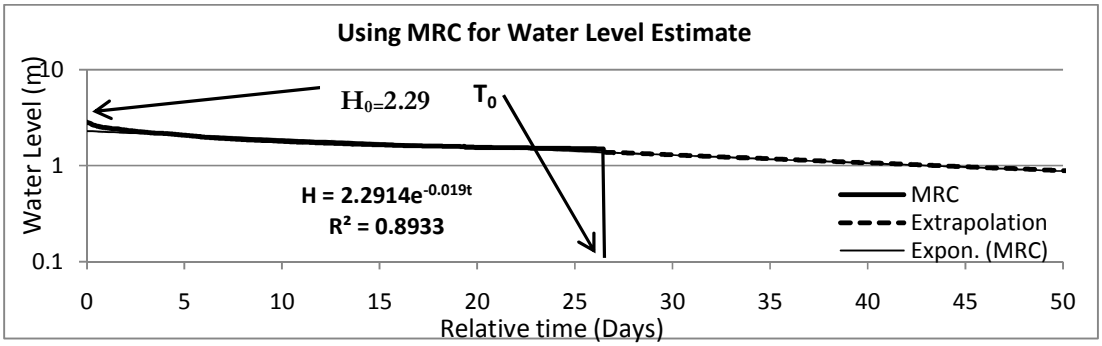

Figure 25. Master recession curve of Trabadillo piezometer and its extrapolation for dry period water level estimate

The hourly records of water levels are averaged to daily to fit with time steps of the models. Some additional information was also obtained from the boreholes that are drilled in September 2010 and finally the point data are interpolated so as to obtain water level at every cell of the model (Figure 2-top right).

❖ **Hydraulic Conductivities (V/H):** In hard rocks, storage and flow of subsurface water mainly depends on the secondary porosities like fractures or lineaments. Therefore hydraulic conductivity of such rocks depends on the degree of weathering or fracturing which varies spatially (both laterally and vertically). Pumping test data or slug tests performed on the existing wells or piezometers are the main sources to estimate hydraulic conductivities for the second layer. Hydraulic conductivity can be calculated using different methods like Maag's, Hvorslev method (example used by Kagaba (1997)) or using slug tests, inverse auger-hole method, where the last two methods were applied to find hydraulic conductivity of the rocks in the catchment. For the first layer, double ring tests, laboratory tests (using permeameter) performed on undisturbed core samples and disturbed samples taken in to bags are the main sources for especially vertical hydraulic conductivities. The horizontal hydraulic conductivities were estimated from the disturbed samples permeameter test as it is commonly used by different researchers as mentioned in manual of Data Collection Hand Book by Yu et al. (1993) Within an anisotropic geological formation, the vertical component of the saturated hydraulic conductivity is usually smaller one to two orders of magnitude than the horizontal component.

According to the field observation permeability, thickness, texture and other hydraulic properties of the soil in the catchment depend on slope and location with the respect to valleys or streams. Double ring tests indicated that areas with flat and gentle slopes have thicker and less permeable soils while those on slopes have coarser textured soils with higher permeability. On the other hand soils in valleys have different conductivity values from that of other places due to the deposition in valleys. For instance they have a number of layers at most of the places like thicker sandy soils (for width of up to fifty meter distance from stream centre) with different permeability from the rest of the study area.

Based on this observation the soils in the study area are classified in to three main soil zones with peculiar hydraulic properties. To each one of these zones different hydraulic conductivity values were assigned as an input for the first layer. Mapping of these zones was done using data integration of different maps like slope map, distance from stream (buffer map) and the point map of hydraulic conductivity tests and review of previous slug tests (Figure 27 maps at the top).

In order to create the zone, slope map is classified in to two classes (plain to gentle) and sloppy. The streams are buffered for fifty meter. From hydraulic head contour map those areas with closer contour lines are selected. Finally the three maps are integrated using ArcGIS so as to create the hydraulic conductivity classes map shown on the figure 27. At the end hydraulic conductivity point maps obtained from data of the double ring, permeameter, texture analysis and sludge test are assigned using the integrated map as a background. Interpolation of the point hydraulic conductivity values was not satisfactory. As a result the use of the point data as a background of the hydraulic conductivity class map is preferred.

Among the measured hydraulic conductivities at closer locations to each other those data that best correlates are taken and assigned to the corresponding zone (Table 4). The remaining might be affected by any of the different factors and that deteriorates their reliability that is why many samples from the same places were taken as shown on Table 4. The selected sample values are also tabulated in this table.

Hydraulic conductivity is estimated from the disturbed samples that are taken in to sample bags from different soil horizon at each point. The average value of each horizon is assigned for that location and finally this number is assigned to the zone in which they are found using soil hydraulic conductivity classes as a background. Table 4 shows the values that are assigned to each zone.

Table 4. Assigned hydraulic conductivity values (md^{-1}) to different zones of the first layer

Zone. No	Zone Description	Sample ID	Location (UTM)		Permeameter	Double Ring	SPAW	Kv_Value Assigned	Kh_Value Assigned	Remark
			X	Y						
0	Plain to gentle out of valley	GD1.2	739381	4555666	1.14	1.67	1.27	1.41	14.1	Finally calibrated
1	Plain to gentle in Valley	GD2.1	739353	4555611	2.21	1.92	0.67	2.07	20.7	Finally calibrated
2	Sloppy	TR_06	739652	4555749	1.09	1.82	1.60	1.09	10.9	Lowest
	Drain							3.0	30.00	DE_1mbgl

Table 5: Assigned hydraulic conductivity values to different MODFLOW input zones (Figure 27) of the second layer

Zone Description	Highly weathered and fractured	Weathered and highly fractured	Highly fractured	Fractured	Slightly fractured
Zone No	1	2	3	4	5
Assigned Kv	0.1	0.08	0.05	0.009	0.005
Assigned Kh	0.5	0.4	0.25	0.045	0.025

❖ **Storage Coefficient:** Similar to hydraulic conductivity storativity of the unconfined alluvium depends on the porosity of the rock which is related to degree of compaction, texture of the deposit and etc. But that of fractured granitic aquifer depends on the density, width, length and connectivity of the fractures, degree of the fracturing and weathering, which again varies both laterally and vertically as referred from groundwater assessment study of Sardon by Kipkoech Ronoh (2001).

Table 6. Results from laboratory analysis and assigned values to different zones of the first layer

Zone No	Zone Description	Sample ID	Location (UTM)		Laboratory Analysis of Core Samples	SPAW (Using Texture Analysis result)	Value Assigned for the Zone
			X	Y			
0	Plain to gentle (out of valley)	GD1.2 & 1.1	739381	4555666	0.044, 0.0625	0.026	0.05325
1	Plain to gentle (in Valley)	GD2.1	739353	4555611	0.0316	0.032	0.0316
2	Sloppy	GD3.1	739386	4555380	0.0253	0.0219	0.0253

These data was obtained from slug test results of the existing wells and also planned to find from those wells which are drilled this year, but unfortunately not done because of the failure of the pump used for the test. The geophysical assessment done by Abubeker (2010) in this area are also used to improve quality of the modeling, like the use of resistivity values to create hydraulic conductivity or storage coefficient zones.

The same zones as that of hydraulic conductivity were used since both Sy & K are hydraulic properties of soils or rocks that are affected by similar geologic conditions. Concerning the assignment of values the

sludge tests were related with resistivity values and then values were assigned to zones with no sludge test result but has geophysical data, based on this relation.

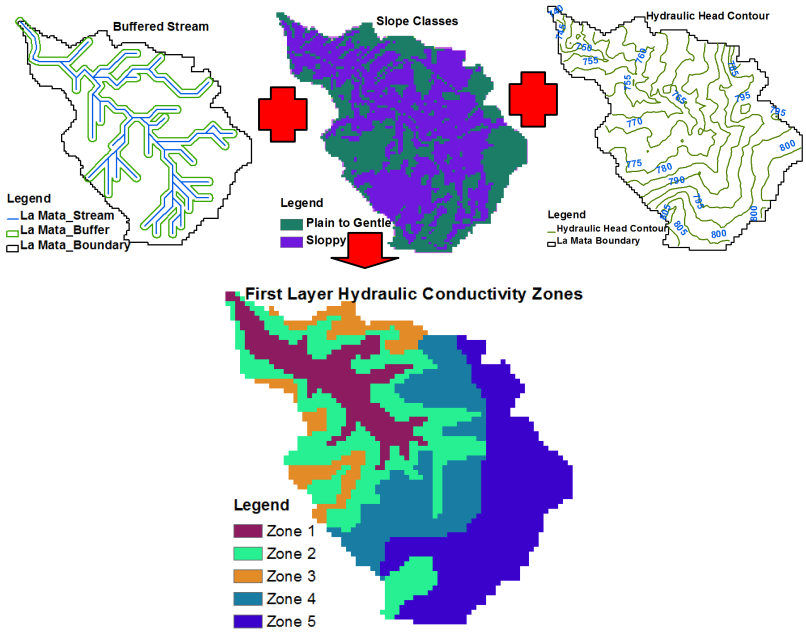

Figure 26. Horizontal and Vertical Hydraulic conductivity zones for the first layer

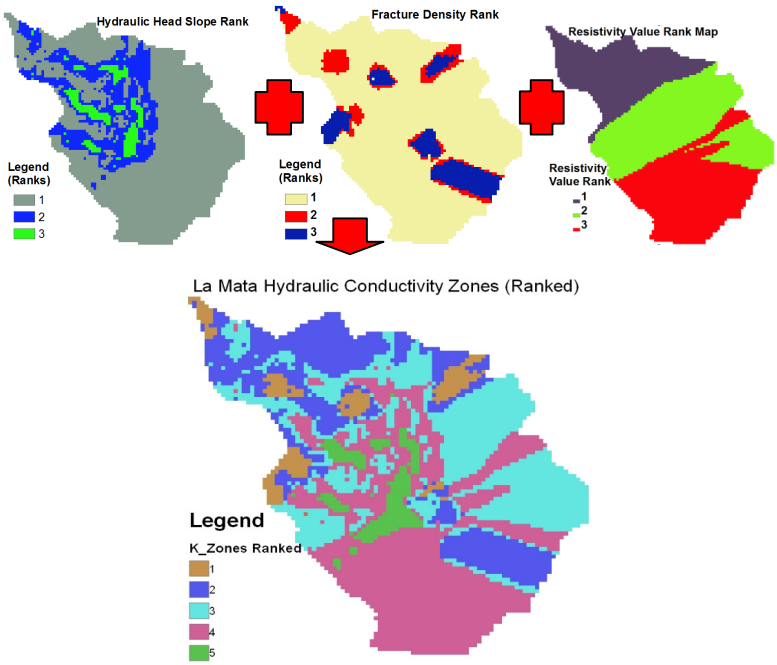

Figure 27. Horizontal and Vertical Hydraulic conductivity zones for the Second layer

Values of storage coefficient obtained by different methods are assigned to their corresponding locations in each zone as shown in Table 6.

For those samples taken from different soil horizons from the same location the average of the top soil layers were assigned to the location. Then average values of those points with small variations between the

values obtained using different methods were assigned to the corresponding zones (soil hydraulic property zones were used as background for the point specific yield estimates).

Table 7. Assigned Storage coefficient values to different zones of the second layer

	Highly weathered and fractured	Weathered and highly fractured	Highly fractured	Fractured	Slightly fractured
Zone No	1	2	3	4	5
Sc Value Assigned	0.00009	0.00002	0.000009	0.000005	0.000002

Similar to hydraulic conductivity, specific yield for the first unconsolidated layer is assigned based on the laboratory results as indicated in the table 7. The assignment of storage coefficient values for the second layer zones is based on the results of the previous studies. The values assigned to the corresponding zone is based the ranking of the hydraulic conductivity zones as shown in table 7.

❖ **Transpiration from Groundwater and Assigning in MODFLOW (Tg):** As described in the flow chart on figure 11; first the area covered by each species should be known in order to assign values of transpiration from groundwater (Tg) rate to each grid of the model. To do so vegetation in the catchment is classified using the August 2009 Quickbird image as shown on Figure 17 (top right).

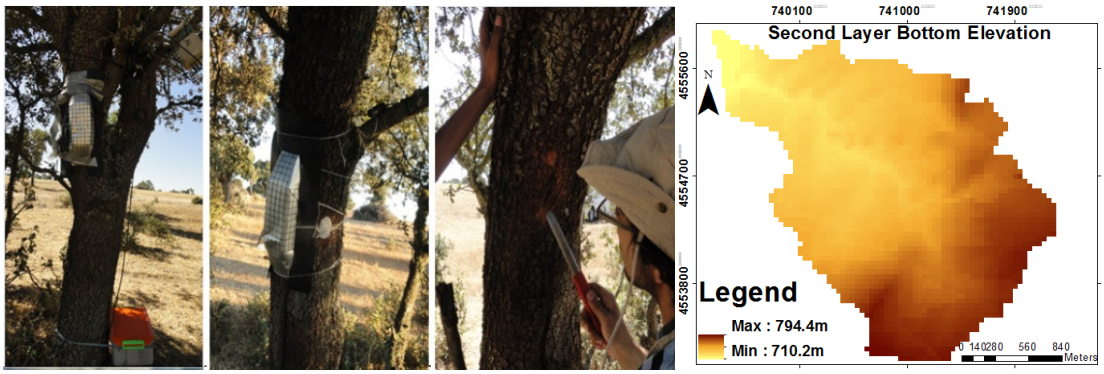

Figure 28. Measuring sap flow (left) second layer bottom elevation (right)

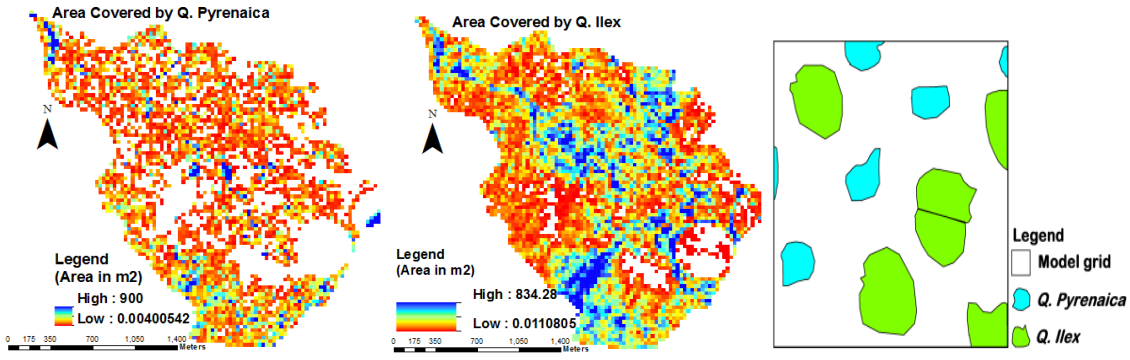

Figure 29. Sum of are covered by *Q. Pyrenaica* (left), *Q. Ilex* (middle) in each MODFLOW Grid (right)

The classified two species were polygonized so as to calculate the area covered by each species in each cell (Figure 29-left & middle). To know their coverage in each grid cell of MODFLOW a mesh of polygon with a size of the MODFLOW grid is created and intersected with the polygon maps of the species. The area covered by each species in each grid is then calculated by summarizing or summing the new polygons in each cell (Figure 29-right). Using the summation (area of each species) as a value the new polygons are

rasterized. These new raster maps of Area Coverage of Q.pyrenaica and Q.Ilex (Figure 29) are multiplied by the daily transpiration rates from groundwater obtained from the sap flow measurement (Figure 28) for each species and are finally imported to MODFLOW. Transpiration rate from groundwater (Figure 41) multiplied by area covered by the corresponding tree species as indicated in table 9 are assigned to the recharge package (negative value) of MODFLOW. A detail of this process is shown on the flow chart on Figure 30.

Time Discretisation

Selection of Time steps is critical step in model design because the value of space and time discretization strongly influences the numerical result. Time is usually discretized in to stress periods based on the fluctuation of precipitation, evaporation, transpiration and abstraction that cause the aquifer to respond through change in groundwater level.

Table 8. The multiplier (the rate of evaporation in md-1) per canopy area of the species in September 2009 & 2010

Stress Period	Days in September	QI_2009		QP_2009		QI_2010		QP_2010	
		Total	From gw	Total	From gw	Total	From gw	Total	From gw
1	1-10	4.96E-06	3.10E-06	2.23E-06	8.92E-07	3.92E-06	1.57E-06	4.19E-06	1.84E-06
2	11-20	4.17E-06	2.55E-06	1.91E-06	7.64E-07	4.06E-06	2.31E-06	4.54E-06	2.35E-06
3	21-30	4.66E-06	3.07E-06	1.83E-06	7.31E-07	3.25E-06	2.00E-06	4.74E-06	2.55E-06

Among the mentioned factors only evaporation and transpiration are considered in this study due to nonexistence of the remaining variables as mentioned in previous sections of this document.

Since evaporation is treated by HYDRUS as discussed in time discretization section of unsaturated zone model design, it is not considered in time discretization of MODFLOW. The only factor left is transpiration, which is measured by the two field campaigns in September of each study year. Since a full record of the whole month of each year could not found, average value of ten days of the existing data is taken and used as a stress period. Therefore three stress periods with ten days of time steps each are used as discretization of time for MODFLOW as shown in table 10. The measured rate of transpiration from groundwater per cell as shown in table 10, of each species is multiplied by the corresponding area covered by each species is summed and assigned to recharge package of MODFLOW (negative values is used as it is against recharge).

Table 9. Rate of transpiration from groundwater in mmd-1 per cell of each tree species for three stress periods

Year	Stress Periods	Time steps	TR_Q.P per cell in mmd-1	TR_Q.I in mmd-1
2009	1	10	0.0000892	0.00031
	2	10	0.0000764	0.000255
	3	10	0.0000731	0.000307
2010	1	10	0.000184	0.000399
	2	10	0.000235	0.000332
	3	10	0.000255	0.000380

2.4.4. Model Calibration and Uncertainty Analysis

The calibration of the model is performed manually as it is unsuitable because of the coupling to use the automatic calibration technique, PEST. The calibration target is minimizing the difference between the measured and or the extrapolated water level values with the simulated ones. Prior to calibration the accurate and dense measurements of water levels should be taken to minimize discrepancy using different optimization techniques mentioned above like make use of recession curve methods as shown on figure 26 & 32, take as much as possible auguring points and go deep as much as possible to reach water level (Figure 6-left), walk around the catchment so as to find naturally exposed water levels (Figure 23-right), use those piezometers dug for isotope tests (Figure on Annex) and etc. Finally minimization the difference between the simulated and measured water levels was done by readjusting reasonably the values of input parameters of the model until the minimum possible value of error is obtained. Details of the calibration result and its comparison with result of Master Recession Curve is discussed in chapter three of this document.

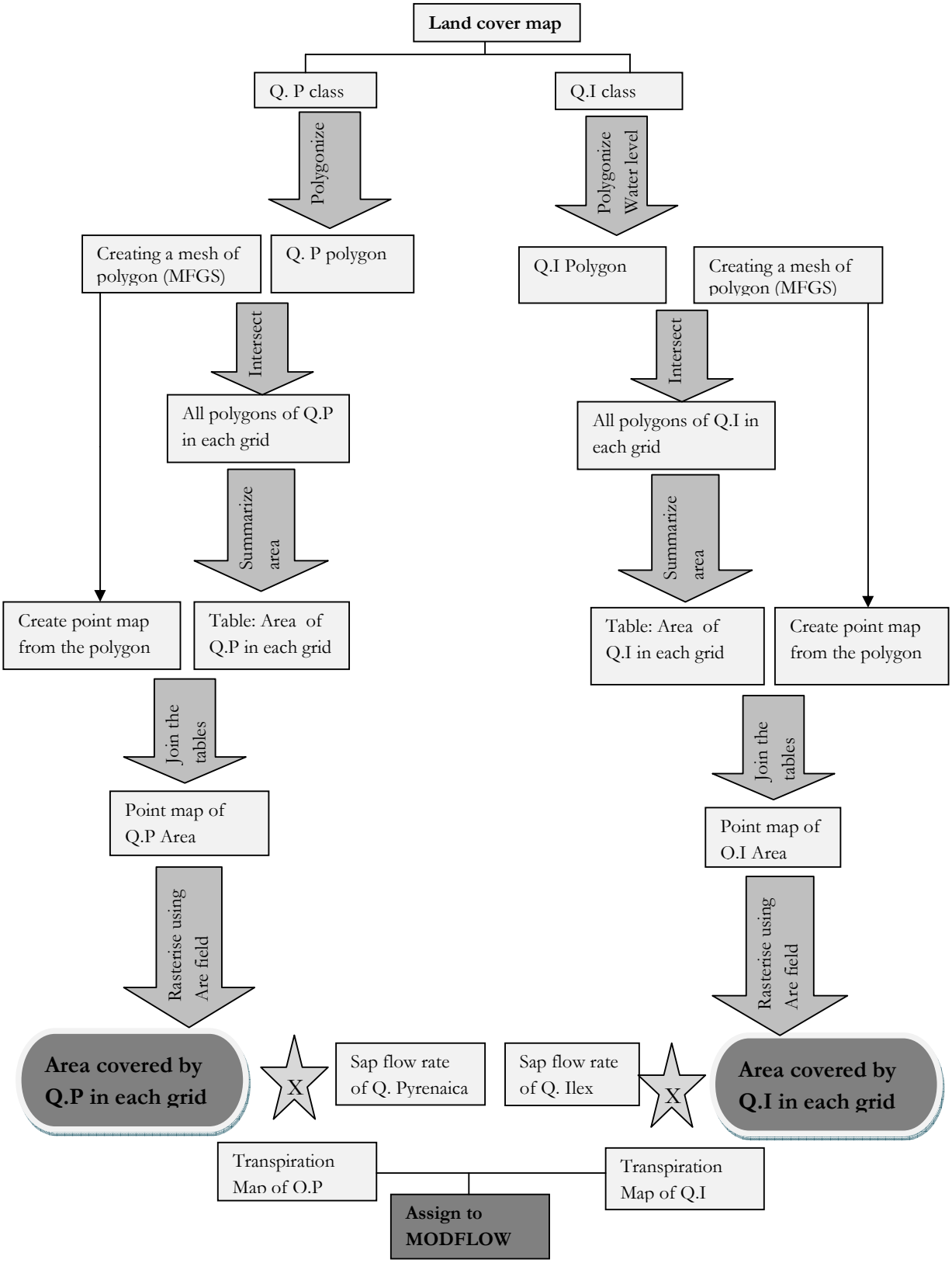

Figure 30. Flow chart: Creating the area covered by each species in each MODFLOW grid

3. Result and Discussion

3.1. Hydraulic properties of the Grantic Rock and Soils in the Catchment

Based on the analysis of field and laboratory samples soils in the catchment are categorized in to three types with slightly different hydraulic properties, as shown in Table 10. The difference is related to slope. Because the parent rock sources and causes of all the soils in the study area is so similar that they have similar hydraulic properties. As it can be observed from this summary table all the methods gave almost similar values of hydraulic parameters and the same texture (sandy loam). The sandy nature of all the soils is due to their being the weathering products of granitic rock.

Table 10. Summary of hydraulic properties (average of all samples from similar location) of the main soil types in La Mata Catchment

Sample Area	Θr SWAP	Θr Wp4	Θs SWAP	Θs Wetting	Ks (m/d) SWAP	Ks Double Ring (m/d)	Ks (m/d) Permea.	α	N	L
Sloppy	0.087	0.090	0.4172	0.375	2.1	1.92	2.21	0.143	2.28	0.5
Gentle	0.059	0.069	0.4038	0.245	1.5	1.82	1.67	0.124	1.89	0.5
Flat	0.031	0.058	0.4038	0.115	0.85	1.67	1.14	0.075	1.51	0.5

NB: α, N & L are derived from Models like HYDUS 1D & Rossetta using texture analysis result as an input,

3.2. Recession Characteristics of Granitic Rocks

Water-table fluctuations occur in unconfined aquifers owing to ground-water recharge or discharge. For instance following precipitation or infiltration and ground-water discharge to streams between storm events the water table may raise or fall. With the presence of continuous record of water level of wells a recession curves can be plotted and some aquifer characteristics such as recharge and transmissivity can be retrieved. Especially Master recession curve (MRC) a characteristic water-table recession hydrograph is more helpful as it represents the average behaviour for a declining water-table at a given site.

In any given system, such as an aquifer or stream, individual recession segments recorded at different times may have different slopes depending on the variability in storage, evaporation loss, and recharge rates. Nathan & Mahon (1990).stated that in many cases it is possible to compile individual recessions into a single recession curve that provides an average characterization of head, flow, or other observed variable response; the MRC. Recession rates are strongly influenced by the antecedent conditions of the system, and thus the MRC represents the most probable recession scenario under a given situation.

In order to plot MRC, variable-length recession periods were manually extracted from five piezometer water level records as shown in Figure 31 and plotted in descending order. Then individual recessions were interactively shifted along the ordinate axis until all the recessions overlap in the desired fashion. For this study the MRCs are mainly used to obtain the missed water levels due to dryness of the piezometer or absence of records during the required simulation period as shown in Table 12. MRC estimate of a piezometer (Ptb) was also compare with the simulated water levels by the coupled model (

Figure 32).

Different aquifer systems react (through fluctuation of the water table) differently for these subsurface fluxes. From a long term record of such reactions it is possible to identify or study some properties of an aquifer. Good example is well hydrograph that can be plotted if a good record of the fluctuation exists (Figure 25 & Figure 31). For instance from quantitative well hydrograph analysis like recession segment technique one can determine recharge (example Shakya (2001)), transmissivity (example Powers & Shevenell (2000)) and discharge from the aquifer.

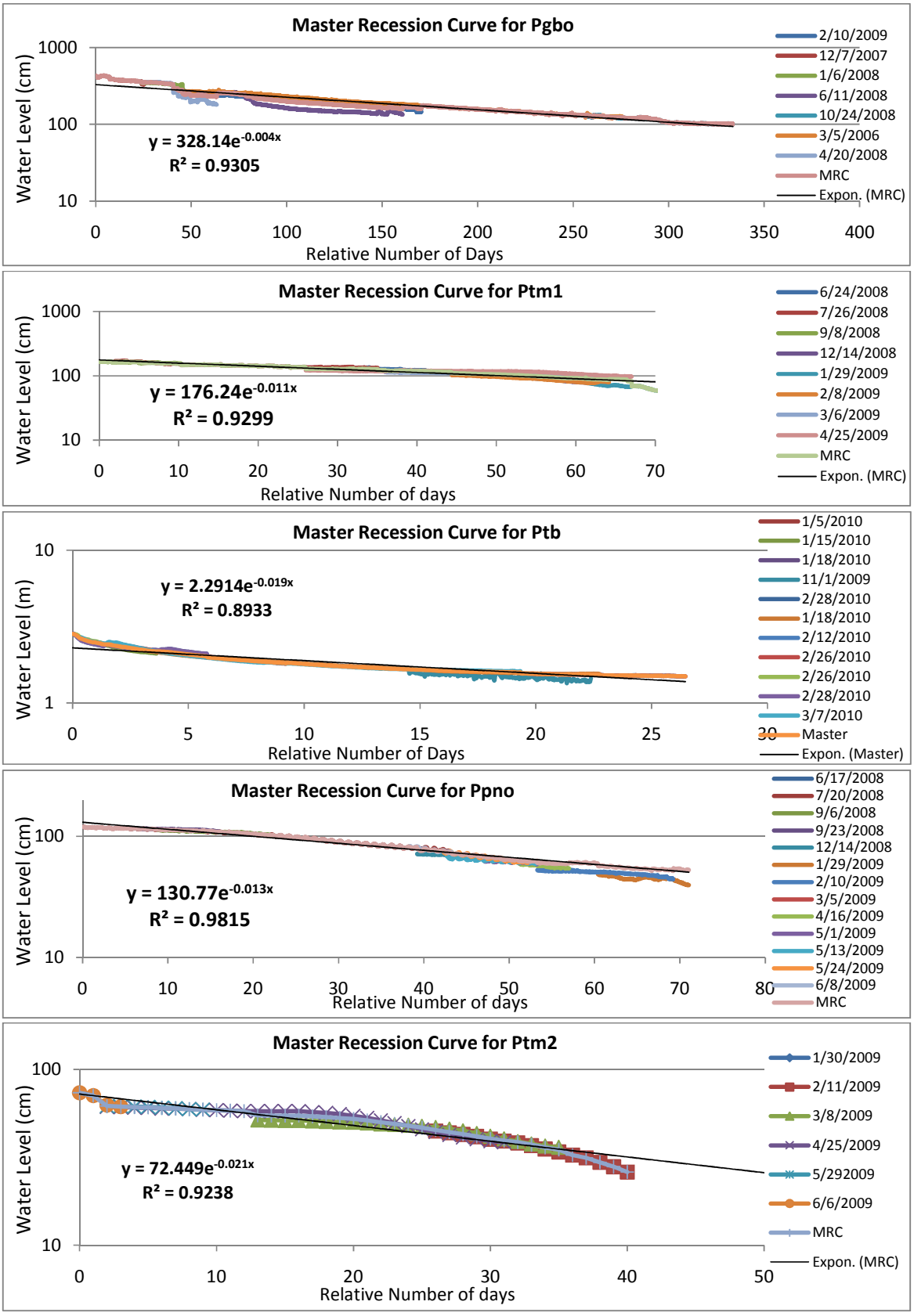

Figure 31. Master recession curves of Well hydrographs of five Piezometers in La Mata Catchment and its vicinity

Table 11. Water levels retrieved from MRC (location in table Table 12 and shown on maps on Figure 3)

No	Piezometer ID	Last reading Date	Last reading Water Level (cm)	Water Level Retrieved from MRC for September 1, the same year (cm)	Equation MRC (H=)
1	**Pgbo**	6/12/2009	134	237.1	$328.14e^{-0.004t}$
		5/25/2010	146	261.05	
2	**Ppno**	6/13/2009	76	204.74	$130.77e^{-0.013t}$
		5/23/2010	52	251.35	
3	**Pmt1**	9/22/2009	250	192.28	$176.24e^{-0.011t}$
		5/23/2010	119	420.57	
4	**Ptb**	7/3/2009	27.54	169.97	$2.2914e^{-0.019t}$
		5/23/2010	2.11	186.61	
5	**Pmt2**	6/12/2009	112	194.73	$76.814e^{-0.025t}$
		5/23/2010	31	147.4	

3.3. Simulation Results Using average Values of transpiration

3.3.1. Comparison of Simulated Measured and MRC estimate of Hydraulic Heads

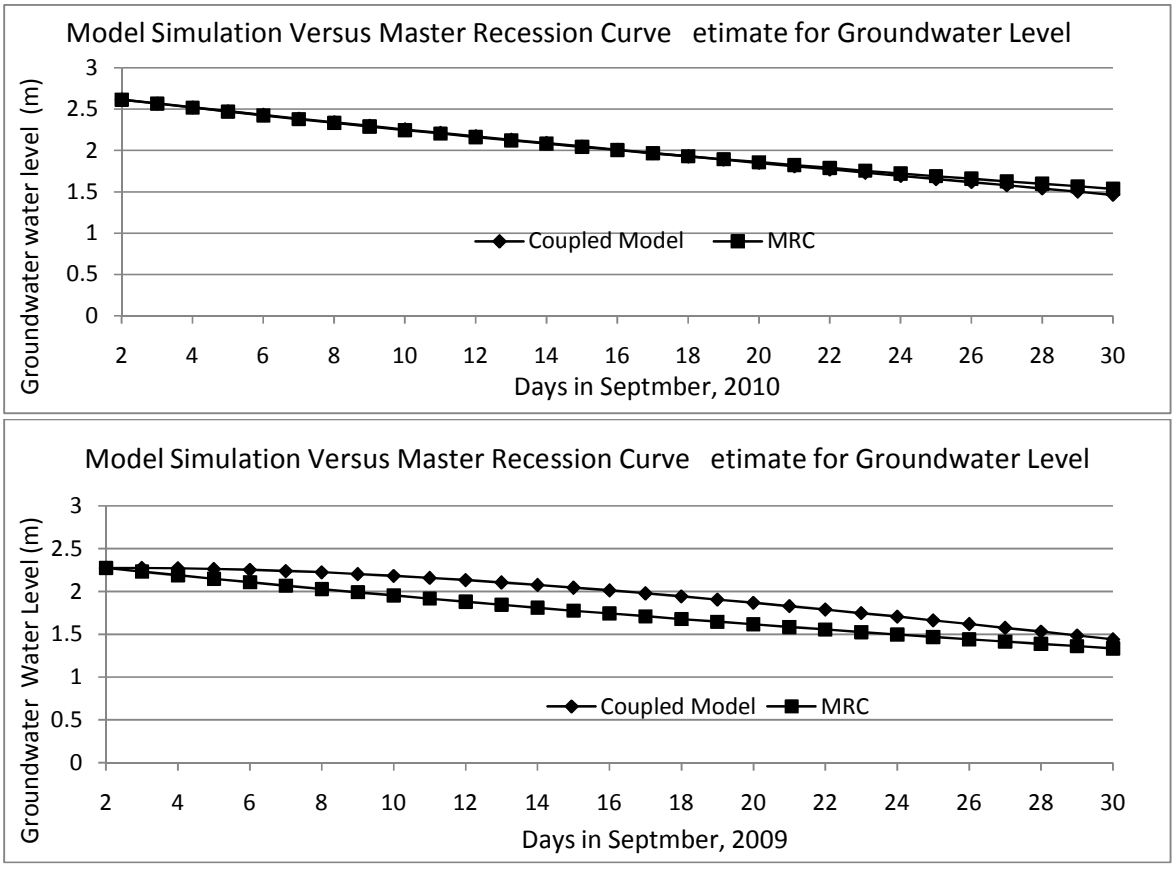

Figure 32. Comparison of groundwater level estimated of Master Recession Curve and Model Simulation for Seotember 2009 (top) and 2010 (bottom); (RMSE = 0.2m for 2009 and 0.02m for 2010)

There exist more than fourteen points (Figure 2 & Figure 3) where measurements of groundwater levels in the catchment can be taken. Since some of them are already dry during the campaign the MRCs discussed above are used to retrieve groundwater levels of the dry piezometers. For the piezometers like the one in the Trabadillo monitoring station recession curves are used to estimate the groundwater level during the study period. Among these existing points including the piezometers drilled for isotope testing (for partitioning of transpiration) measurements from thirteen points listed in Table 12 were used to interpolate initial hydraulic heads and finally to analyze the uncertainty of the model.

The model is calibrated so as to reduce the error between the measured and simulated hydraulic heads and the obtained values in cm for the errors for the simulation period of September 2010 are –o.645, 0.645 and 0.731 for ME, AME and RMSE, while –o.625, 0.535 and 0.621 respectively for September 2009 (Figure 35).

The simulated water level at Trabadillo piezometer was compared with that of the estimate by Master recession curve as indicated on

Figure 32. The two estimates were fit as shown on the graph with an error of 0.2m and 0.02m RMSE for September 2009 and 2010 respectively. The two estimates of water table fitted best for 2010 as compared to 2009, because the calibration of the model was done using 2010 data. Also it should be noted that water level estimate of the coupled model doesn't represent a point (rather zone) in the model while recession cureve is a result of single piezometer.

Different aquifer systems react (through fluctuation of the water table) differently for these subsurface fluxes. From a long term record of such reactions it is possible to identify or study some properties of an aquifer. Good example is well hydrograph that can be plotted if a good record of the fluctuation exists (Figure 25 & Figure 31). For instance from quantitative well hydrograph analysis like recession segment technique one can determine recharge (example Shakya (2001)), transmissivity (example Powers & Shevenell (2000)) and discharge from the aquifer.

Table 12. Water level points used for interpolation, MRC and calculation of errors

No	Piezometer/Point measurement name	Location (UTM)		Description	Remark
		X	Y		
1	Pisotope1	739471.1	4555899	Piezometer for isotope measurement	
2	Pisotope2	739562	4555779	Piezometer for isotope measurement	
3	Pisotope3	739514	4555851	Piezometer for isotope measurement	
4	Aug1	740341	4555154	Groundwater level obtained from augering	
5	Aug2	740141	4555210	Groundwater level obtained from augering	
6	Aug3	740751	4554766	Groundwater level obtained from augering	
7	NE1	739504.6	4555794	Naturally existing	
8	NE2	739385	4555808	Naturally existing	
9	Pgbo	741435.1	4551574	Piezometer	Using MRC
10	Ppno	738315.9	4554146	>>	>>
11	Ptm1	737006.2	4551116	>>	>>
12	Ptb	739505	4555886	>>	>>
13	Ptm2	737067.2	4551353	>>	>>

3.3.2. Comparison of PM Actual Evapotranspiration with the Model Estimate

Actual evapotranspiration using penman Monteith equation (taking soil hydraulic property in to account) is calculated and compared with the total ET which is the sum of Eu, Eg, Tu and Tg, where Eu and Eg are obtained from the HYDRUS 1D and the coupled model while Tu and Tg are sap flow measurements. The two estimates for both years excluding the first five days fitted better and the errors (ME, AME and RMSE) between the two for 2009 are -0.0084, 0.0092 and 0.00011 while -0.013, 0.014 and 0.00025 for 2010 respectively.

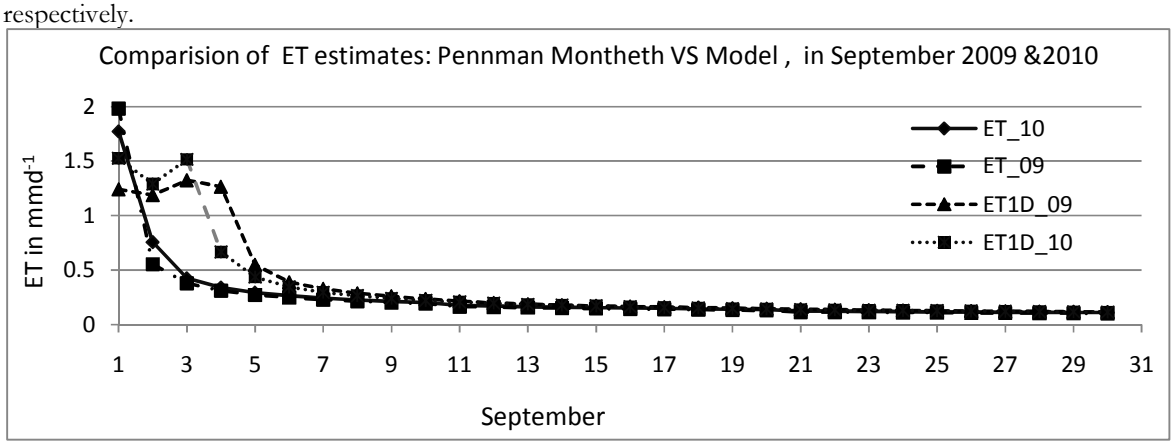

Figure 33. Comparison of ET estimates of Penman Monteith with Total ET simulated by the Model

The two estimates are nicely correlated except for the first few days where there exists model instability due to the initial conditions at the beginning of the simulation period as shown on Figure 33.

3.3.3. Spatial and Temporal Distribution of Subsurface Fluxes in the Catchment

The fluxes & definitions of terms used in this section: as shown in Figure 36 **UZSC (+CS)** is Unsaturated zone storage change, **Eg**: evaporation from groundwater **Eu**: evaporation from unsaturated zone; **BF** (Bottom flux)=Eg+UZSC; **TF** (Top flux) or evaporation (**E**)= Eg+Eu, **D**: flow through drain; **Tg** & **Tu** are transpiration from saturated & unsaturated zone respectively (their sum **Tt**).

The main source of inflow in the catchment is considered recharge from rainfall (nil during this study) while the out flow is caused by drains or streams Sardon & La Mata along the out let of the catchment, Evaporation and Transpiration (Figure 36). No extraction in the catchment. The values of these fluxes, their spatial distribution and discussion concerning the values and the distribution are presented below.

Color representation used for mapping is reddish for low and bluish for high evaporation or transpiration or evapotranspiration, referred from (Tomczak, 2010)

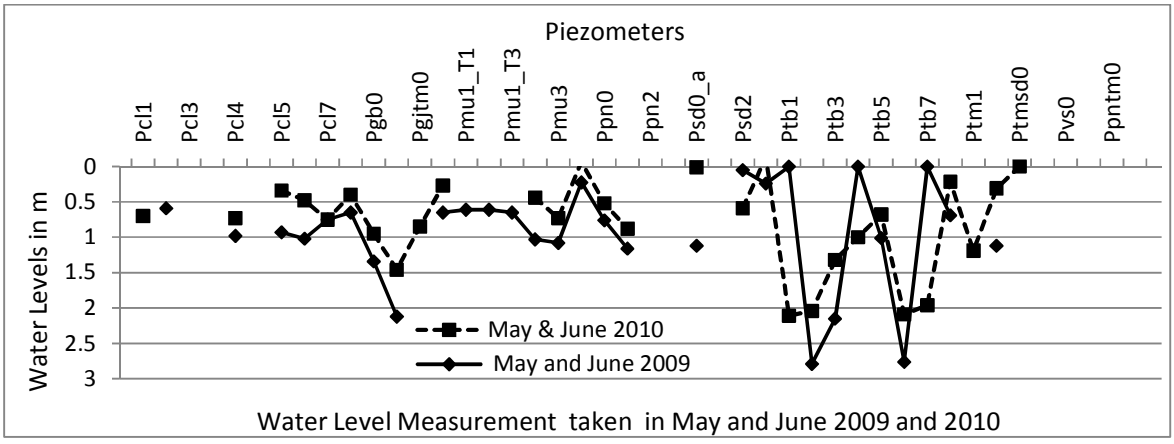

Figure 34. Depth to groundwater in year 2009 and 2010

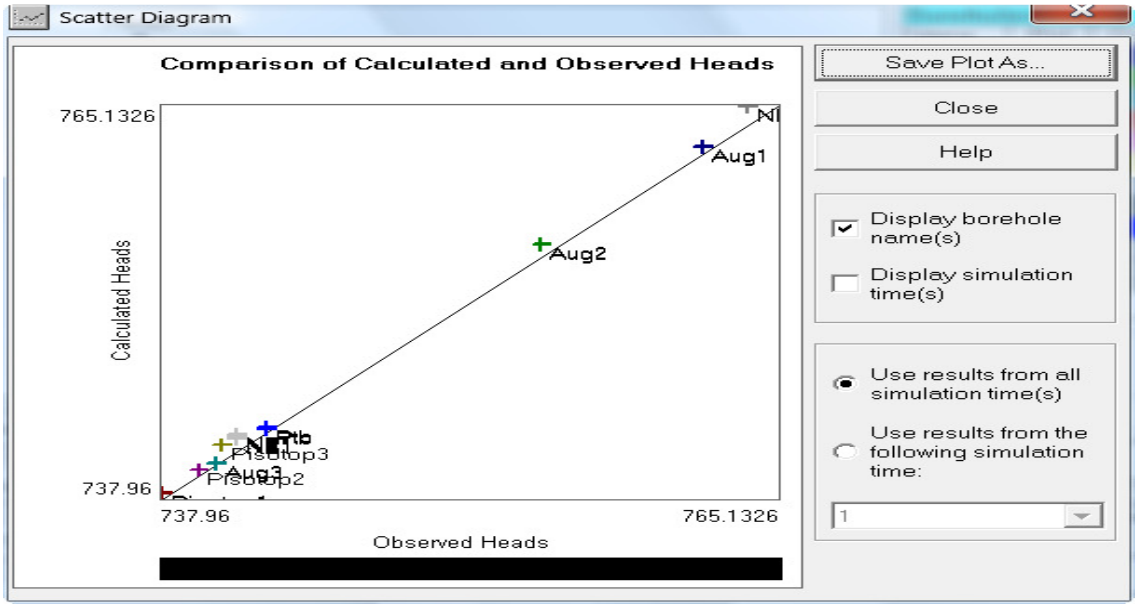

Figure 35. Comparison of the simulated and measured or retrieved hydraulic heads

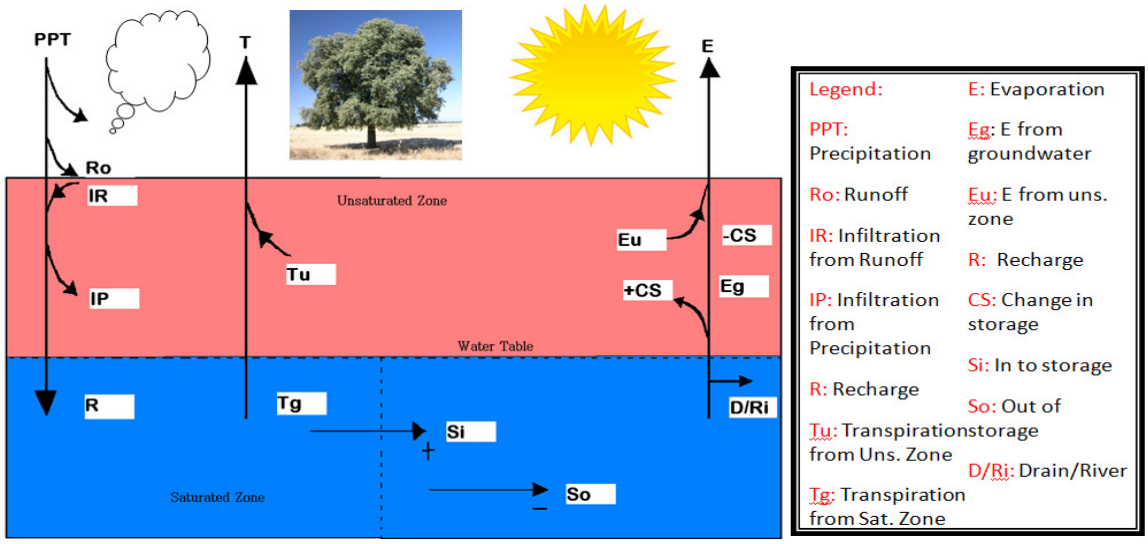

Figure 36. Subsurface fluxes

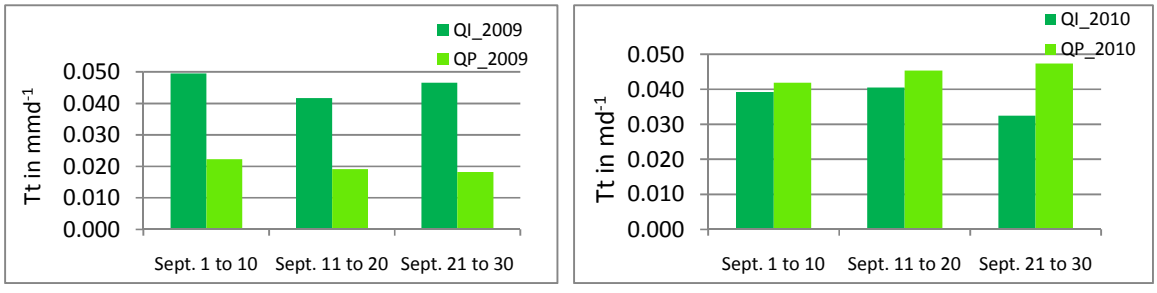

Figure 37. Tt of the two species every ten days (averaged) per cell, September 2009 (left) & 2010 (right)

i. Total Transpiration

As it was also discussed earlier the annual precipitation in the year 2009 is lower than that of 2010. Its effect can be recognized from measurements of water levels of the piezometers taken in May and June of the two years, 2009 and 2010 as shown on

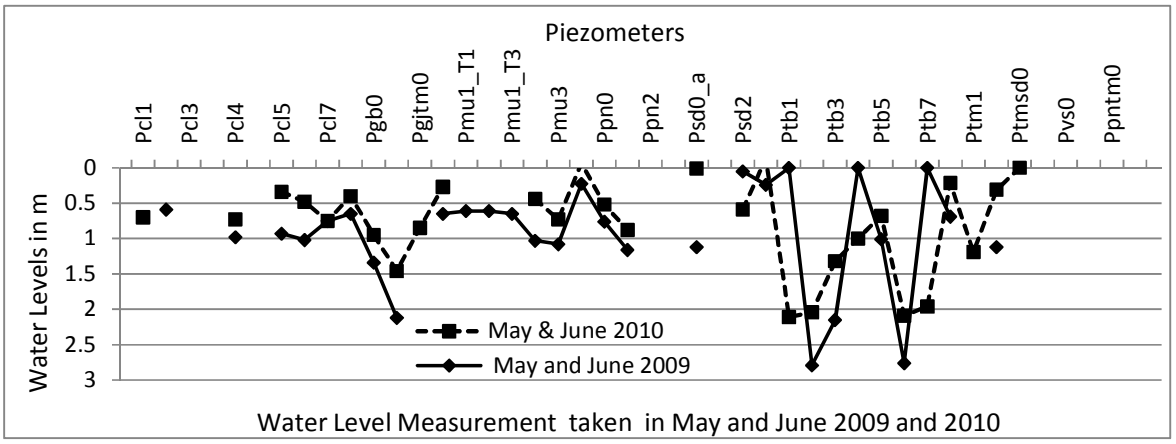

Figure 34 where the average decrement in water levels was 0.44m.

As a result the rate of transpiration of trees was also changed as the main causes for the change is either the weather condition or the availability of water. Since September was sunny during both years, the change in water level can be considered as the reason for the change of transpiration. This was justified by the response of the two species, *Quercus Pyrenaica* and *Quercus Ilex* to the change as shown on Figure 38 (A) and (B). If the cause was weather condition the rate of transpiration of both species will rise or fall together. But water level change may cause the two species to act differently. It can be observed from the graphs on Figure 38, in 2010 when depth to groundwater is shallower the amount of transpiration by *Q. pyrenaica* is higher while during the less water in the unsaturated zone (the water table is deeper) *Q. ilex* takes more water may be because of the deeper roots of *Q. ilex* as compared to *Q. pyrenaica* and the mechanism of *Q. pyrenaica* that varies its rate of transpiration with availability of water.

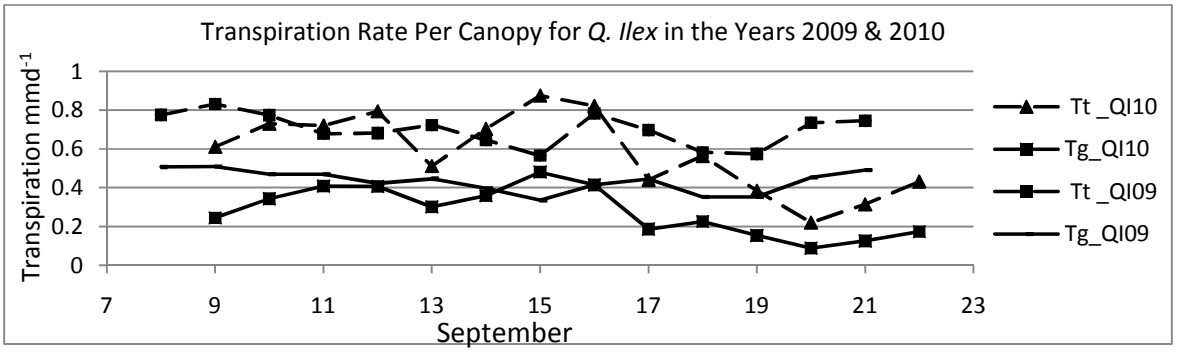

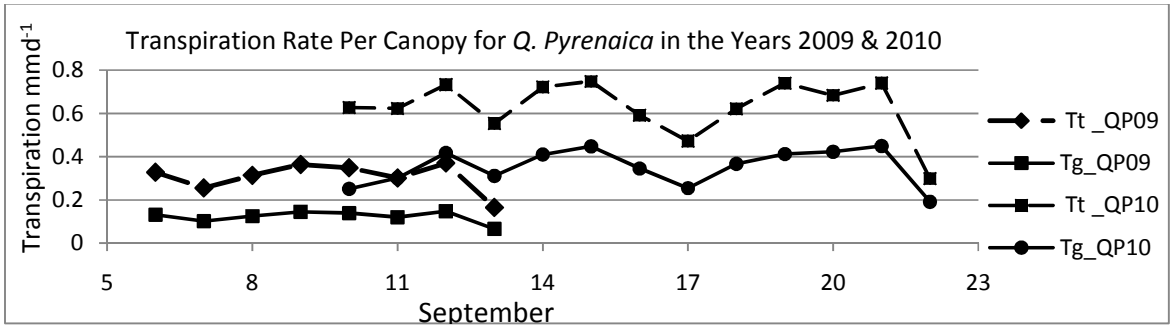

Figure 38. Transpiration rate (Total & Tg) of Q.I (top) and Q. P (bottom) for September 2009 & 2010

ii. Correlation between Transpiration rate and Meteorological Variables and ETo

Sap flow measurements are sometimes inturrepted by technical failurities and because of other unknown factors. As a result it was tried to see if they have some relation with meteorological variables and ET0. From the data used for the two simulation periods (full month of September 2009 and 2010), September 9 to 14, 2010 was taken for further analysis because of the data quality and continuous measurement for both species in this range. The daily weather variables and ETo were plotted versus tree transpiration rate as illustrated on Figure 63. From this graph one can observe that temperature, relative humidity and ETo have a correlation with the transpiration rates of both species. The correlation coefficient is also calculated for both species versus each weather variables as shown on Table 13. So it was observed that the two species have similar correlation with the variables where temperature has better correlation with transpiration rate of both species while ETo has highest correlation with transpiration rate of *Q. Ilex*. Further study and data of long period is required inorder to conclude fully about the relation between these variables ane transpiration.

Table 13. Value of correlation coefficient of weather variable versus tree transpiration rate per species

Species	Weather Variable and Corresponding Correlation coefficient		
	Temperature	**Relative Humidity**	**ETo**
Q. Ilex	0.21	0.08	0.30
Q. Pyrenaica	0.21	0.09	0.10

iii. Transpiration from unsaturated Zone

The rate of transpiration of each species is calculated based on the sap flow measurement rates found from sample tree species during the field campaigns of September 2009 & 2010. The measurement is partitioned in to saturated and unsaturated transpiration based on the study of the (Leonardo J Reyes-Acosta, 2010) who used stable isotope tracing method to study the proportion of water taken from the different zones.. The partitioned rate is multiplied by the corresponding area covered by the species and divided to the area of the model grid to find transpiration rate per cell; finally summed to create map of Tu for the catchment. Based on this Tu map (Figure 39) is created for the interval of September 1-10, 11-20 and 21-30 , 2009 & 2010.
From the result it was observed that transpiration from unsaturated zone was higher in September 2010 (up to 0.2996mmd^{-1}) than in 2009 (which is only up to 0.1842mmd^{-1}). Tu decreased from an average of 0.077mmd^{-1} during the the begning of September to 0.092mmd^{-1} during the end of the month in 2009. Tu decreased from an average of 0.15mmd^{-1} to 0.12mmd^{-1} in September 2010.

iv. Transpiration from groundwater (Tg)

Similar to the Tu the partitioned proportion of Tg by *Q.P* and Tg by *Q.I* in each grid cell of the model was calculated (Figure 41) and summed to create the Tg map. As shown on Figure 42 the maps were created for the time intervals; September 1-10, 11-20 and 21-30 and also exported to the MODFLOW for the corresponding stress periods to assign as negative recharge.
As it is shown on maps on Figure 42 transpiration from groundwater per day was a bit higher in September 2009 (up to 0.26 mm) than in 2010 (which is up to 0.25mm) unlike that of from unsaturated zone. Within each year it was observed that the transpiration per day from this zone decreased from an average of 0.13 mm during the beginning of the month to 0.067 mm during the end of the month in 2009 and from an average of 0.126mm to 0.084mm in the years 2010.

V. Evaporation and Change in Storage of Unsaturated Zone (UZSC)

Daily Eu, Change in unsaturated zone storage and evaporation from groundwater are calculated using a HYDRUS 1D model. The inputs are daily bottom fluxes or pressure head at the bottom of each profile obtained from the coupled model. The remaining inputs are daily potential evaporation rate the same to the

input of the coupled model and soil profile that has similar discretization as that of the coupled profile. The output from this model is top flux from which the remaining fluxes can be calculated.

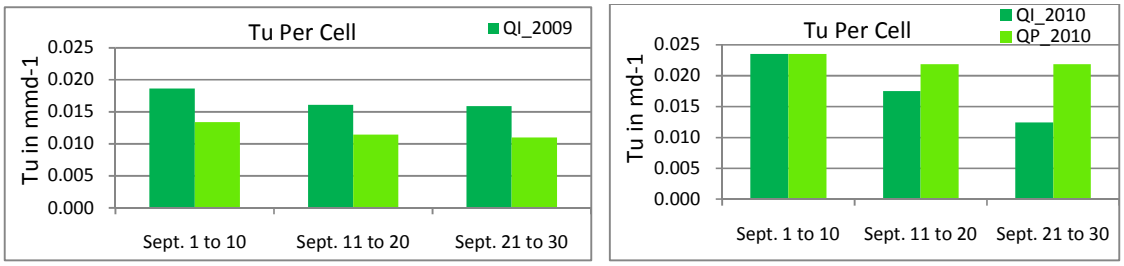

Figure 39. Tg rate of the two species every ten days (average) per cell, September 2009 (left) & 2010 (right)

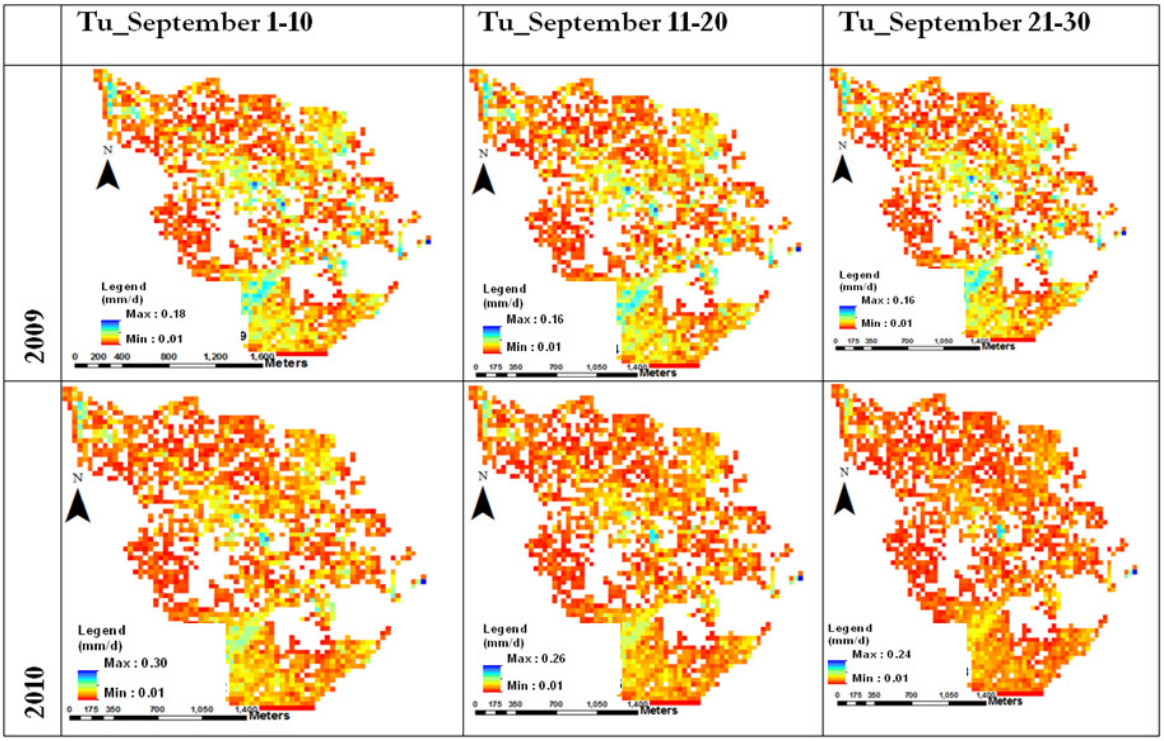

Figure 40. Map of Tu in mmd^{-1} for the given interval in September 2009 and 2010

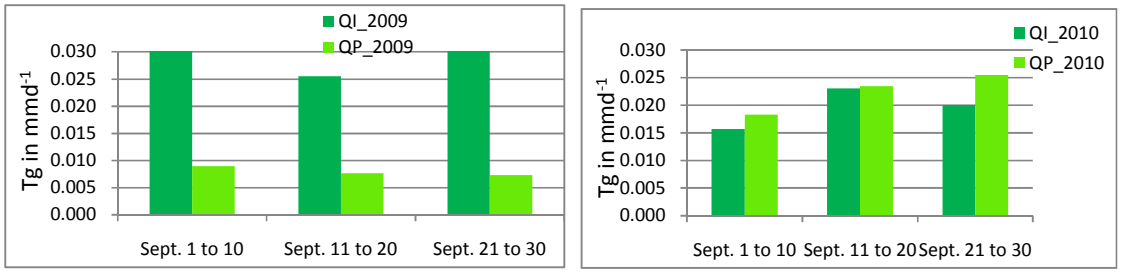

Figure 41. Average Tg rate of the two species every te n days per cell, September 2009 (left) & 2010 (right)

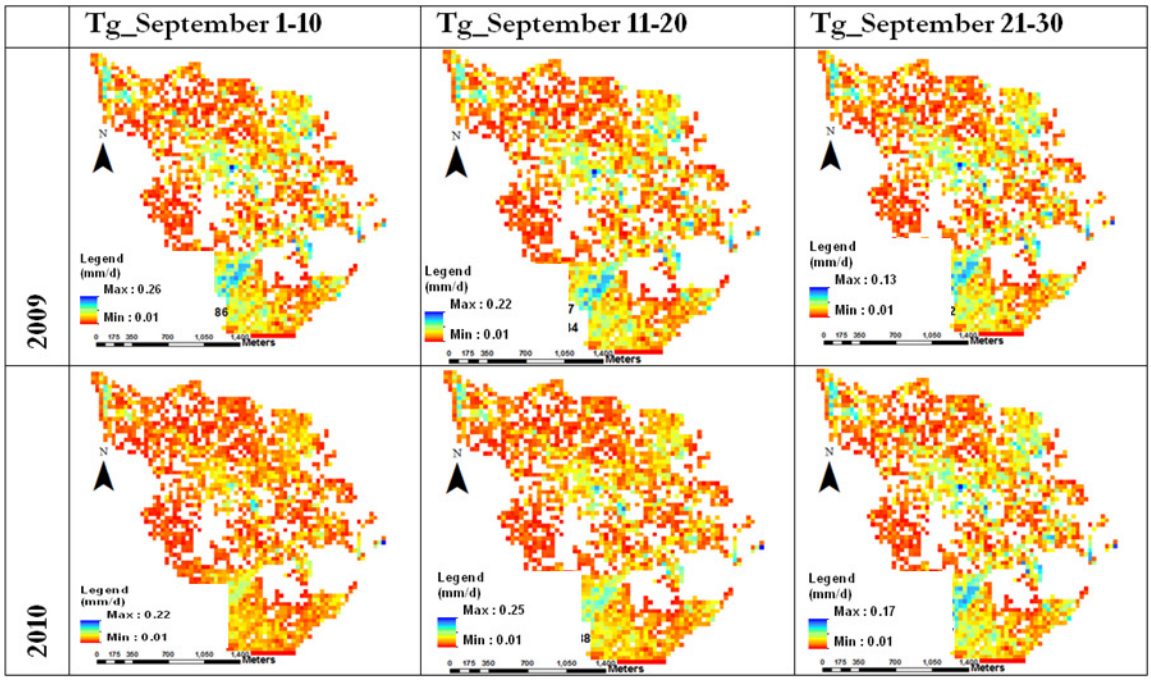

Figure 42. Map of Tg in mmd^{-1} for the given interva in September 2009 and 2010

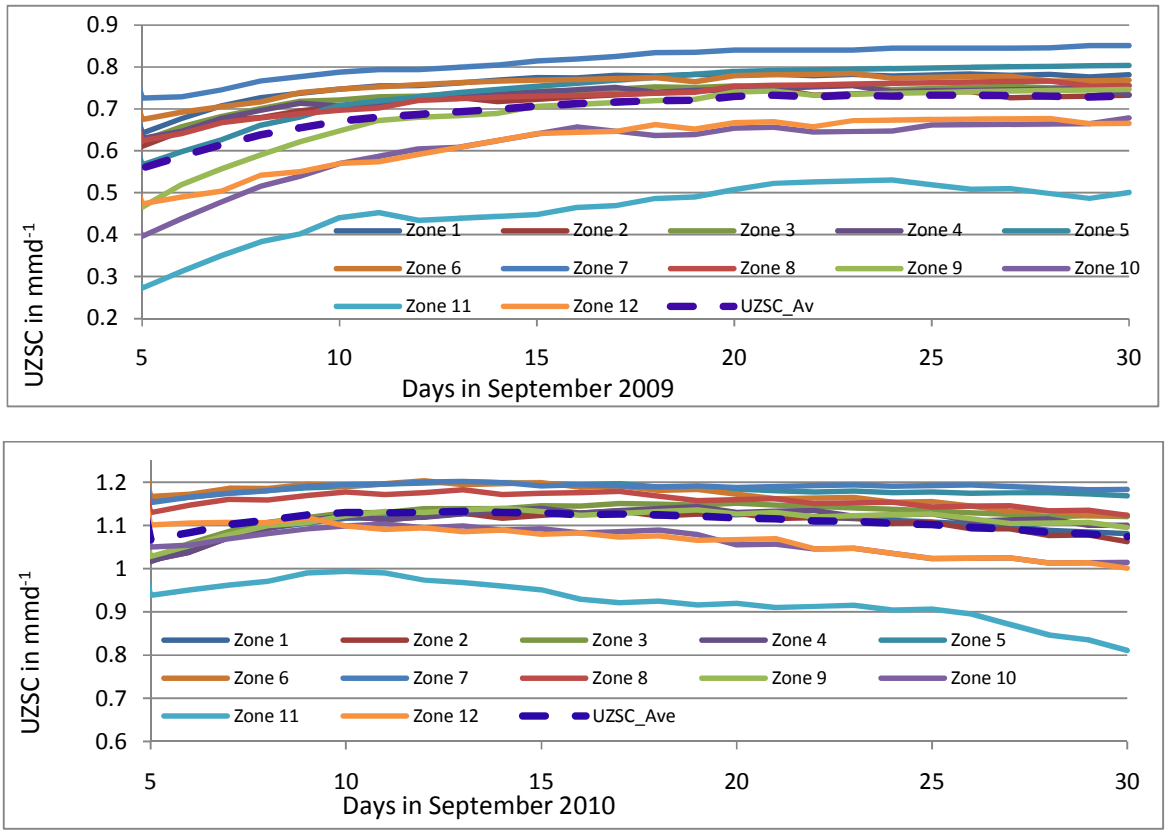

Figure 43. Zonal UZSC September 2009 (the first) and 2010 (the second)

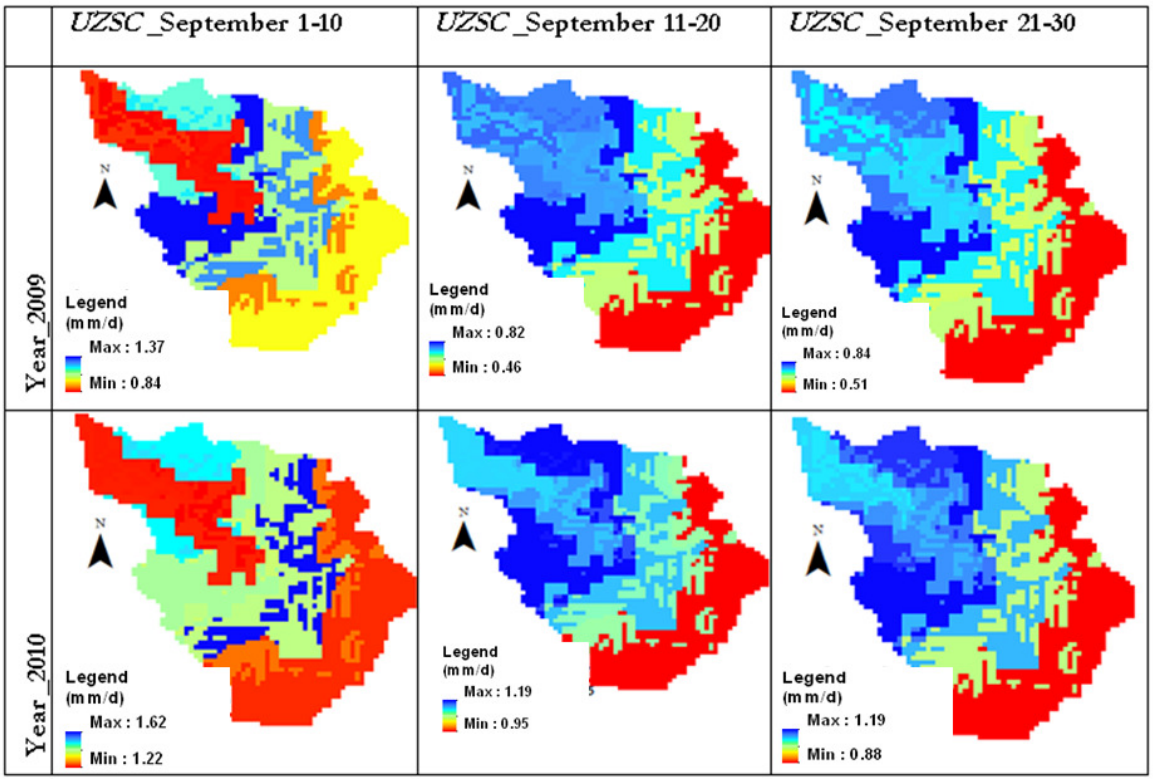

Figure 44. Unsaturated zone average change in storage (mmd-1) every 10 days in September 2009 and 2010

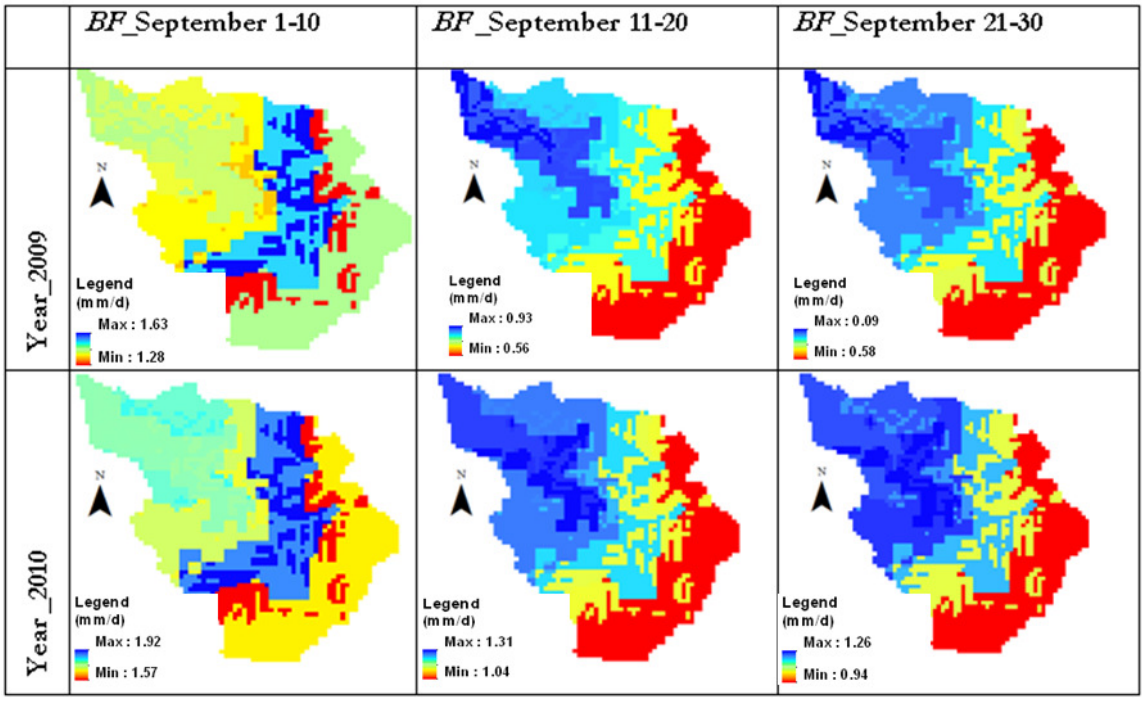

Figure 45. Maps of average bottom flux every 10 days of September 2009 and 2010.

The difference between the top and bottom flux is either Eu if top flux exceeds or change in storage otherwise. It is obtained by simply subtracting the top flux from the bottom flux. The calculation is done separately for each profiles of HYDRUS input zone. The result was zero for Eu at every zone and the

average value of change of unsaturated zone storage for every ten days is calculated to create a map of change in storage Figure 44. From this map it can be observed that change in storage varies both temporally and spatially. As shown on the maps the change in storage showed a decrement towards the end of the month during both years. Spatially the downstream part of the catchment showed more increment in storage while zones at the upstream periphery of the catchment remain the lowest in change of storage.
As shown on Figure 44 unlike Tu the average value of change in storage is less in September 2010 (average 0.8059 mmd^{-1}) than in September 2009 (average 1.145 mmd^{-1}). It was already observed that the weather condition favors ET and water table decline is also more in the year 2009 than in 2010. The high temperature, humidity and solar radiation and the shallow groundwater table might cause the more evaporation to exist in 2009 than in 2010. As a result more water is removed from unsaturated zone in 2009 than in 2010. However the rate of Eu decreases towards the end of the month during both years.
It was also observed that UZSC varied temporally more in 2009 than in 2010 while the trend of spatial variation remains the same every year. From figure 46 one can observe that zone 9 and 10 have lower UZSC rate while zone 11 and 12 had higher value every time. This is might be due to the hydraulic property of soil around the water table in zone 9 & 10 favors bottom flux better than the soil in zone 11 & 12.

VI. Evaporation from Groundwater and Bottom Flux

As also mentioned earlier bottom flux is calculated by the coupled model while the top flux is by HYDRUS 1D model using the bottom flux (output of coupled model) and the same weather and soil parameters as the coupled one as an input. Evaporation from groundwater in this document refers to the amount of water that leaves groundwater to the atmosphere which is less or equal to the top flux. If the bottom flux exceeds the top flux evaporation from groundwater is considered to be the top flux which is the bottom flux otherwise according to its definition in this document.
Like transpiration bottom flux is also higher in September 2010 (average 1.233mmd^{-1}) than that of September 2009 (average 1.047mmd^{-1}) as showed on Figure 45 and Figure 46.
During both years 2009 and 2010 the general trend of bottom flux from the beginning to the end of the month showed a decrement as it can be observed from the maps and the graphs of bottom flux at each zone. The average values of bottom flux have lower values at zone 10 and 11 while the remaining zones have no such significant difference as shown on graph of Figure 46.
Daily evaporation rate from groundwater in general showed a decrement in every zone (Figure 47) in the catchment. But it was observed for instance in September 2009 that the decrement is faster in zones with shallower water table than the deeper ones where the decrement is up to 0.74mmd-1 for the former and up to only 0.009mmd-1 for the later (Figure 48).
Evaporation from groundwater as it can be observed from maps on figure 49 and graphs on figure 48 has higher values at zones with shallow groundwater, and lower at deeper ones especially around zones with finer soil material around the water table, like zone 7. Zones with coarser material around the water table and deeper water table like zone 11 and 12 have always lower Eg as shown on Figure 47 and Figure 48. Eg is also higher in September 2010 than in 2009 like the subsurface fluxes discussed earlier. The rate of Eg has a declining trend during both years from beginning to the end of the month.

VII. Average Values of BF VS Eg and UZSC for the entire Catchment

All the fluxes during September 2010 are higher than in 2009 (figure 49 and 50) and their trend in each month of the year is decreasing. Concerning the comparisons of the fluxes among each other average value of BF is higher and Eg is lowest during both years (2009 and 2010) as shown on figure 49 and 50.
As it was shown on figure 51 for 2009 and figure 52 for 2010, Eg has always highest average value at the first ten days of the month, up to 0.585mmd^{-1} in 2009 and 0.536mmd^{-1} in 2010 at zones with shallow water table like zone 1, while lowest at zones with deeper water table up to 0.00227mmd^{-1}at the end of the month in 2009 (zone 7) and up to 0.0377mmd^{-1} in 2010 (zone 10).

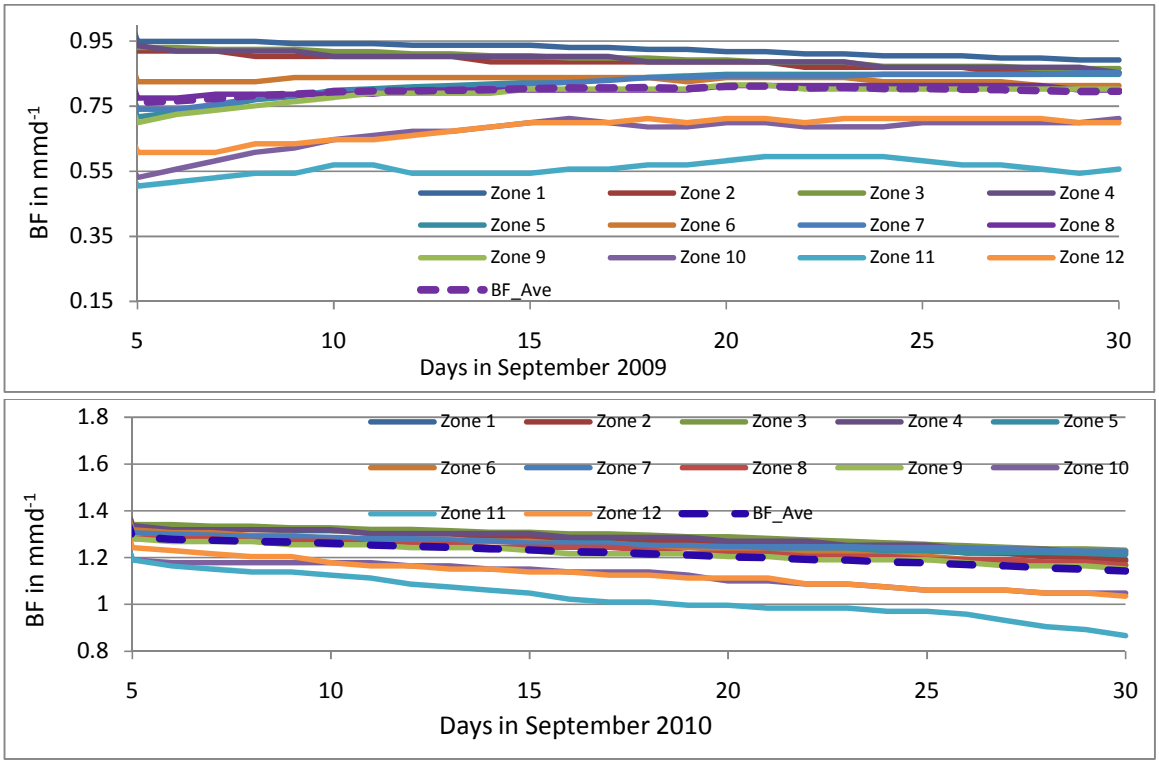

Figure 46. Daily bottom flux per zone for September 2009 (top) and 2010 (bottom)

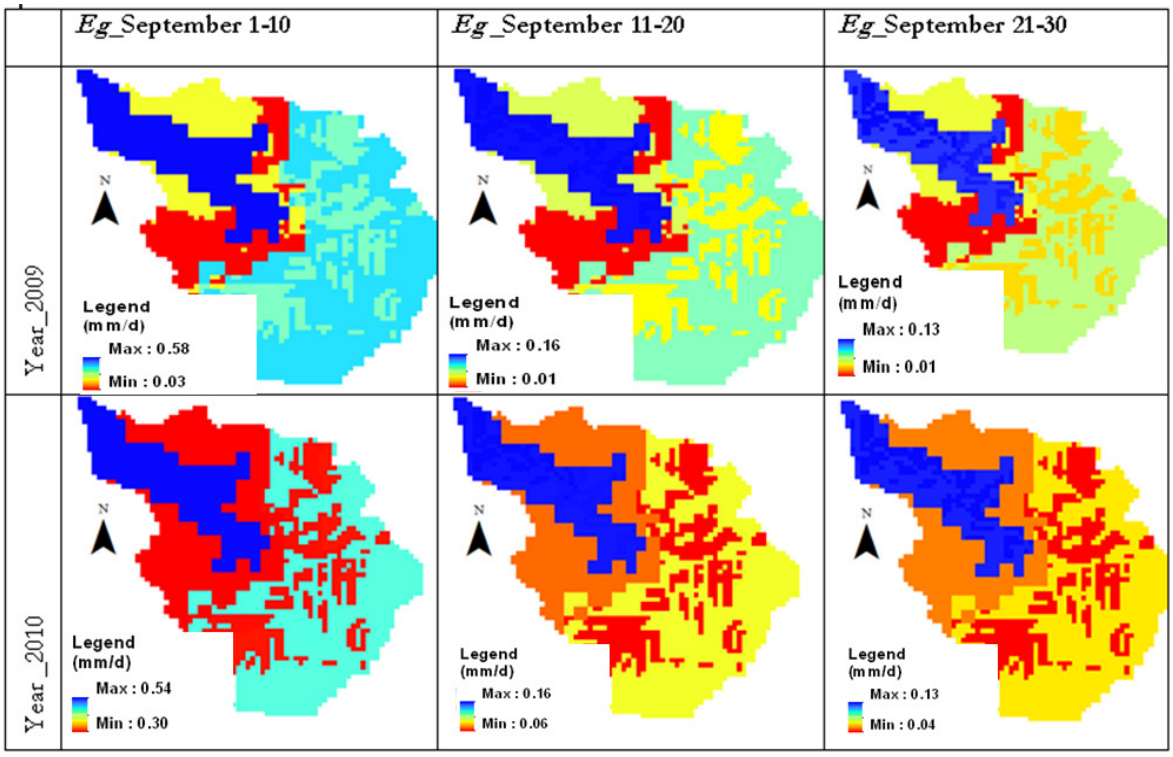

Figure 47. Maps of average Eg every 10 days of September 2009 and 2010.

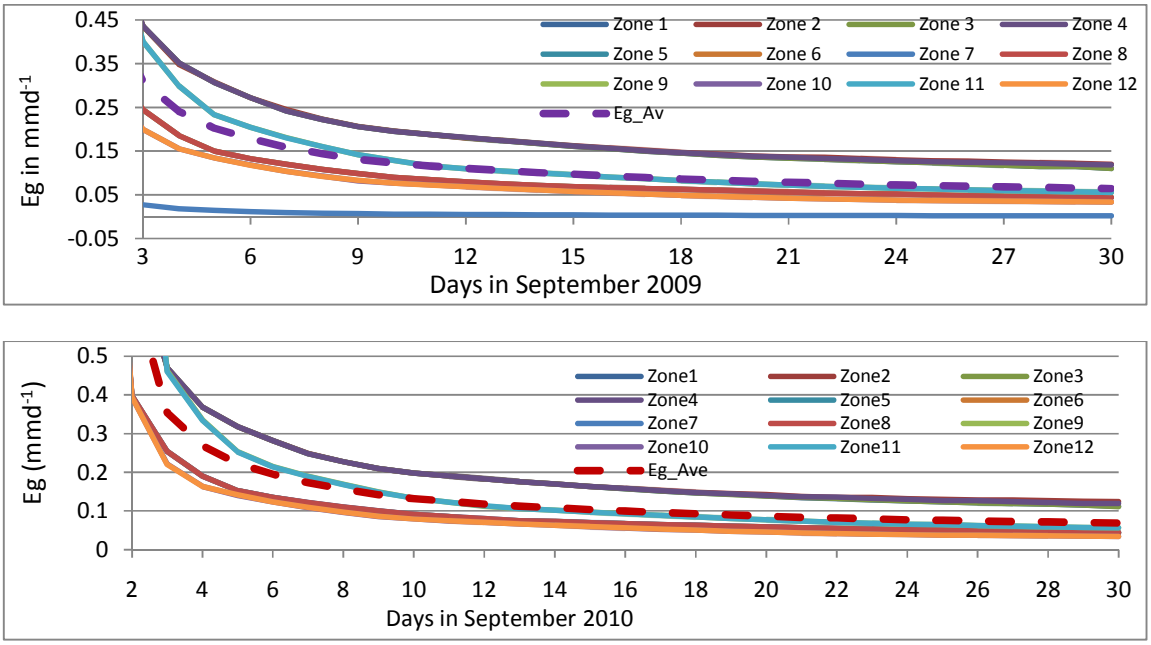

Figure 48. Daily groundwater evaporation per zone for September 2009 (A) and 2010 (B)

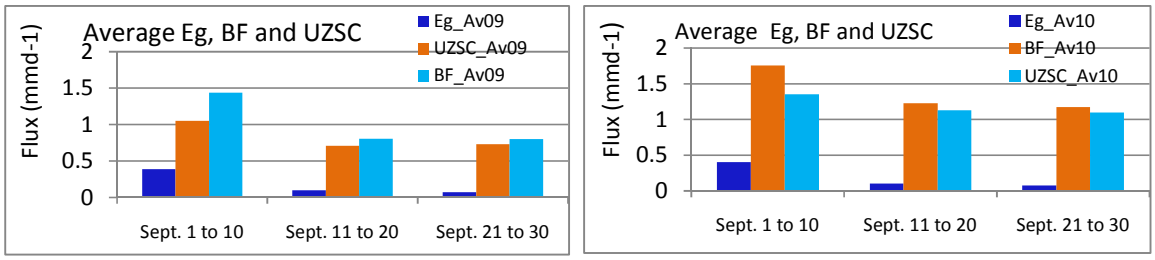

Figure 49. Average values of BF, Eg and UZSC every ten days, for September 2009 and 2010

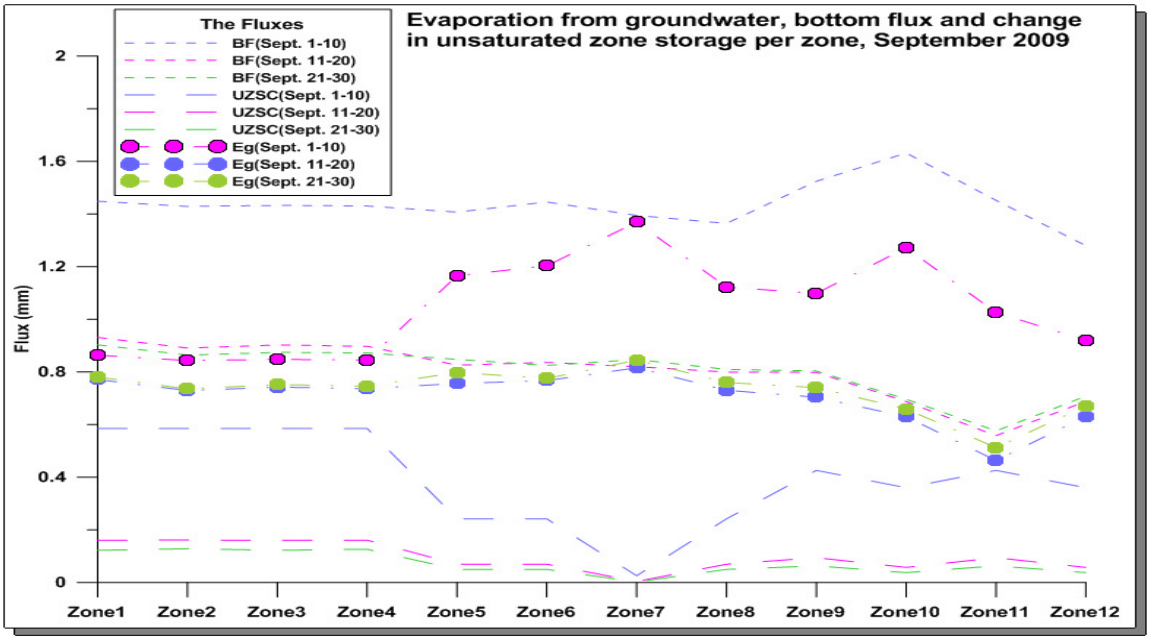

Figure 50. Average values of Eg, BF and UZSC every ten days per zone, September 2009

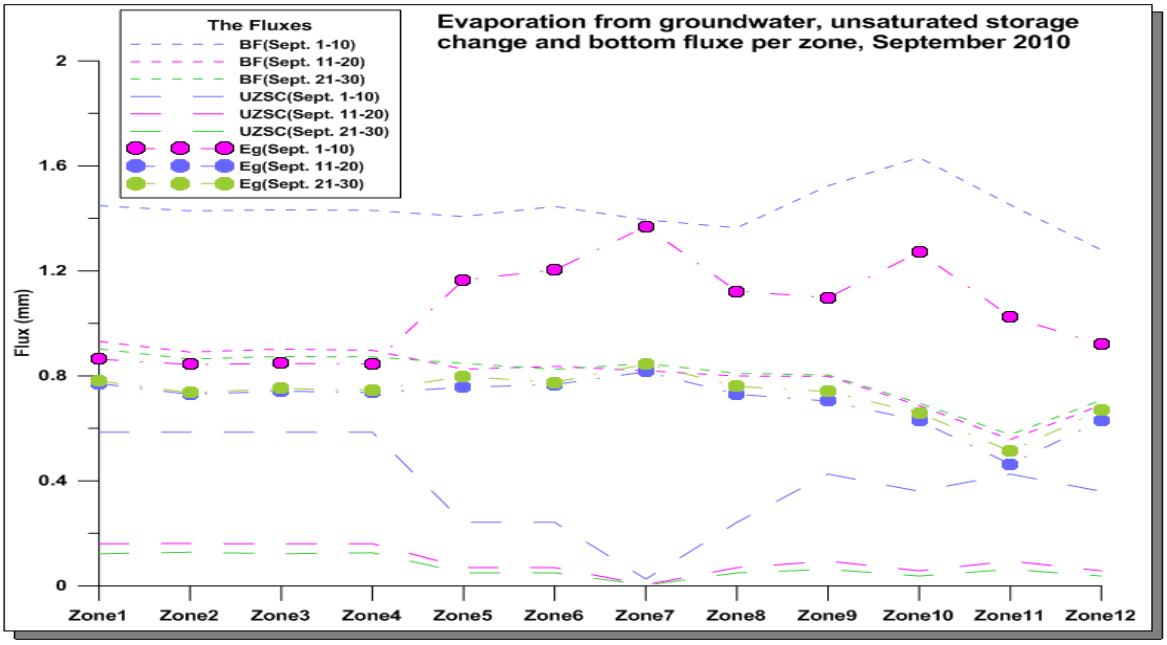

Figure 51. Average values of Eg, BF and UZSC every ten days per zone, September 2010

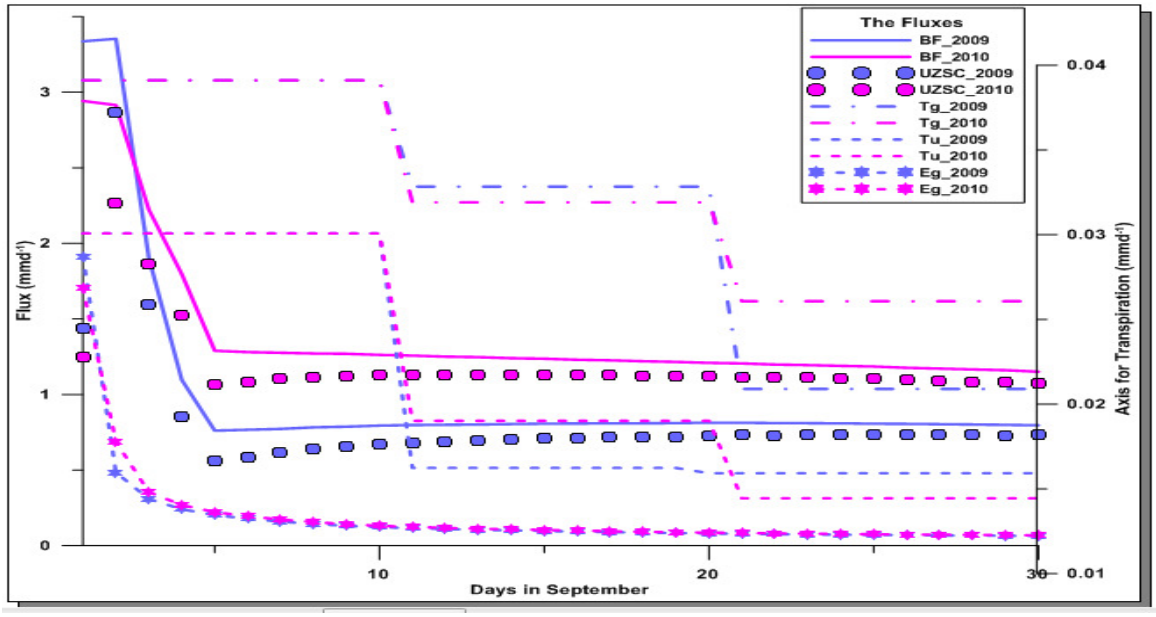

Figure 52. Daily average value of the main fluxes in september 2009 and 201

The BF values as shown on figures 51 and 52 has always highest average value at the first ten days of the month, up to 1.524mmd^{-1} in 2009 and 1.921 mmd^{-1} in 2010 (Zone 10), while lowest at zones with deeper water table up to 0.00227mmd-1at the end of the month in 2009 (Zone 7) and up to 0.0377 mmd^{-1} in 2010. Similarly unsaturated zone storage change (UZSC) is also lower in zones with deeper water table. For instance up to 0.5128mmd^{-1} in 2009 and 0.88mmd^{-1} in 2010 at zone number 11.

The average value of the main fluxes in September 2009 and 2010 were summarized on figure 58; and it was observed that all the fluxes showed a decreasing trend during both years. Again all the fluxes in 2010 are higher than in 2009 except Tg in the middle of the month and Tu at the end of the month.
During the first five days of both simulation periods the values are a bit higher than the rest of time. This is I think because of the model instability and initial condition at the begging of every simulation period.

3.4. Draw down and Water Budget of the Catchment

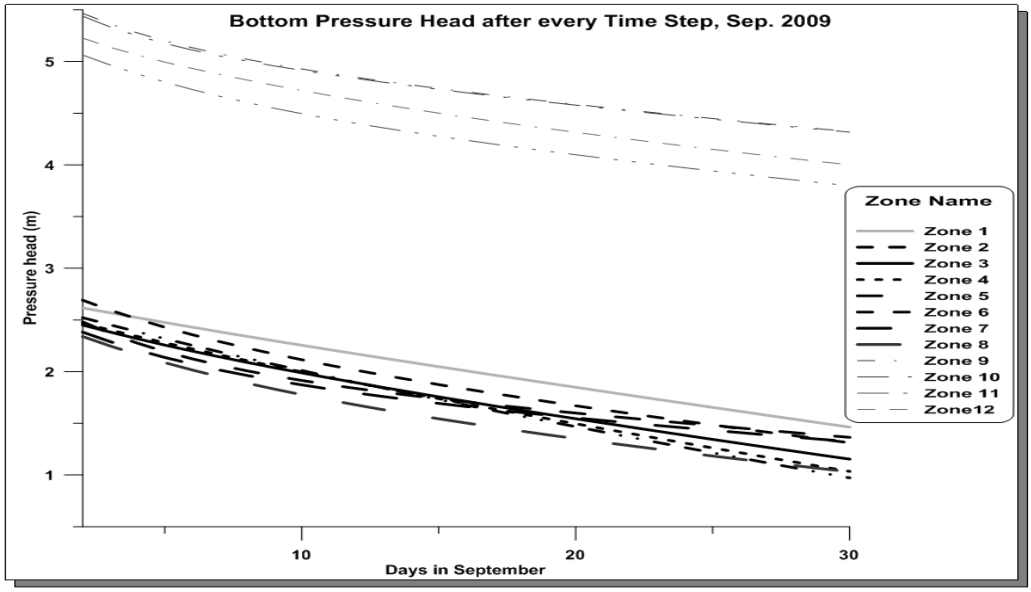

Figure 53. Pressure head at the bottom of each profile (HYDRUS input zones) after every time step

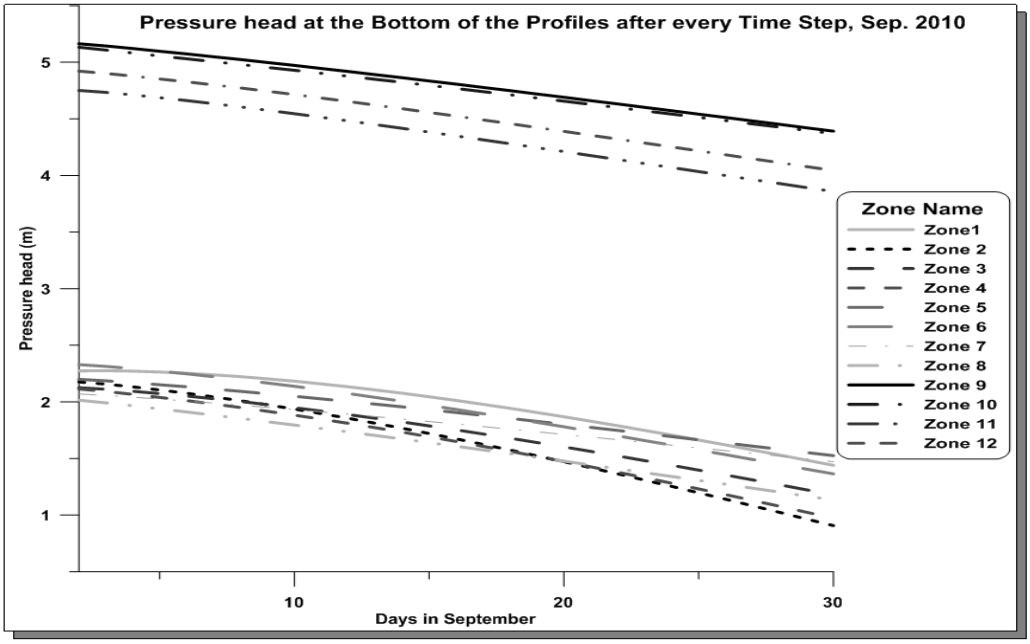

Figure 54. Pressure head at the bottom of each profile after every time step, September 2010

Draw down

The draw down at every profile in September 2009 has similar trend as shown on figure 56, where there was a drawdown of up to 1.22m at zones with deeper water table and 1.55m at zones with shallower water table. The draw down in September 2010 was up to 0.88m at zones with deeper water table and 1.27m at zones with shallower water table (Figure 57). When the draw down during the two simulation periods are compared there was high draw down in 2009 than in 2010 during which the initial hydraulic head was lower. As it was observed from the recession curves of the piezometers, the average monthly draw down was 45cm and the average drawdown simulated during both September 2009 and 2010 was 46cm and 49cm respectively, which indicates the two estimates showed good agreement.

Water Budget

Due to the dry season there is no rain during the both simulation periods (September 2009 and 2010) and nonexistence of either Perennial River or any surface water with external source in the study area there is no inflow to the catchment. The out flow agents in the study area are; Transpiration, Evaporation, capillary rise and drains. Here capillary rise plus evaporation are considered as positive unsaturated flow. The negative value of this sum is recharge which is nil during these simulation periods. The daily volumetric rate of each of these fluxes as shown on figures 59 (A) to (C) are higher in 2010 than in 2009. In addition on the figures it can be observed that all the fluxes showed a decrement from the beginning to the end of the month during both simulation periods.

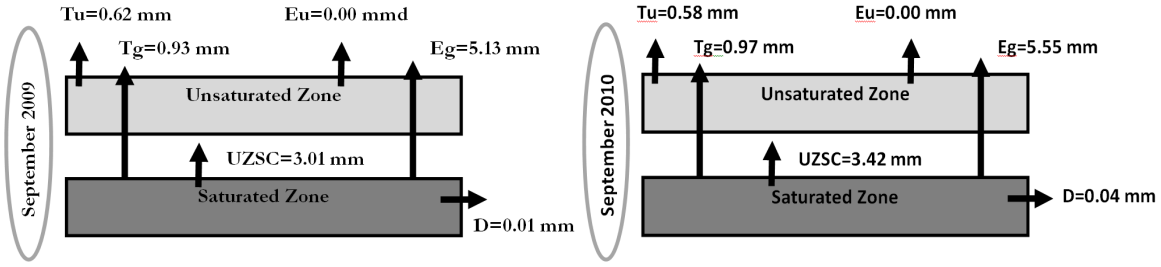

Figure 55. Montly average value of the fluxes September 2009 and 2010 (UZSC: Unsaturated zone storage change D: Drain)

Table 14. Water Budget at the end of each simulation period

Year	Fluxes	In to Storage (m^3)	Out of Storage (m^3)	In-Out (m^3)
2009	Storage	136335.48	2148.69	
	Drains	0	53.72	
	Unsat Flow	0	129934.95	
	Transpiration	0	4206.32	
	Total	136335.48	136343.69	-8.20
2010	Storage	188418.59	1156.73	
	Drains	0	158	
	Unsat Flow	0	182703.27	
	Transpiration	0	4398.67	
	Total	188418.59	188416.67	1.92

For instance at the beginning of the month (the first day) 177.18m^3 of water left groundwater through transpiration, 31.15m^3 out flow through drains, 90.85m3 in to storage, 90.4m3 out of storage and 15575.65m^3 to unsaturated zone in September 2009. While the fluxes; transpiration is reduced to 94.69.18m3, out flow through drains to 0m3, in to storage to 0.80m3, out of storage to 3.62m3and to unsaturated zone to 3481.48m^3 at the end of September 2009 (the last day).

In the same way as 2009, at the beginning of the month (the first day) 177.18m3 of water left groundwater through transpiration, 77.1m^3 out flow through drains, 127.49m^3 in to storage, 126.63m^3 out of storage and

13204m³ to unsaturated zone in September 2010. While the fluxes; transpiration is reduced to 118.12m³, out flow through drains to 0m³, in to storage to 1.76m³, out of storage to 0.44m³ and to unsaturated zone to 5074.9m³ at the end of September 2010 (the last day).

From the entire catchment total amount of water left groundwater in the month September 2009 through transpiration is m³, out flow through drains is 77.1m³, in to storage is 127.49m³, out of storage is 126.63m³ and to unsaturated zone 13204m3. While in September 2009 the amount through transpiration is m³, out flow through drains is 77.1m³, in to storage is 127.49m³, out of storage is 126.63m³ and to unsaturated zone 13204m³ as shown on figures 59 and 60.

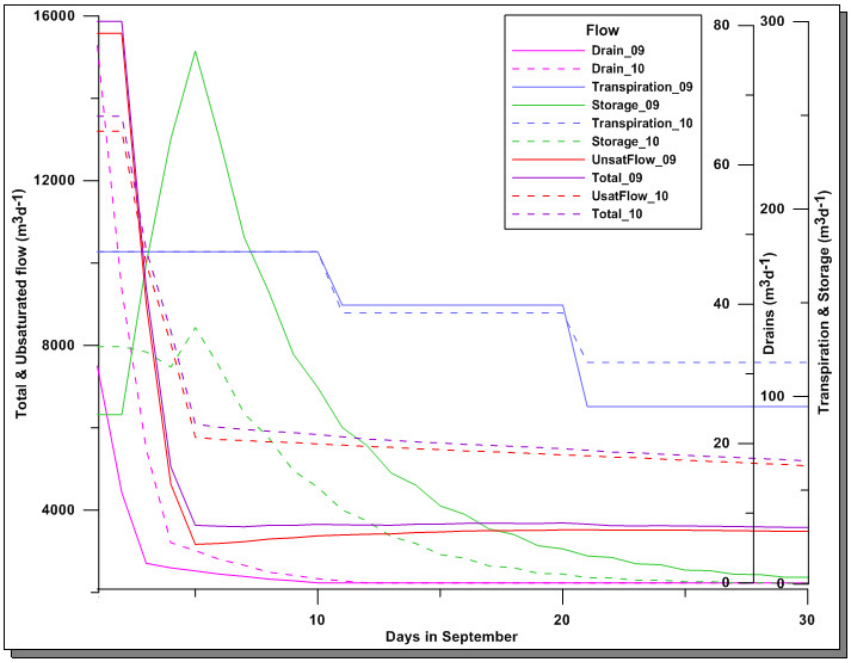

Figure 56. Daily Average volumetric Rates of Outflow (from groundwater) components in September 2009 &10

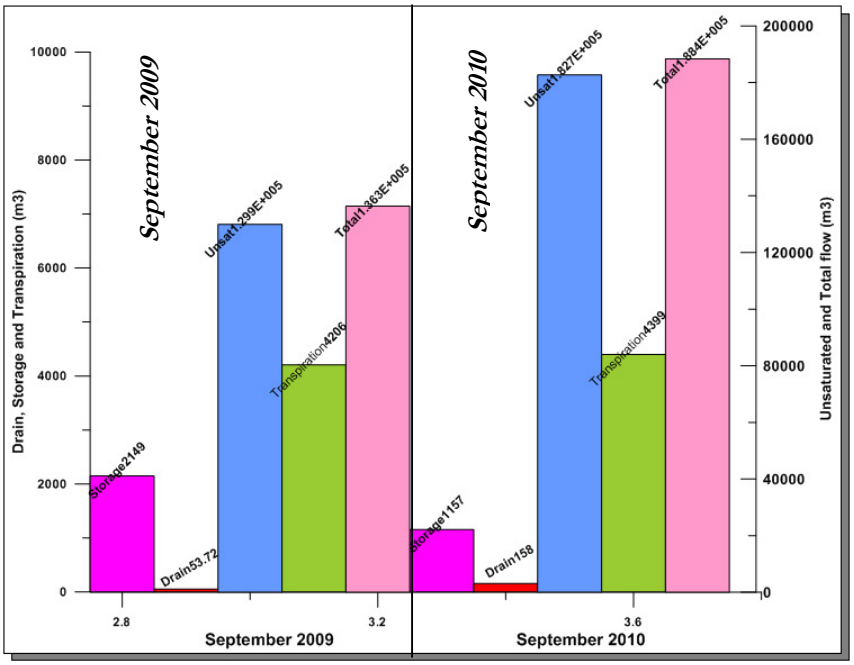

Figure 57. Groundwater Budget in September 2009 &2010

3.5. Sensitivity Analysis of the Model to Main Input or Hydraulic Parameters

The primary outputs of the coupled model are hydraulic heads at the end of every time steps of MODFLOW and fluxes like water through drain and bottom flux (Eg+UZSC. These fluxes were tested for sensitivity of the main input parameters such as reference evaporation rate, hydraulic conductivity, specific yield, inverse of air entry value, saturated and residual water content and etc. Among the inputs the moel (tested for bottom flux) was more sensitive to the unsaturated zone inputs like especially ETo and Ksat than others and the saturated zone inputs as shown on Figure 58, Figure 59, Figure 60, Figure 61, Figure 62. On the figures volume of water that leaves groundwater increases with increase of ETo, decrease with increase of Ksat while it is not much sensitive to inputs like hydraulic conductivity of the saturated zone model of the first layer and alpha (inverse of air entry value) of the unsaturated zone model.

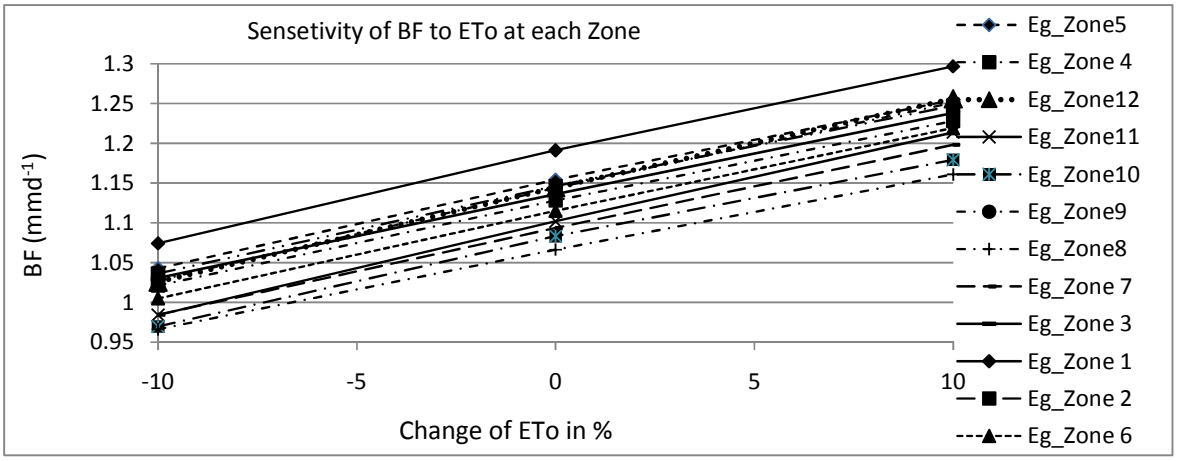

Figure 58. Sensitivity of the model calculated bottom flux to reference evaporation rate

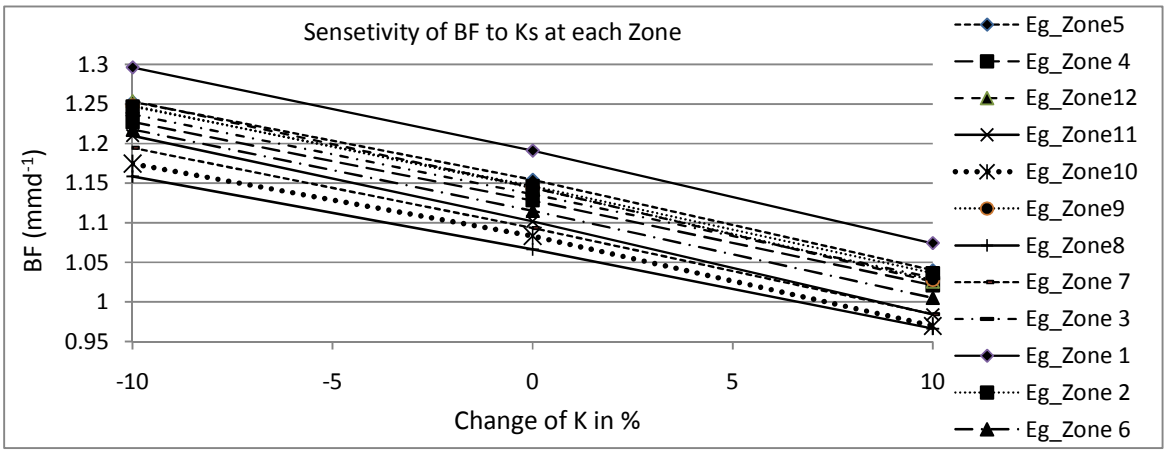

Figure 59. Sensitivity of the model calculated to saturated hydraulic conductivity

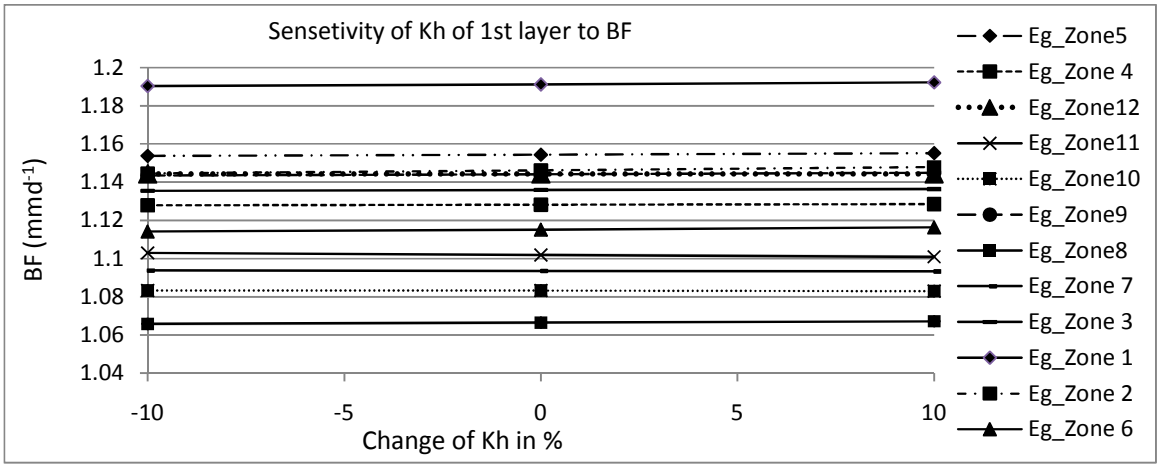

Figure 60. Sensitivity of the model calculated to saturated hydraulic conductivity

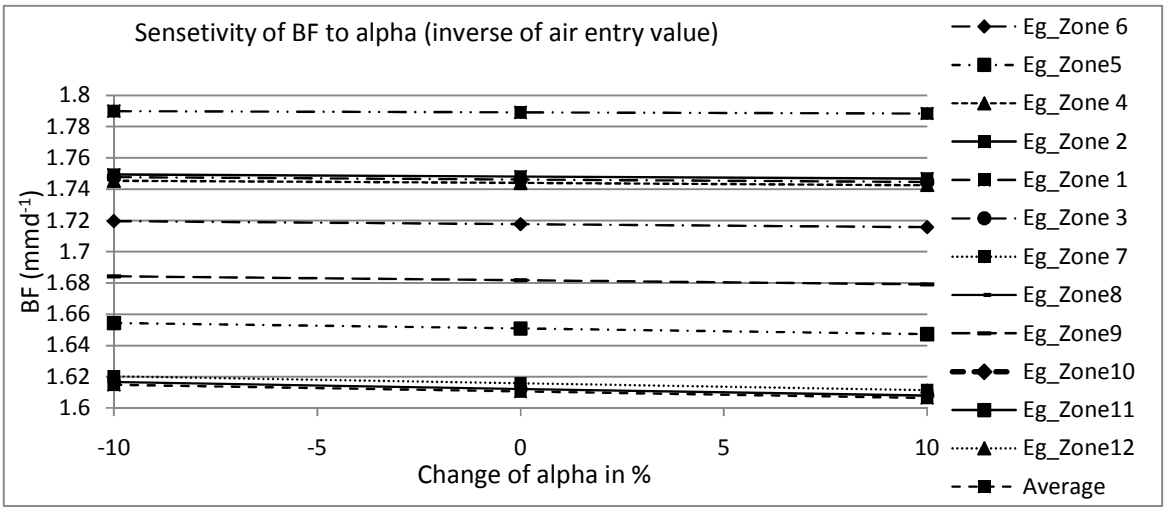

Figure 61. Sensitivity of BF to alpha (inverse of air entry value)

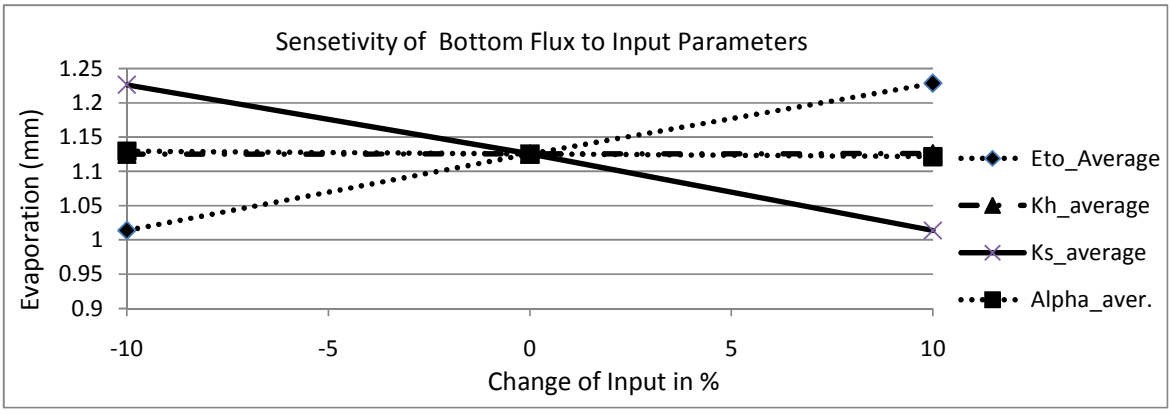

Figure 62. Sensitivity of the model to saturated hydraulic conductivity average of all zones

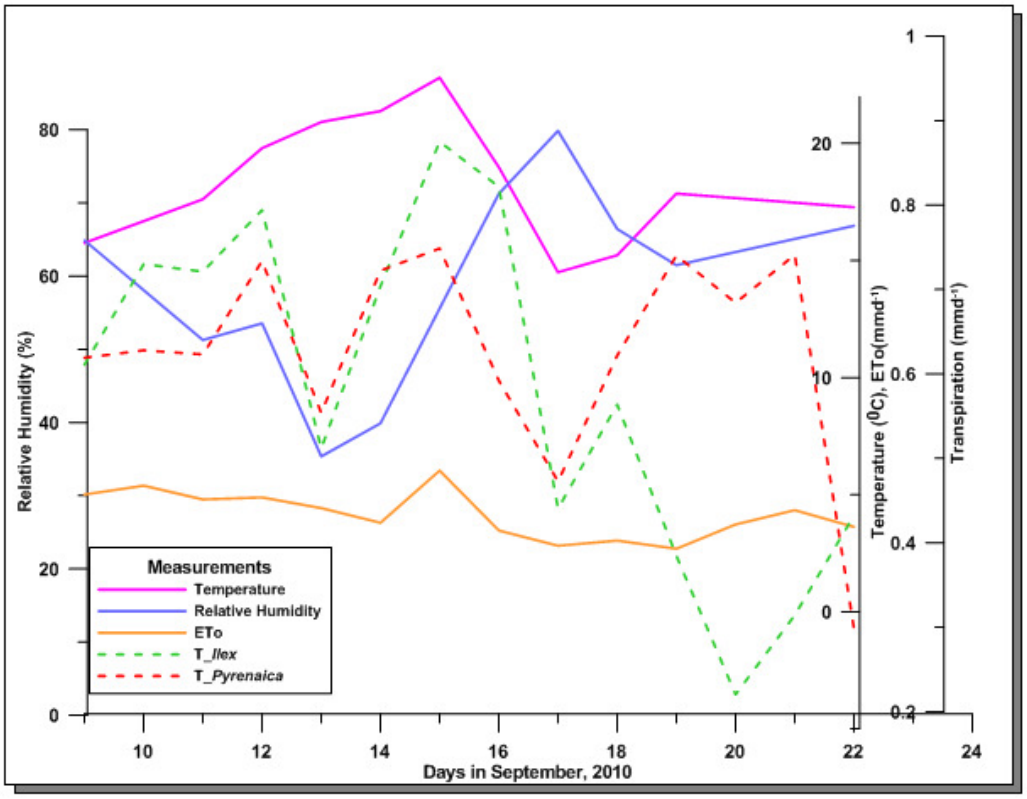

Figure 63. Correlating weather variables with daily transpiration rate of *Q. Pyrenaica* & *Q. Ilex*

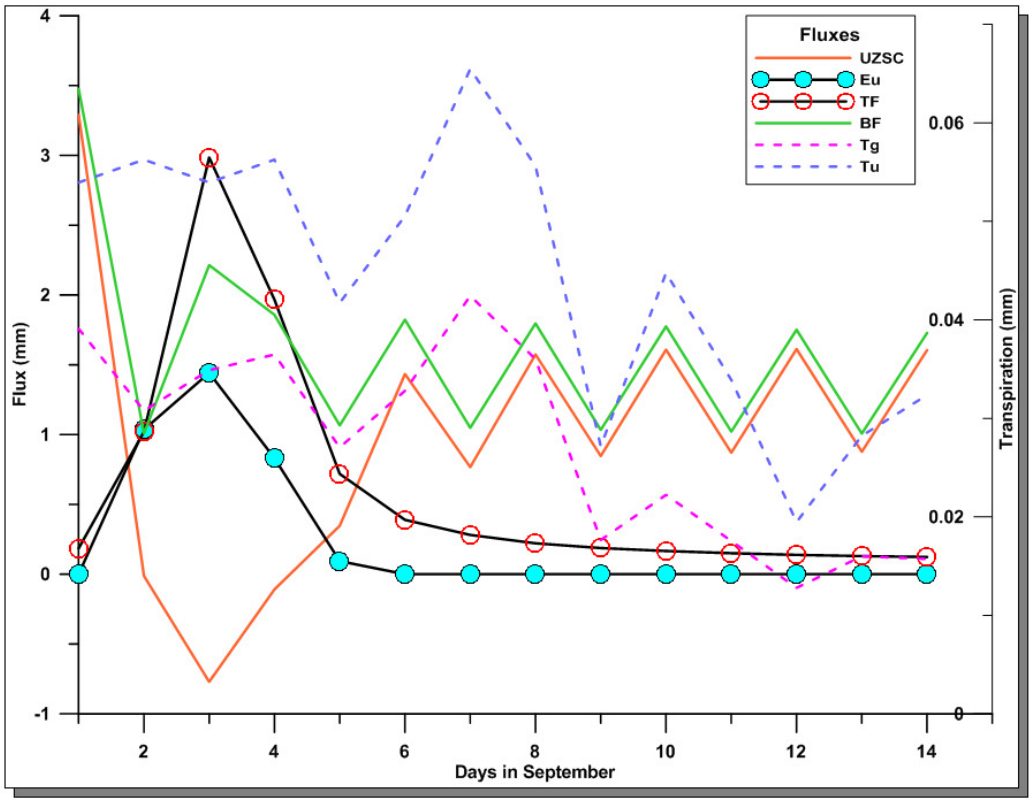

Figure 64. Daily average values of the fluxes

3.6. Simulation Result Using Daily Transpiration Rate (September 9 to 22, 2010)

The initial head for this simulation period was retrieved from extrapolation of the recession curves and finally interpolated to obtain initial head at each model cell.

Temporal and Spatial Distribution of the Subsurface Fluxes

From figure 65 daily average values of all the fluxes is decreasing towards the end of the month. Particularly evaporation from unsaturated zone only existed for the first few days of the simulation period. From these graphs one can observe that more proportion of the daily bottom flux remains in the unsaturated zone where it can be taken plants or increases the moisture content of the unsaturated zone.

Maps showing the daily spatial distribution of the subsurface fluxes for September 11, 2010 to September 22, 2010 were also produced as shown on figures 67-70. From figure 67 it can be observed that part of the catchment with shallow groundwater and coarser material at and above water table like zone 1, has higher bottom fluxes, while the deep groundwater zone has lower bottom flux value. Johnson, et al. (2010) who used a mor direct way of measuring groundwater evaporation was also indicated that shallow groundwater table and coarser materials are in favour of evaporation from groundwater. Partitioned transpiration rate shown on figure 68 and 69 varies spatially with distribution of the trees, where higher values of Tu and Tg are observed along the streams. Especially Q. Pyrenaica grows following stream. Like others, these fluxes also showed a decrement towards the end of the month. However they are more dependent on weather condition than the minor water table fluctuation as indicated on the preceding section and observed from sensitivity of the model not attached to this document.

As it can be observed from the map on figure 70 the top flux which is equivalent to evaporation from groundwater in this case, varies spatially. The spatial variation of this flux is also more dependent on weather condition like transpiration, so the cause for the spatial variation of this flux can be due to water table depth and hydraulic properties of soil above water table. For instance top fluxes of profiles like that of zone 1, 3 and 4 where there exist coarse material above water table are lower though the water table is relatively shallow. But those zones like zone number 6, 9 and 11 with fine material above water table have high top flux value though the water table is relatively deep. As a result it is difficult to generalize the cause for the spatial variation in the catchment. But this flux is also decreasing temporally like all others.

3.7. Result limitations and its comparision with previous works

This study is not concerned with a direct way of measuring the subsurface fluxes. So the results of this study cannot be used for those works that require accurate values of the subsurface water fluxes. In addition the fluxes depend on particular site condition and daily weather condition. However there could be an agreement between different methods of measuring similar fluxes. The result should also agree with the mean value of the fluxes if any in the study area. Accordingly the mean dry season transpiration rate of Q. Ile and Q. Pyrenaica calculated by 2010 MSc graduate, Agbakpe (2010) was 0.61 mmd-1 and 0.72 mmd-1 respectively and the one calculated in September 2009 as indicated on figure 65 was 0.58 and 0.63 mmd-1 respectively, which is closer to the average dry season value.

The mean value of measurements (chamber method) of evaporation from groundwater at 49 locations in closed basin of Chilean Altiplano, which has similar groundwater depth (0.09 to 3.3m) and climate (semi-arid) like the study area, was 0.1 mmd-1 for deepest groundwater table, 1.64 mmd-1 for water table depth of 0.11m and 3.7mmd-1 for open water (Johnson, et al., 2010). By this study the values of evaporation from groundwater was 0.185mmd-1 and 0.194mmd-1 in September 2009 and September 2010 respectively, which are closer to the first value of the mentioned study. This estimate agreed with the chamber method estimate as the first estimate of the chamber method was for groundwater deeper than 0.11m where the depth to groundwater of La Mata catchment was also between 0.3m and 3.4m for September 2009 and between 0.7 and 4m in September 2010.

Tanvir (2008) used stable isotope method to estimate Eg and compare Eg estimate of a transient model using 1D EARTH model as recharge package for MODFLOW. This study area, Pisoes catchment in Portugal has also semi-arid climate and average depth to groundwater in the catchment is between 4 to 5m

(Tanvir Hassan, 2008). He found an average value of 0.094mmd^{-1} (using $\delta^{18}O$) and 0.109mmd^{-1} (using $\delta^{2}H$) for dry season groundwater evaporation, which is also closer to the result of La Mata catchment.

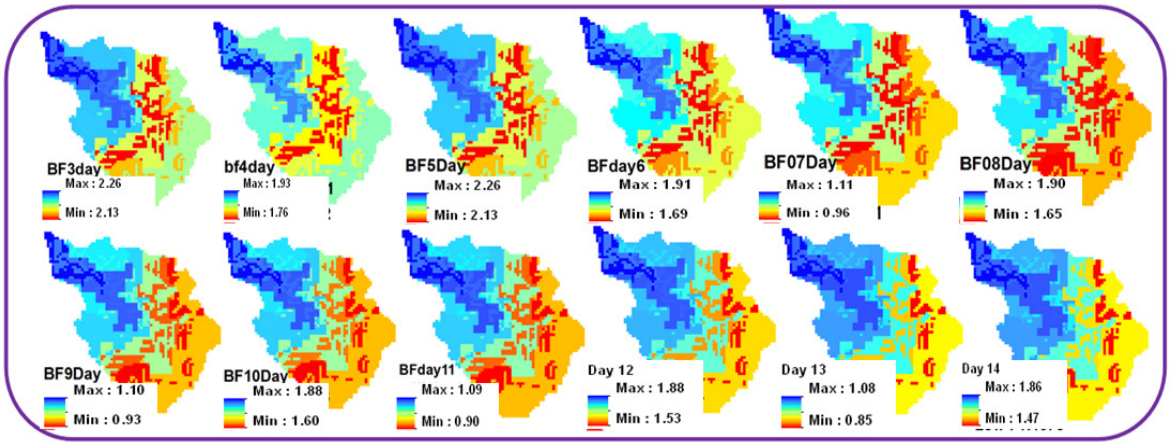

Figure 65. Map of daily Bottom flux (water leaving groundwater up towards unsaturated zone) in mmd^{-1} (September 11 to September 22, 2010)

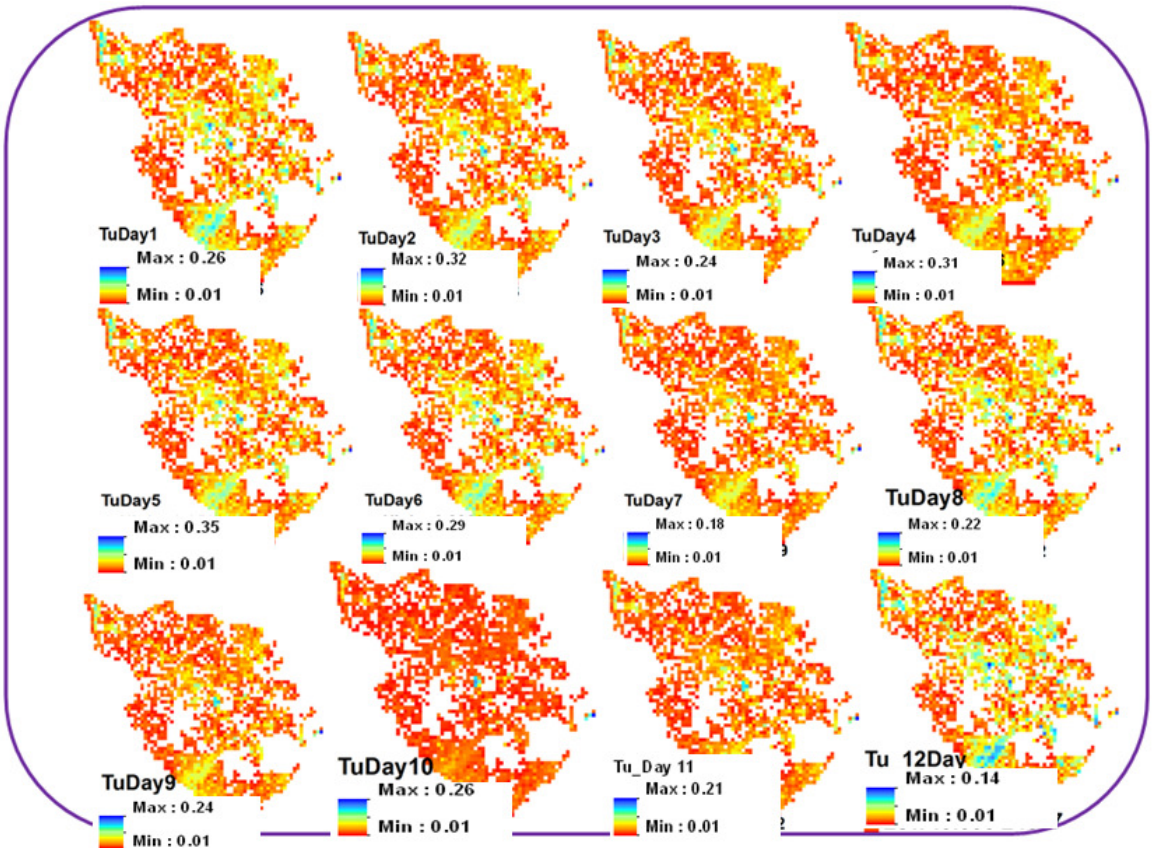

Figure 66. Daily Tu map in mmd^{-1} (September 11 to September 22, 2010)

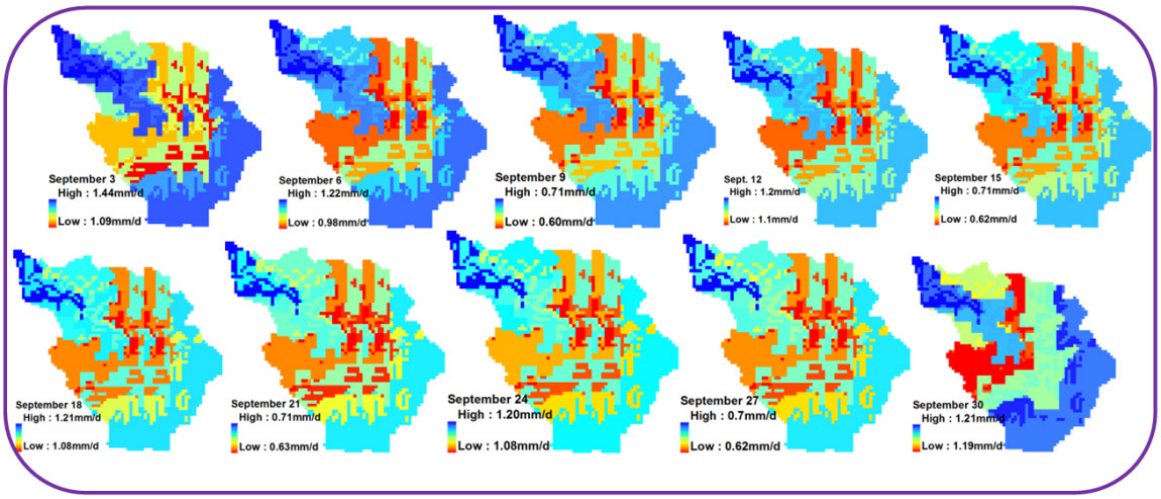

Figure 67. Daily Tg map in mmd^{-1} (September 11 to September 22, 2010)

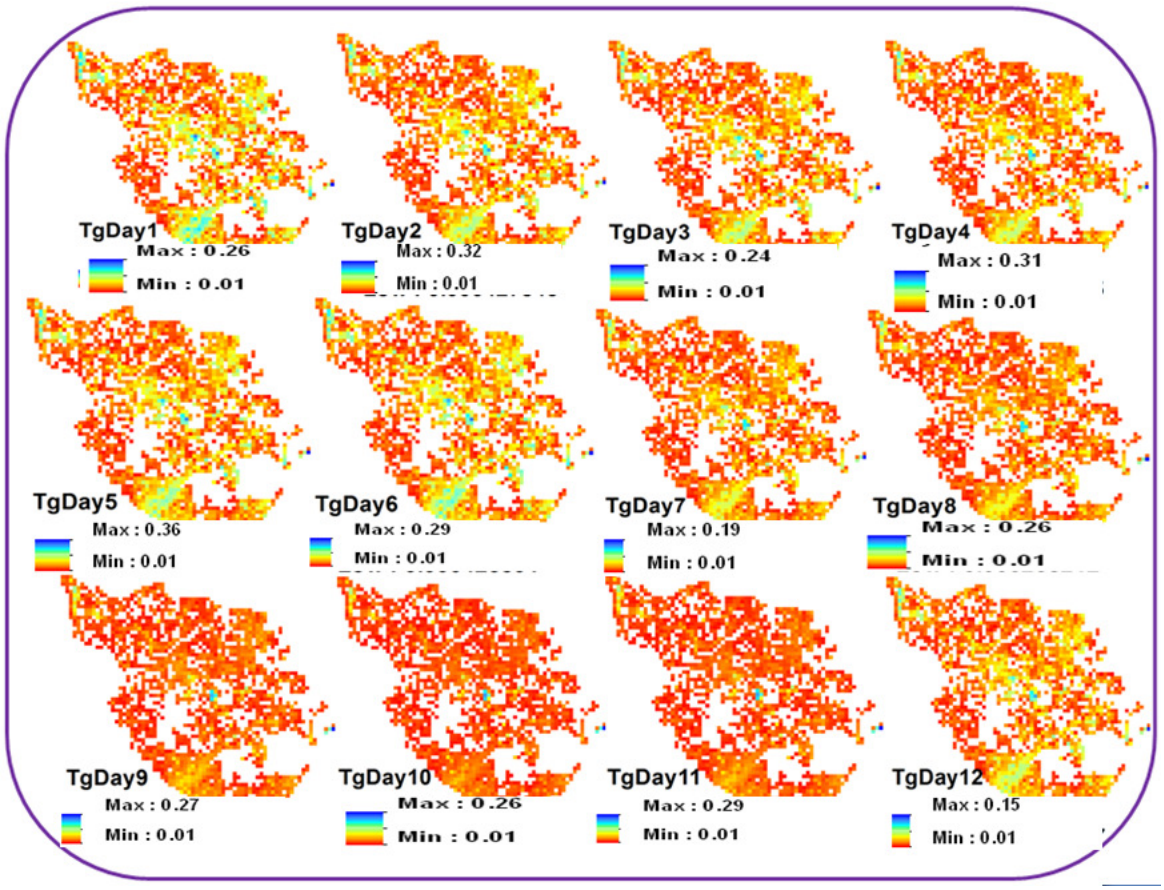

Figure 68. Daily Eg map in mmd^{-1} (September 11 to September 22, 2010)

4. Conclusion and Recommendation

4.1. Conclusion

Modelling subsurface fluxes in areas with semi-arid climate and shallow groundwater table is important because these fluxes are significant in hydrologic cycle and if not estimated, the water resource evaluation by management models can fail.. The accurate quantification of water balance components cannot be possible without taking the unsaturated flow into account next to groundwater flow. Nowadays this is done by coupled saturated-unsaturated zone models as done in this study through coupling of HYDRUS with MODFLOW. Such copled approach requires however an intensive monitoring and field data acquisition on saturated and unsaturated zone parameters and state variables such as soil moisture and matric potential, water levels and microclimatic variables. The studied La Mata catchment is an ideal place for such application because it has extensive data base and monitoring network active already since 1997.

As a result of the La Mata research the following conclusions can be drawn:

- The high resolution, temporal data acquired during the course of this study and through the monitoring network (available since 1997) allowed to constrain successfully the coupled model.
- The recession curves of water table were particularly helpful in constraining transient model calibration, because in La Mata catchment only partial groundwater recession data was available (the piezometers were dry in peak dry season); the missing data was extrapolated according to Maillet equation $H= H_o e^{-\alpha t}$ which allowed to generate missing water table records.
- The tree sap flow measurement gave valuable information on source of water oak trees use in dry season to survive; the partitioning of transpiration into saturated and unsaturated zone components was implemented in the model after the PhD research Leonardo J Reyes-Acosta (2010).
- Remote sensing upscalling of sap flow measurements (classifying the tree species with high spatial resolution over the Quickbird image), based on the available, species-dependent relations between canopy area and corresponding sap flow estimates, proved to be efficient in the spatial assessment of transpiration i.e. in estimation of Tt, Tu and Tg; all these fluxes were used as input in the coupled saturated-unsaturated zone model.
- The use of GIS in combination with coupled model allowed to integrate data of various sources such as: field sampling, laboratory analysis, geophysical measurements, hydrological monitoring, remote sensing.
- The coupling of saturated and unsaturated zone fluxes, in this case MODFLOW and HYDRUS models, provided more realistic solution for estimation of upward and downward fluxes than Hydrus 1D alone, because it accounts for lateral flow that otherwise is not accounted for.
- In September 2009, groundwater discharge was 0.80 mm out of that 0.7 mm (87.5%) is partly utilized by plants or change the unsaturated zone water storage. The remaining 0.1mm (12.5%) evaporates daily. In 2010 the groundwater discharge was 1.11mm, out of that 1.00mm (90.1%) was partly utilized by plants or change the unsaturated zone water storage while the remaining 0.11mm (9.9%) evaporated.
- In September 209, 0.11 mm of water was taken up daily by trees from groundwater while 0.092mm from unsaturated zone. In September 2010 the amount of water taken daily by trees directly from groundwater and unsaturated zone was 0.11mm and 0.09mm respectively.
- The total amount of water that left the catchment because of all the subsurface fluxes was 0.3024 mmd^{-1} in September 2009 and 0.311mmd^{-1} in September 2010, which was significant as compared to the annual mean value of precipitation (~500mmy^{-1}) or recharge (10-100mm y^{-1}).

4.2. Recommendations

The following are recommended for any study related to groundwater modeling of La Mata and or Sardon catchment.

- Although the existing piezometers have good temporal data, their spatial distribution in the study area was not still sufficient to make more reliable and easier numerical model calibration.
- Data organization is very important; there should be a means in the future to accesses the existing data online for the monitoring network stations.
- By organizing the existing water level measurement of the piezomers further studies can be carried out concerning reterive some properties of the aquifer in Sardon catchment using recession curve method.
- More piezometers are required taking their spatial distribution into account so that any study concerning groundwater modeling is closer to the reality.
- The existence of the non-comfortable farmers while interring to their fences and the Spanish Bulls almost everywhere in the catchment make the data gathering a scary work.
- Sap flow measurements were very important for this study. Therefore it is also better to have a record of sap flow measurements at least some days in dry season every year.
- Relation between sap flow and some meteorological variables can be studied and if there exist some relation it can be used to estimate or obtain at least the missing sap flow values.

LIST OF REFERENCES

About.com Spain Travel. (2010). Weather in Spain: Average Monthly Temperature. Retrieved August 7, 2010, from http://gospain.about.com/od/spanishclimate/ss/weather_6.htm

Abubeker, A. M. (2010). *Hydro - geophysical assessment of sub surface to improve groundwater models : Sardon case study, Spain.* Unpublished MSc Thesis, ITC, Enschede.

Agbakpe, B. A. (2010). *Estimating tree groundwater transpiration in La Mata catchment, Spain.* Unpublished MSc Thesis, ITC, Enschede.

Allen, R. G., Pereira, L. S., Raes, D., & Smith, M. (1998). Crop evapotranspiration - Guidelines for computing crop water requirements - FAO Irrigation and drainage paper 56. August 25, 2010, from http://www.fao.org/docrep/x0490e/x0490e00.htm#Contents

Anderson, M. P., & Woessner, W. W. (1972). *Applied Groundwater Modeling Simulation of Flow and Advective Transport*. San Diego Harcourt Brace Javanovich.

Attanayake, N. B. A. (1999). *Analysis of fractures in a granitic terrain and their tectonic and hydrogeological implications : a study from Sardon catchment area, Salamanca province, Spain.* Unpublished MSc Thesis, ITC, Enschede.

Bellingham, K. (2007). The Stevens Hydra Probe Inorganic Soil Calibration. Retrieved August 15, 2010, from http://www.stevenswater.com/catalog/products/soil_sensors/datasheet

Cary, J. W., & Hayden, C. W. (1973). AN INDEX FOR SOIL PORE SIZE DISTRIBUTION. November 26, 2010, from http://eprints.nwisrl.ars.usda.gov/244/1/263.pdf

David, T. S., Henriques, M. O., Kurz-Besson, C., Nunes, J., Valente, F., Vaz, M., et al. (2007). Water-use strategies in two co-occurring Mediterranean evergreen oaks: surviving the summer drought. *Tree Physiology, 27*(6), 793-803.

Earth. (2010). A Graphic Look at the State of the World,The World's Water. Retrieved May 28, 2010, from www.theglobaleducationproject.org/earth/fresh-water

Eijkelkamp. (2010). Eijkeljamp Agrisearch Equipment. August 28, 2010, from http://www.eijkelkamp

Ermias, T. B. (2010). *Improving groundwater model reliability by coupling unsaturated and saturated models : a case study of Sardon catchment, Spain.* Unpublished MSc Thesis, ITC, Enschede.

Fetter, C. W. (2001). *Applied Hydrogeology* (4th ed.). New Jersey Upper Saddle River, New Jersey : Prentice Hall.

Harbaugh, A. W., Banta, E. R., Hill3, M. C., & McDonald, M. G. (2000). MODFLOW-2000, The U.S. Geological Survey Modular Ground Water Model—User Gide to Modularization Concepts and the Ground-Water Flow Process. Retrieved August 11, 2010, from http://www.gama-geo.hu/kb/download/ofr00-92.pdf

Johnson, E., Yáñez, J., Ortiz, C., & Muñoz, J. (2010). Evaporation from shallow groundwater in closed basins in the Chilean Altiplano. *Hydrological Sciences Journal, 55*(4), 624-635.

Kipkoech Ronoh, W. (2001). *Groundwater assessment of the Sardon catchment, Spain.* Unpublished MSc Thesis, ITC, Enschede.

Kosner, B., Granier, A., & Cermak, J. (1998). Sapflow measurements in forest stands: methods and uncertainties. Ann. Sci. For. 55: 13-27.

Kumar, M. D., & Shah, T. (2010). Groundwater Pollution and Contamination in India:. Retrieved May 28, 2010, from www.iwmi.cgiar.org/iwmi-tata/files/pdf/ground-pollute4_FULL .pdf

Lu, P., Urban, L., & Zhao, P. (2004). Granier's thermal dissipation probe (TDP) method for measuring sap flow in trees: Theory and practice. *46*(6), 631-646.

Lubczynski, M. W., & Gurwin, J. (2005). Integration of various data sources for transient groundwater modeling with spatio-temporally variable fluxes - Sardon study case, Spain. *Journal of Hydrology*.

Makoto, T., & lan, p. H. (2010). Groundwater Response to Changing Climate. *IAH - Selected Papers on Hydrogeology*, Retrieved August 09, 2010, from http://ezproxy.itc.nl

Menking, K. M., Anderson, R. Y., Brunsell, N. A., Allen, B. D., Ellwein, A. L., Loveland, T. A., et al. (2000). Evaporation from groundwater discharge playas, Estancia Basin, central New Mexico. *Global and Planetary Change, 25*(1-2), 133-147.

Nathan, R. J., & McMahon, T. A. (1990). Evaluation of automated techniques for base flow and recession analyses. *Water Resour. Res., 26*(7), 1465-1473.

Posavec, K., Parlov, J., & Nakić, Z. (2010). Fully Automated Objective-Based Method for Master Recession Curve Separation. *Ground Water, 48*(4), 598-603.

Powers, J., & Shevenell, L. (2000). Transmissivity estimates from well hydrographs in karst and fractured aquifers. *Ground Water, 38*(3), 361-369.

Ratnayake, R. M. S. (2000). *Groundwater resources evaluation and grounwater modelling in hard rock terrain : Sardon catchment, Salamanca province, Spain.* Unpublished MSc Thesis, ITC, Enschede.

Reyes-Acosta, L. J. (2010). Groundwater transpiration (Tg) discretization using enrichment of naturally abundant isotopes coupled with sap-flow and hydrological variables. Unpublished PhD Thesis. University of Twente, Faculty of Geo-information and Earth Observation (ITC).

Reyes-Acosta, L. J., & Lubczynski, M. W. (2011). Spatial assessment of transpiration, groundwater and soil-water uptake by Oak trees in dry-season at a semi-arid open-forest in Salamanca, Spain. *Press*.

Ruwan Rajapakse, R. R. G. (2009). *Numerical groundwater flow and solute transport modelling : a case study of Sardon catchment in Spain.* Unpublished MSc Thesis, ITC, Enschede.

Rwasoka, D. T. (2010). *Evapotranspiration in water limited environments : up - scaling from crown canopy to the eddy flux footprint.* ITC, Enschede.

Salinas, R. A. I. (2010). *A study case on the upscaling of tree transpiration in Water Limited Environments.* Unpublished MSc Thesis, ITC, Enschede.

Scanlon, B. R., Mace, R. E., Barrett, M. E., & Smith, B. (2003). Can we simulate regional groundwater flow in a karst system using equivalent porous media models? Case study, Barton Springs Edwards aquifer, USA. *Journal of Hydrology, 276*(1-4), 137-158.

Seo, H. S., Šimunek, J., & Poeter, E. P. (2007). Documentation of the HYDRUS Package for MODFLOW-2000, the US Geological Survey Modular Ground-Water Model. *IGWMC-International Ground Water Modeling Center*.

Shakya, D. R. (2001). *Spatial and temporal groundwater modeling integrated with remote sensing and GIS : hard rock experimental catchment, Sardon, Spain.* Unpublished MSc Thesis, ITC, Enschede.

Smakhtin, V. (2008). Basin Closure and Environmental Flow Requirements. *International Journal of Water Resources Development, 24*(2), 227 - 233.

Stephen, K. (1997). *Evaluation of groundwater resources in hard rocks by numerical flow modelling combined with GIS : lower Rio Tormes basin, Salamanca province, Spain.* ITC, Enschede.

Tanvir Hassan, S. M. (2008). *Assessment of groundwater evaporation through groundwater model with spatio - temporally variable fluxes : case study of Pisoes catchment, Portugal.* Unpublished MSc Thesis, ITC, Enschede.

Tesfai, B. H. (2000). *Subsurface characterization of granitic basement from structural and resistivity data : a case study from Sardon catchment area, Salamanca, Spain.* Unpublished MSc Thesis, ITC, Enschede.

Thornthwaite, C. W. (1948). An Approach toward a Rational Classification of Climate. *Geographical Review, 38*(1), 55-94.

Tomczak, M. (2010). Water Cycle from the U.S. Geological Survey. December 23, 2010, from http://oceansjsu.com/105d/exped_briny/6.html

Twarakavi, N. K. C., Simunek, J., & Seo, S. (2008). Evaluating Interactions between Groundwater and Vadose Zone Using the HYDRUS-Based Flow Package for MODFLOW. *Vadose Zone J, 7*(2), 757-768.

Uria cornejo, S. P. (2000). *Groundwater recharge modelling in hard rocks area : Sardon case study, Spain.* Unpublished MSc Thesis, ITC, Enschede.

Yang, J., Li, B., & Shiping, L. (2000). A large weighing lysimeter for evapotranspiration and soil-water-groundwater exchange studies. *Hydrological processes, 14*(10), 1887-1897.

Yu, C., Loureiro*, C., Cheng, J.-J., Jones, L. G., Wang, Y. Y., Chia*, Y. P., et al. (1993). Data Collection Handbook to Support Modeling Impacts of Radioactive Material in Soil November 2, 2010, from http://web.evs.anl.gov/resrad/documents/data_collection.pdf

APPENDICES

Appendix A:

I. Profile 1

1	Z	WC	AT	SINK
1	750.22	-1.088	3	0
2	750.21	-1.078	3	0
3	750.2	-1.068	3	0
4	750.19	-1.058	3	0
5	750.17	-1.038	3	0
6	750.15	-1.018	3	0
7	750.13	-0.998	3	0
8	750.1	-0.968	3	0
9	750.07	-0.938	3	0
10	750.04	-0.908	3	0
11	750	-0.868	3	0
12	749.96	-0.828	3	0
13	749.91	-0.778	3	0
14	749.86	-0.728	3	0
15	749.76	-0.628	2	0
16	749.66	-0.528	2	0
17	749.36	-0.228	2	0
18	749.06	0.072	2	0
19	748.56	0.572	4	0
20	748.06	1.072	4	0
21	747.06	2.072	5	0

II. Profile 2

2	Z	WC	MAT	SINK
1	750.22	-1.088	3	0
2	750.21	-1.078	3	0
3	750.2	-1.068	3	0
4	750.19	-1.058	3	0
5	750.17	-1.038	3	0
6	750.15	-1.018	3	0
7	750.13	-0.998	3	0
8	750.1	-0.968	3	0
9	750.07	-0.938	3	0
10	750.04	-0.908	3	0
11	750.00	-0.868	3	0
12	749.96	-0.828	3	0
13	749.91	-0.778	3	0
14	749.86	-0.728	3	0
15	749.76	-0.628	3	0
16	749.66	-0.528	3	0
17	749.36	-0.228	3	0
18	749.06	0.072	1	0
19	748.56	0.572	1	0
20	748.06	1.072	1	0
21	747.06	2.072	1	0

III. Profile 3

3	Z	WC	MAT	SINK
1	764.29	-1.088	3	0
2	764.28	-1.078	3	0
3	764.27	-1.068	3	0
4	764.26	-1.058	3	0
5	764.24	-1.038	3	0
6	764.22	-1.018	3	0
7	764.2	-0.998	3	0
8	764.17	-0.968	3	0
9	764.14	-0.938	3	0
10	764.11	-0.908	3	0
11	764.07	-0.868	3	0
12	764.03	-0.828	3	0
13	763.98	-0.778	3	0
14	763.93	-0.728	3	0
15	763.83	-0.628	2	0
16	763.73	-0.528	2	0
17	763.43	-0.228	2	0
18	763.13	0.072	2	0
19	762.63	0.572	4	0
20	762.13	1.072	4	0
21	761.13	2.072	5	0

IV. Profile 4

4	Z	WC	MAT	SINK
1	764.29	-1.088	3	0
2	764.28	-1.078	3	0
3	764.27	-1.068	3	0
4	764.26	-1.058	3	0
5	764.24	-1.038	3	0
6	764.22	-1.018	3	0
7	764.2	-0.998	3	0
8	764.17	-0.968	3	0
9	764.14	-0.938	3	0
10	764.11	-0.908	3	0
11	764.07	-0.868	3	0
12	764.03	-0.828	3	0
13	763.98	-0.778	3	0
14	763.93	-0.728	3	0
15	763.83	-0.628	3	0
16	763.73	-0.528	3	0
17	763.43	-0.228	3	0
18	763.13	0.072	1	0
19	762.63	0.572	1	0
20	762.13	1.072	1	0
21	761.13	2.072	1	0

V. Profile 5

5	Z	WC	AT	SINK	
	1	762.19	-2.097	3	0
	2	762.18	-2.087	3	0
	3	762.17	-2.077	3	0
	4	762.16	-2.067	3	0
	5	762.14	-2.047	3	0
	6	762.12	-2.027	3	0
	7	762.1	-2.007	3	0
	8	762.07	-1.977	3	0
	9	762.04	-1.947	3	0
	10	762.01	-1.917	3	0
	11	761.97	-1.877	3	0
	12	761.93	-1.837	3	0
	13	761.88	-1.787	3	0
	14	761.83	-1.737	3	0
	15	761.73	-1.637	2	0
	16	761.63	-1.537	2	0
	17	761.33	-1.237	2	0
	18	761.03	-0.937	2	0
	19	760.53	-0.437	4	0
	20	760.03	0.063	4	0
	21	759.03	1.063	5	0

VI. Profile 6

6	Z	WC	MAT	SINK	
	1	762.19	-2.097	3	0
	2	762.18	-2.087	3	0
	3	762.17	-2.077	3	0
	4	762.16	-2.067	3	0
	5	762.14	-2.047	3	0
	6	762.12	-2.027	3	0
	7	762.1	-2.007	3	0
	8	762.07	-1.977	3	0
	9	762.04	-1.947	3	0
	10	762.01	-1.917	3	0
	11	761.97	-1.877	3	0
	12	761.93	-1.837	3	0
	13	761.88	-1.787	3	0
	14	761.83	-1.737	3	0
	15	761.73	-1.637	3	0
	16	761.63	-1.537	3	0
	17	761.33	-1.237	3	0
	18	761.03	-0.937	1	0
	19	760.53	-0.437	1	0
	20	760.03	0.063	1	0
	21	759.03	1.063	1	0

VII. Profile 7

7	Z	WC	MAT	SINK	
	1	773.41	-2.097	3	0
	2	773.4	-2.087	3	0
	3	773.39	-2.077	3	0
	4	773.38	-2.067	3	0
	5	773.36	-2.047	3	0
	6	773.34	-2.027	3	0
	7	773.32	-2.007	3	0
	8	773.29	-1.977	3	0
	9	773.26	-1.947	3	0
	10	773.23	-1.917	3	0
	11	773.19	-1.877	3	0
	12	773.15	-1.837	3	0
	13	773.1	-1.787	3	0
	14	773.05	-1.737	3	0
	15	772.95	-1.637	2	0
	16	772.85	-1.537	2	0
	17	772.55	-1.237	2	0
	18	772.25	-0.937	2	0
	19	771.75	-0.437	4	0
	20	771.25	0.063	4	0
	21	770.25	1.063	5	0

VIII. Profile 8

8	Z	WC	MAT	SINK	
	1	773.41	-2.097	3	0
	2	773.4	-2.087	3	0
	3	773.39	-2.077	3	0
	4	773.38	-2.067	3	0
	5	773.36	-2.047	3	0
	6	773.34	-2.027	3	0
	7	773.32	-2.007	3	0
	8	773.29	-1.977	3	0
	9	773.26	-1.947	3	0
	10	773.23	-1.917	3	0
	11	773.19	-1.877	3	0
	12	773.15	-1.837	3	0
	13	773.1	-1.787	3	0
	14	773.05	-1.737	3	0
	15	772.95	-1.637	3	0
	16	772.85	-1.537	3	0
	17	772.55	-1.237	3	0
	18	772.25	-0.937	1	0
	19	771.75	-0.437	1	0
	20	771.25	0.063	1	0
	21	770.25	1.063	1	0

IX. Profile 9

9	Z	WC	AT	SINK
1	782.74	-3.3	5	0
2	782.73	-3.29	5	0
3	782.72	-3.28	5	0
4	782.71	-3.27	5	0
5	782.69	-3.25	5	0
6	782.67	-3.23	5	0
7	782.65	-3.21	5	0
8	782.62	-3.18	5	0
9	782.59	-3.15	5	0
10	782.56	-3.12	5	0
11	782.52	-3.08	5	0
12	782.48	-3.04	5	0
13	782.43	-2.99	5	0
14	782.38	-2.94	5	0
15	782.28	-2.84	5	0
16	782.18	-2.74	5	0
17	781.88	-2.44	5	0
18	781.58	-2.14	5	0
19	781.08	-1.64	5	0
20	780.58	-1.14	2	0
21	779.58	-0.14	2	0
22	778.58	0.86	2	0
23	776.58	2.86	1	0
24	774.58	4.86	1	0

X. Profile 10

10	Z	WC	MAT	SINK
1	782.74	-3.3	3	0
2	782.73	-3.29	3	0
3	782.72	-3.28	3	0
4	782.71	-3.27	3	0
5	782.69	-3.25	3	0
6	782.67	-3.23	3	0
7	782.65	-3.21	3	0
8	782.62	-3.18	3	0
9	782.59	-3.15	3	0
10	782.56	-3.12	3	0
11	782.52	-3.08	3	0
12	782.48	-3.04	3	0
13	782.43	-2.99	3	0
14	782.38	-2.94	3	0
15	782.28	-2.84	3	0
16	782.18	-2.74	3	0
17	781.88	-2.44	3	0
18	781.58	-2.14	1	0
19	781.08	-1.64	1	0
20	780.58	-1.14	1	0
21	779.58	-0.14	1	0
22	778.58	0.86	1	0
23	776.58	2.86	1	0
24	774.58	4.86	1	0

XI. Profile 11

11	Z	WC	MAT	SINK
1	798.51	-3.3	5	0
2	798.5	-3.29	5	0
3	798.49	-3.28	5	0
4	798.48	-3.27	5	0
5	798.46	-3.25	5	0
6	798.44	-3.23	5	0
7	798.42	-3.21	5	0
8	798.39	-3.18	5	0
9	798.36	-3.15	5	0
10	798.33	-3.12	5	0
11	798.29	-3.08	5	0
12	798.25	-3.04	5	0
13	798.2	-2.99	5	0
14	798.15	-2.94	5	0
15	798.05	-2.84	5	0
16	797.95	-2.74	5	0
17	797.65	-2.44	5	0
18	797.35	-2.14	5	0
19	796.85	-1.64	5	0
20	796.35	-1.14	2	0
21	795.35	-0.14	2	0
22	794.35	0.86	2	0
23	792.35	2.86	1	0
24	790.35	4.86	1	0

XII. Profile 12

12	Z	WC	MAT	SINK
1	798.51	-3.3	3	0
2	798.5	-3.29	3	0
3	798.49	-3.28	3	0
4	798.48	-3.27	3	0
5	798.46	-3.25	3	0
6	798.44	-3.23	3	0
7	798.42	-3.21	3	0
8	798.39	-3.18	3	0
9	798.36	-3.15	3	0
10	798.33	-3.12	3	0
11	798.29	-3.08	3	0
12	798.25	-3.04	3	0
13	798.2	-2.99	3	0
14	798.15	-2.94	3	0
15	798.05	-2.84	3	0
16	797.95	-2.74	3	0
17	797.65	-2.44	3	0
18	797.35	-2.14	1	0
19	796.85	-1.64	1	0
20	796.35	-1.14	1	0
21	795.35	-0.14	1	0
22	794.35	0.86	1	0
23	792.35	2.86	1	0
24	790.35	4.86	1	0

The twelve Profiles

Appendix B

Sample ID	Location		Soil texture	Depth (cm)	Ksat (md-1)			Θsat		Θr		n
	X	Y			SPAW	FIELD DR_	LAB (Per	LAB (WB)	SPAW	WP4	SPA	
GD1.2	739381	4555666	Sandy loam	60-65	1.34		1.14	0.31	0.39	0.70	0.05	0.5
GD3.1	739386	4555380	Sandy loam	0-5			1.30	0.23		0.65		0.5
GD1.1	739381	4555666	Sandy loam	0-5	1.03	1.67	4.46	0.33	0.39	0.95	0.031	0.5
SVIL02-02R	740348	4555212	Sandy loam	30-35			4.55	0.34				0.5
GD2.1	739353	4555611	Sandy loam	0-5	0.64	1.9	2.21	0.45	0.41	1.05	0.007	0.5
SVIL12-06R	740348	4555212	Sandy loam	90-95	0.7		3.74	0.29		0.83		0.5
LAMATA (GD_DR)	739653	4555667	Sandy loam	15-20	1.4	1.8	2.27	0.29		0.55		0.5
TB08R	739140	4555870	Sandy loam	20-25	1.6		0.41	0.41				0.5
LAMATA(P#2)	739679	4555746	Sandy loam	20-25	0.7		0.16	0.17				0.5
SVIL-01R	740452	4555232	Sandy loam	20-25	0.77		0.09	0.1				0.5
TB-08R2	739140	4555870	Sandy loam	50-55	1.6		0.07	0.07				0.5
TB06B1	739652	4555749	Sandy loam		0.77	1.1						0.5
TRAB00	739658	4555672	Sandy loam		0.8	1.2						0.5
TRABSS	738522	4556380	Loam		0.75	4.2	1.13					0.5
MU02	739697	4546864	Sand		1.58	8.5	0.06					0.5
MU03	739702	4546875	Sandy clay			7.5						0.5
GD7_1	740197	4554934	Sandy loam	0-25	1.29				0.40		0.044	0.5
GD6_1	740321	4555017	loamy sand	0-25	2.17				0.41		0.03	0.5
GD5_1	739644	4555255	Sandy loam	0-25	0.65				0.39		0.08	0.5
GD8_1	739279	4555669	Sandy loam	0-25	0.50				0.50		0.42	0.5
GD4_1	739386	4555380	Sandy loam	0-25	0.69				0.40		0.08	0.5
GD1_3	739381	4555666	Sandy loam	60-65	1.27				0.39		0.017	0.5
GD1_4	739381	4555666	Sandy loam	65-70	1.22				0.39		0.016	0.5
GD8.2	739279	4555669	Sandy loam	25-65	1.20				0.41		0.035	0.5
GD2.2	739353	4555611	Sandy loam	25-65	0.67				40.3	7.8		0.5
GD4.3	739386	4555380	Sandy loam	40-45	0.82				38.4	5.2		0.5
GD1.2E	739391	4555671	Sandy loam	25-45	1.27				39.0	3.4		0.5
GD5.2	739644	4555255	Sandy loam	25-30	0.57				39.0	7.3		0.5
GD4.2	739386	4555380	Sandy loam	25-45	1.01				40.2	3.0		0.5
GD1.1E	739391	4555671	Sandy loam	0-25	1.13				39.3	3.2		0.5
GD1.3E	739391	4555671	Sandy loam	40-45	1.25				40.1	3.20		0.5
GD5.1E	739956	4555110	Sandy loam	0-20	2.40				41.8	1.70		0.5

Soil hydraulic parameters of sample s reterived using different methods with their locations and depths of samplingΘr: Residual soil moisture, Θsat: Saturated soil moisture, Ksat: Saturated hydraulic conductivity

Appendix C

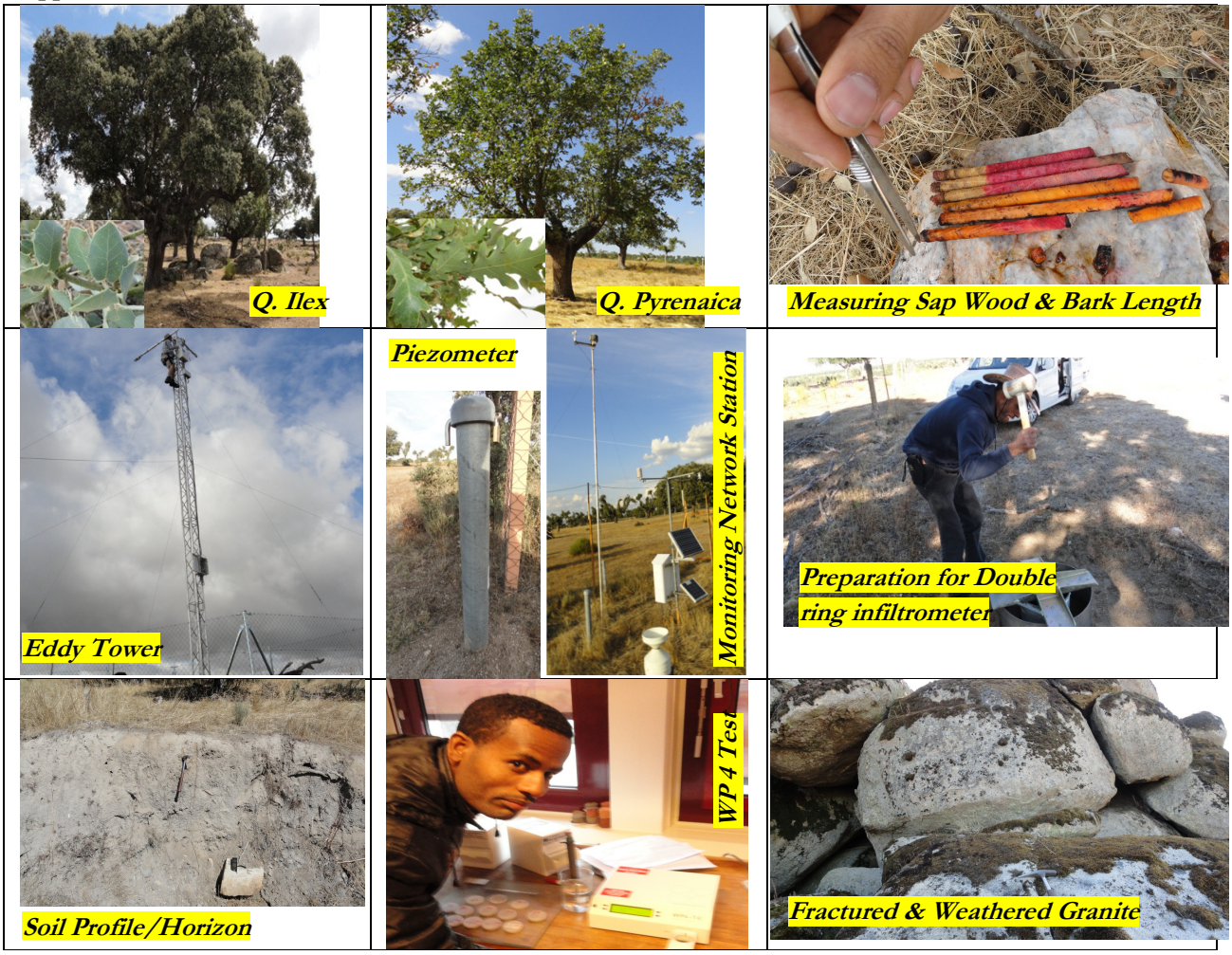

Tree Species and Data Sources: The two tree Species, Sap wood & Bark, Eddy Tower, ...
Map of Bottom Fluxes every three days starting from September 3, 2009

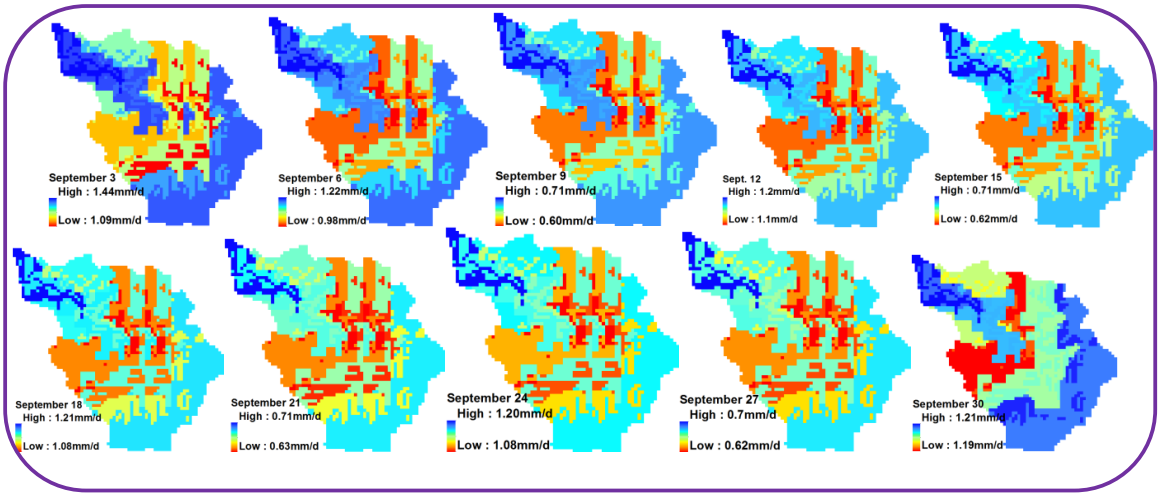

Appendix D

Reference Evapotranspiration

Most part of the study area is covered by grasses, which is usually regarded (example FAO) as a reference for calculation of potential evaporation of crops using Penman-Monteith equation. The FAO Penman-Monteith method is selected as the method by which the evapotranspiration of this reference surface (ET_o) can be unambiguously determined, and as the method which provides consistent ET_o values in all regions and climates (Allen et al.,1998). As mentioned in this paper the relatively accurate and consistent performance of the Penman-Monteith approach in both arid and humid climates has been indicated in both the ASCE and European studies. The Penman-Monteith form of the combination equation is:

$$\lambda ET = \frac{\Delta(Rn-G)+\varrho_a c_p \frac{(e_s-e_a)}{r_a}}{\Delta+\gamma\left(1+\frac{r_s}{r_a}\right)}$$

where R_n is the net radiation, G is the soil heat flux, (e_s - e_a) represents the vapor pressure deficit of the air, ϱ_a is the mean air density at constant pressure, c_p is the specific heat of the air, Δ represents the slope of the saturation vapor pressure temperature relationship, γ is the psychrometric constant, and r_s and r_a are the (bulk) surface and aerodynamic resistances.

The transfer of heat and water vapor from the evaporating surface into the air above the canopy is determined by the aerodynamic resistance:

$$r_a = \frac{ln\left[\frac{Zm-d}{Zom}\right]-ln\left[\frac{Zh-d}{Zoh}\right]}{k^2 U_z}$$

Where; r_a aerodynamic resistance [s m^{-1}], z_m height of wind measurements [m], z_h height of humidity measurements [m], d zero plane displacement height [m], z_{om} roughness length governing momentum transfer [m], z_{oh} roughness length governing transfer of heat and vapour [m], k von Karman's constant, 0.41 [-], u_z wind speed at height z [m s^{-1}].

For a wide range of crops the zero plane displacement height, d [m], and the roughness length governing momentum transfer, z_{om} [m], can be estimated from the crop height h [m] by the following equations:

d = 2/3 h

z_{om} = 0.123 h

The roughness length governing transfer of heat and vapour, z_{oh} [m], can be approximated by:

z_{oh} = 0.1 z_{om}

Assuming a constant crop height of 0.12 m and a standardized height for wind speed, temperature and humidity at 2 m (z_m = z_h = 2 m), the derivation of the aerodynamic resistance r_a [s m^{-1}] for the grass reference surface as used by FAO (Allen et al.,1998) becomes (Eq. 3):

$$r_a = \frac{ln\left[\frac{2-2/3(0.12)}{0.123(0.12)}\right]ln\left[\frac{2-2/3(0.12)}{(0.1)0.123(0.12)}\right]}{(0.41)^2 U_2} = \frac{208}{U_2}$$

where u_2 is the wind speed [m s^{-1}] at 2 m.

The 'bulk' surface resistance, r_s describes the resistance of vapour flow through the transpiring crop and evaporating soil surface. Where the vegetation does not completely cover the soil, the resistance factor should indeed include the effects of the evaporation from the soil surface. If the crop is not transpiring at a potential rate, the resistance depends also on the water status of the vegetation. An acceptable approximation to a much more complex relation of the surface resistance of dense full cover vegetation according to this paper of FAO is:

$$r_s = \frac{r_1}{LAI_{active}}$$

Where r_s (bulk) surface resistance [s m^{-1}], r_l bulk stomatal resistance of the well-illuminated leaf [s m^{-1}], LAI_{active} active (sunlit) leaf area index [m^2 (leaf area) m^{-2} (soil surface)].

A general equation for LAI_{active} is: **LAI_{active} = 0.5 LAI,** which takes into consideration the fact that generally only the upper half of dense clipped grass is actively contributing to the surface heat and vapour transfer. For clipped grass a general equation for LAI is: LAI = 24 h, where h is the crop height [m].

The stomata resistance, r_l, of a single leaf has a value of about 100 s m^{-1} under well-watered conditions. By assuming a crop height of 0.12 m, the surface resistance, r_s [s m^{-1}], for the grass reference surface becomes (Eq. 5):

$$r_s = \frac{100}{0.5(24)(0.12)} \approx 70 s m^{-1}$$

Therefore by defining the reference crop as a hypothetical crop with an assumed height of 0.12 m having a surface resistance of 70 s m^{-1} and an albedo of 0.23, closely resembling the evaporation of an extension surface of green grass of uniform height, actively growing and adequately watered, the FAO Penman-Monteith method was developed.

- fluxes spatial significance in relation to conditions like hydrogeology and climate of the area
- Discussing the encountered difficulties or shortcomings in implementing the selected methodology for the study
- Discussing the result by comparing with results of related previous studies such as recharge, ET, Tg and etc.
- Discuss the significance of subsurface fluxes and the importance of improving quantification of subsurface fluxes based on the result obtained.
- Discussion based on the trends or (contribution of Eg and Tg to the total evaporation)

Daily average value for Tu is calculated: daily transpiration per cell of each species summed and divided by total area of the catchment in ArcGIS. How Eg is calculated also (this should be under discussion)

Biometric measurements (cm) of sampled trees

Biometric Variable	***Q.P.*_01**	***Q.P.*_02**	***Q.P.*_03**	***Q.I.*_01**	***Q.I.*_02**	***Q.I.*_03**
Measured Xylem Length (Ai)	0.9	0.6	0.6	1	0.5	0.5
DBH	21.7	24.6	21	34	33.2	32
Height of First Branch	270	210	265	200	210	175
Height of Sensor	155	160	155	155	158	160
Tree Height	599	425	406	1050	1143	1332
Canopy Area	83252	104065	83252	883730	1124768	789561
X Coordinate	0739491	0739491	0739491	0739588	0739577	0739574
Y Coordinate	4555663	4555661	4555663	4555737	4555741	4555738